Impact and Energy Absorption of Laminated and Sandwich Composites

by

Yavuz Kilic

B.S., Naval Architecture and Marine Engineering

Turkish Naval Academy, 2003

SUBMITTED TO THE DEPARTMENT OF MECHANICAL ENGINEERING IN PARTIAL FULFILLMENT OF THE REQUIREMENTS FOR THE DEGREE OF

MASTER OF SCIENCE IN NAVAL ARCHITECTURE AND MARINE ENGINEERING

AT THE

MASSACHUSETTS INSTITUTE OF TECHNOLOGY

June 2008

Signature of Author____

Department of Mechanical Engineering
May 10, 2008

Certified by_____

James H. Williams, Jr.
School of Engineering Professor of Teaching Excellence
Thesis Supervisor

Accepted by_____

Lallit Anand
Professor of Mechanical Engineering
Chair, Department Committee on Graduate Students

Impact and Energy Absorption of Laminated and Sandwich Composites

by

Yavuz Kilic

Submitted to the Department of Mechanical Engineering, on May 11, 2008 in Partial Fulfillment of the Requirements for the Degree of Master of Science in Naval Architecture and Marine Engineering

Abstract

Advanced fiber reinforced composites combine high specific strength and stiffness. Advanced composites are currently being introduced into modern U.S. Navy ships to achieve weight savings, maintenance reduction, and signature reduction. These advancements manifest themselves in Naval ships as increases in survivability, payload, range, speed, and weapon systems performance.

In this thesis, **vinyl ester** resin matrix laminates and sandwich composites are emphasized since they are increasingly being used in naval applications. Impact damage of laminated and sandwich composites under low-velocity and high-velocity impact are investigated. Delamination damage is explored in detail since delamination is one of the major failure modes of many advanced composites structures. Delamination initiation loads for various laminates having different stacking sequences are compared. In many laminates containing various stacking sequences, placing the 90° laminae on the outside (as opposed to the inside) will reduce the delamination initiation load under impact. Moreover, an open literature survey of numerous laminated and sandwich composites having different stacking sequences and

thicknesses and subjected to low-velocity impact is undertaken. The failure mode, failure load, and displacement at failure of these composites are summarized.

Other topics investigated include (1) effects of a composite's constituents on damage susceptibility, (2) post-impact residual characterization and strength, and (3) nondestructive testing techniques. Prediction methods for residual strength are tabulated based on the impact damage type for laminated and sandwich composites. Further, NASA and Boeing compression-after-impact tests are summarized for laminated composites after low-energy impacts. Damage and residual strength are analyzed for epoxy and PEEK resin laminates. An initial sorting for the selection of nondestructive testing methods for specific composite discontinuities is summarized.

Extensive presentations of tables and figures are used to summarize the results of the literature surveys on impact resistance and energy absorbing capabilities of composites. Particular attention is given to methods for impact resistance improvement. Impact resistance improvement methods are compared according to increases in interlaminar Mode I and Mode II fracture toughness and in residual strength. These comparisons support data for the selection of impact resistance improvement.

Numerous laminates having different lamina orientations are compared to understand the influence of stacking sequence on impact damage resistance and energy absorption capability. Matrix properties are investigated for many laminates and it is noted that higher interlaminar fracture toughness of matrix materials will increase energy absorption capability. The effects of other constituents of a laminate on impact resistance and energy absorbing capability are also summarized. Among the types of composites investigated in this thesis, carbon fiber/PEEK laminates exhibited the highest specific energy absorption.

Recommendations for further studies are offered based on these summaries.

Thesis Supervisor: James H. Williams, Jr.

Title: School of Engineering Professor of Teaching Excellence

Acknowledgements

In the preparation of this thesis, I wish to acknowledge my appreciation and thanks to the following:

To Professor James H. Williams, Jr., my thesis advisor, for his valuable guidance and suggestions, patience, and unlimited availability.

To my parents, Mustafa and Gultaze, for their love and concern.

To my fiancée, Zehra, for her love and continuous support of my goals at M.I.T.

To Turkish Navy, for its financial support to fulfill my degree at M.I.T.

I am also grateful for the financial contribution of the DDG-1000 Program Manager (NAVSEA PMS 500) and the technical guidance of the DDG-1000 Ship Design Manager (NAVSEA 05D).

Table of Contents

List of Figures

List of Tables

1. Introduction

1.1. Overview

In recent years, composite materials have been increasingly replacing conventional metallic materials in the aerospace, civil, marine, and automotive industries, since they offer excellent specific strength and stiffness properties. Composites' intrinsic high strength-to-weight and stiffness-to-weight ratios, corrosion and chemical resistance, improved impact and fatigue resistance, and potential for lower fabrication and life-cycle costs are making them more attractive.

Currently, **carbon fiber** reinforced plastics (CFRP) are widely used in both military and civil aircraft, due to their superior specific stiffness and strength compared to conventional metallic materials. **Glass fiber** composites have been used in the marine industry for decades because of their corrosion resistance, low cost, ease of fabrication, and low maintenance. Specifically, **E-glass vinyl ester** composites are also used in marine structures because of their low cost and resistance to a seawater environment.

1.2. Definition of Problem

One concern in the use of composite materials is their response to localized **impact loading** such as that caused by dropped tools. Low-energy impacts can cause extensive internal damage, taking the form of fiber fracture, delamination, and matrix cracking. At high impact energies, perforation may occur and the impactor may cause cracking and spalling. Such damage will degrade the load-bearing ability of the structure, and their effects can be approximated using mechanics principles.

Some applications of composite materials involve dynamically loaded components and structures. Hence, there is a need to understand the dynamic behavior of composite materials for the analysis and design of composite structures subjected to anticipated **impact loadings**. The mechanical properties of composite materials under dynamic loading conditions are not well understood.

Impact damage can significantly reduce **residual strength** of composite laminates. The prediction of the post-impact load-bearing capability of damaged composite structures is more difficult than for metals since the damage zone is generally complex in nature and consequently difficult to characterize. The problem is further complicated by a lack of existing standards or established testing techniques for impact of composite materials. Much of the work published in the literature has been conducted on purpose-built machines using convenient specimen geometries. As a result, direct comparisons between different material systems and tests are difficult.

Energy absorption capability is an important property of composites subjected to impact loading, in part, since there is a correlation between energy absorption and failure modes. It is therefore useful to understand the effect of a composite constituent parameter on the energy absorption capability of a composite structure. To understand the penetration resistance of composites subjected to **ballistic impact**, there is a need to investigate **penetration** and **perforation threshold energies**. Further, the **ballistic limit velocity** and the material parameters affecting it should be studied to better understand ballistic impact behavior.

1.3. Overview of Thesis

The majority of this thesis is undertaken on continuous fiber reinforced **vinyl ester** resin matrix composites since these materials are finding use in naval applications. In this thesis, low-velocity impact is defined and damage modes, including their interactions due to low-velocity impact loading, are described from the onset of damage to final failure.

Damage characterization and nondestructive inspection methods are reviewed. Among these methods, **visual**, **ultrasonic,** and **laser shearography** are considered in detail since they are currently the primary testing techniques for damage evaluation in the United States Navy. Moreover, damage assessment and post-impact residual strength prediction are discussed. The effects of the composite's constituents such as matrix, fiber, interphase, and fiber stacking sequence on residual strength are also explored.

Numerous techniques, ranging from the use of tough resins to the optimization of fiber stacking sequence, have been proposed to improve impact damage resistance. Energy absorption characteristics of composites under low-velocity impact and ballistic impact, as well as the impactor speed, are analyzed. Finally, effects of the composite's constituents such as matrix, fiber type and geometry, and fiber volume fraction on energy absorption capability are discussed.

2. Characterization of Impact Properties of Composite Materials

Impact may be defined as the relatively sudden application of an impulsive load, generally to a limited volume of material or part of a structure. Often, impacts are classified into either low or high velocity (and sometimes hyper velocity), but the transition between categories are vague and authors vary on their definition.

Low velocity is defined up to 10 $m \cdot s^{-1}$, by considering the test techniques which are generally employed in simulating impact events [Charpy, Izod, instrumented falling weight impact testing (IFWIT), etc.] [1]. Low-velocity impact was defined depending on the material properties, target stiffness, and the impactor's mass and stiffness. Low-velocity impact was designated as quasi-static events, the upper limit of which can vary from one to tens of $m \cdot s^{-1}$ [2,3]. However, in another study it was asserted that low-velocity impacts occur for impact speeds of less than 100 $m \cdot s^{-1}$ [2]. It was further suggested that the type of impact can be classified according to the damage incurred, especially if damage is the main concern. Thus, low-velocity impact is characterized by delamination and matrix cracking and high-velocity impact is characterized by penetration-induced fiber breakage [4,5].

High-velocity impact response is dominated by stress wave propagation through the material, and since the structure does not have time to respond, it leads to localized damage. Often, boundary condition effects can be ignored because the impact event is over before the stress waves reach the edge of the structure.

In low-velocity impact, as the contact duration is long enough for the entire structure to respond to the impact, more energy is absorbed elastically and the dynamic structural response of the target is of highest importance. It is indicated that the low- and high-velocity impact responses of a composite structure may vary considerably and under low-velocity impact loading

where the elastic energy absorbing capability of the structure is important, the structural geometry determines the target's impact response. Conversely, under conditions of high-velocity impact loading where the projectile generates a localized form of target response, geometrical parameters such as the width and length of the target appear to have very little effect on the impact response [1]. A simple model is offered to determine the transition to high velocity by defining a low-velocity impact as being one in which the through-thickness stress wave plays no significant part in the stress distribution [6,7]. A cylindrical zone under the impactor is considered to undergo a uniform strain as the stress wave propagates through the plate, and for epoxy composites this gives the transition to stress-wave-dominated events at 10-20 $m \cdot s^{-1}$ for failure strains between 0.5 and 1% [6].

2.1. Modes of Failure and Failure Load in Low-velocity Impact

Although many failure modes can be cited after low-velocity impact, the heterogeneous and anisotropic nature of fiber-reinforced plastic (FRP) laminates gives rise to four major modes of failure.

1) **matrix mode:** Cracking occurs parallel to the fibers due to tension, compression or shear;

2) **delamination mode:** Produced by interlaminar stresses;

3) **fiber mode:** In tension fiber breakage and in compression fiber buckling;

4) **penetration:** The impacted surface is completely perforated by the impactor. It is important to identify the mode of failure because this will yield information not only about the impact event, but also about the structure's residual strength. Interaction between failure modes is also very important in understanding damage mode initiation and propagation [4].

2.1.1. Matrix Damage

Matrix damage generally takes the form of matrix cracking and debonding between fiber and matrix. It is the first type of failure induced by transverse low-velocity impact [8]. The majority of the impact test research has involved low-energy testing, in the range of 1 to 5 J (i.e. that which causes only minimal damage). Matrix cracks are usually oriented in planes parallel to the fiber direction in unidirectional layers and occur due to property mismatching between the fiber and matrix. A typical crack and delamination pattern is shown in **Figure 1.**

Matrix cracks in the upper layers **(Figure 1a)** and the middle layer **(Figure lb)** begin under the edges of the impactor. These ***shear cracks*** [9] are formed by the very high transverse shear stress through the material, and are inclined at approximately 45°. The transverse shear stresses are related to the contact area and contact force. In **Figure 1a** the crack on the bottom layer is called a ***bending crack*** since it is induced by high tensile bending stresses and is characteristically vertical. The bending stress is related to the flexural deformation of the laminate [10]. Lee and Sun [11] reached the same conclusions in their analyses.

The type of matrix cracking is dependent on the global structure of the impacted specimens [12]. Due to excessive transverse deflection, bending cracks in the lower layers occur and subsequent membrane effects predominate for long thin specimens, whereas short thick specimens are stiffer and so higher peak contact forces induce transverse shear cracks under the impactor in the upper plies. A detailed view of matrix cracking which agreed with the above was presented by Liu and Malvern [4], while Wu and Springer [13] reported detailed locations of matrix cracking for graphite epoxy plates of various stacking sequences. Many studies have been conducted in this area, and it was postulated that the bending crack in the 90° layer is caused by a combination of out-of-plane normal stress (σ_{33}) , in-plane tensile stress (σ_{11}), and

interlaminar longitudinal shear stress (σ_{13}) (**Figure 2**) for line-loading impact damage [9,14,15,16,17,18]. These studies concluded that σ_{33} was very small relative to σ_{11} and σ_{13} throughout the impact event, and there is a critical energy below which no damage occurs.

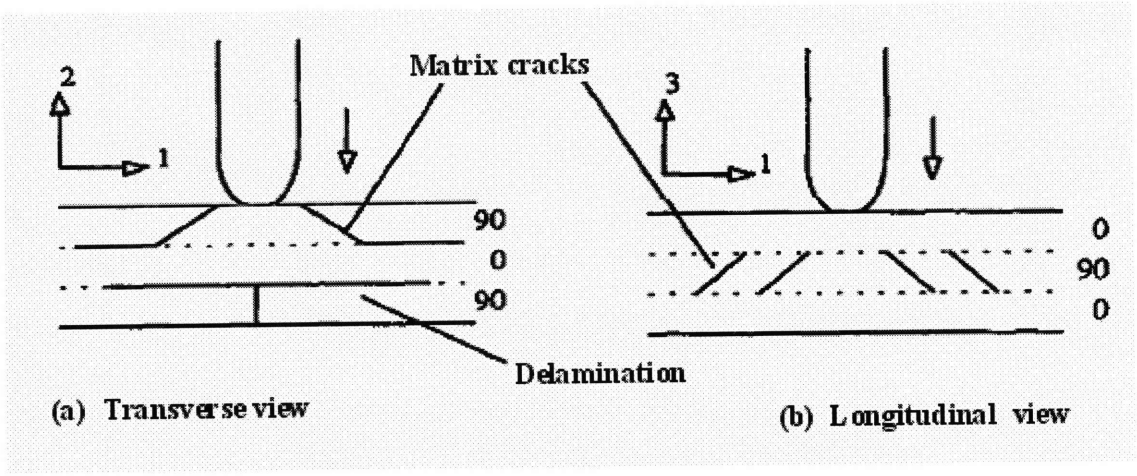

Figure 1: Initial damage in an impacted 0/90/0 composite plate [8].

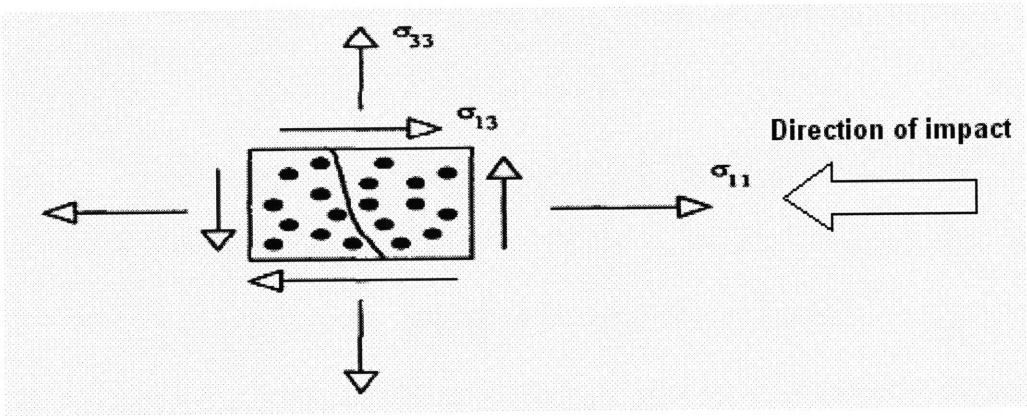

Figure 2: Diagram of stress components contributing to bending matrix crack in transverse layer [15].

2.1.2. Delamination

The impact induced delamination is the most important damage mode because the level of impact energy to initiate delamination is low and the post-impact compressive strength is dramatically reduced to delamination [19]. A delamination is a crack which runs in the resin-rich area (approximately 0.0007 mm in graphite/epoxy laminates [20]) between plies of different fiber orientation and not between lamina in the same ply group [13,21,22].

Detailed connections between delaminations and the areas over which matrix cracks were found for various lay-ups were compiled [4]. It was explained that delamination was a result of the bending stiffness mismatch between adjacent layers, i.e. the different fiber orientations between the layers and delamination areas were generally oblong-shaped with their major axis being coincident with the fiber orientation of the layer below the interface [23]. For 0/90 laminates the shape became that of a distinct peanut. These results have been widely reported in the literature [8,13,15,24,25,26,27].

Further, the bending-induced stresses, which are the major cause of delamination, as both experiment and analysis revealed that along the fiber direction the plate tends to bend concave, while the bend is convex in the transverse direction [23]. A bending mismatch coefficient between two adjacent laminates was defined, which includes bending stiffness terms and predicts the peanut shape reported for 0/90 laminates. The greater the mismatch (0/90 is the worst-case fiber orientation), the greater the delamination area. This is also affected by , stacking sequence, material properties and laminate thickness [28]. This damage mode is more likely to occur for short spans and thick laminates with low interlaminar shear strength [29,30,31].

2.1.2-1. Prediction of Delamination

If the impact-induced delamination crack growth is a quasi-static event, the maximum delamination size should correspond to the magnitude of the maximum impact load. Hence, for a given impact condition, if the peak contact force is known, one can obtain the delamination crack length by using the linear relationship between the peak contact force and delamination crack length. Moreover, if the peak force is unknown, it can be estimated by using the linear relationship between the peak force and impact velocity acquired from experimental data [10].

2.1.2-2. Delamination Initiation and Interaction with Matrix Cracking

Above a threshold energy, delamination caused by transverse impact occurs and a transverse matrix crack usually extends across the entire lamina with the crack tips touching the interfaces [32]. It has also been observed that delamination only occurs in the presence of a matrix crack [18]. Many detailed studies have been conducted to verify this fact and to explain the stress states that could cause this interaction.

Among these studies, one that revealed for the first time the association between matrix cracking and delamination was performed by Takeda [33]. This research explicitly revealed that delaminations do not always run precisely along the interface region, but can run slightly to either side. In another study [8], delamination-matrix crack interaction was examined for 0/90/0 laminates subjected to transverse point impact. It was concluded that when the inclined shear crack in the upper layer (**Figure 1a**) reaches the interface, it is halted by the change in orientation of the fibers and so it propagates between the layers as a delamination. Generally, this delamination is restricted by the middle transverse crack (**Figure 1b**). The vertical bending

crack (**Figure 1b**) is thought to initiate the lower interface delamination, the growth of which is not constrained. Matrix cracks which lead to delamination are known as **critical matrix cracks** [15]. For a 0/90/0 composite, many line-loading, low-velocity impact tests were performed and a typical damage pattern emerged as shown in **Figure 3** [9,15,18,34]. Three-dimensional finite element analysis was used to simulate these matrix cracks in studying the stress in the vicinity of the cracks [15]. It was concluded that delamination was initiated as a mode I fracture process due to very high out-of-plane normal stresses caused by the presence of the matrix cracks and high interlaminar shear stresses along the interface. In another study on this topic [35], it was proposed that matrix crack initiated-delamination was due to the interlaminar normal and shear stresses at the interfaces.

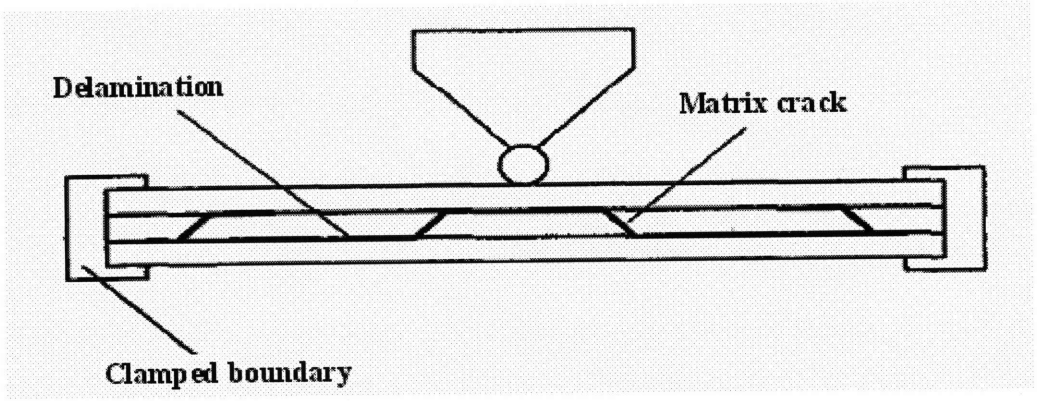

Figure 3: Typical matrix crack and delamination pattern from line-load impact on a 0/90/0 composite [15].

Utilizing a fracture mechanics approach, an analytical model to study the interaction of damage mechanisms due to line-load impact was developed [34]. It was shown that both bending cracks and shear cracks could initiate delamination, but that delamination induced by shear cracks is unstable and that bending crack induced delaminations grow in a stable manner, proportional to the applied load.

The stresses producing impact-induced delamination were described in detail [28,36]. All the modes which could be induced by impact-bending, twisting, and transverse shear were considered, as were the restraints on the affected ply due to layers above and below. It was concluded that if the cracked ply group is above the interface, then (if the upper interface of the ply group is unrestrained) interlaminar transverse shear stresses (σ_{12} and σ_{23}) contribute to delamination; if the cracked ply group is below the interface, transverse in-plane stress and interlaminar transverse shear stress (σ_{22} and σ_{12}) contribute to delamination as long as the ply group lower interface is unrestrained. $\sigma_{12}, \sigma_{23}, \sigma_{22},$ can be drawn from **Figure 2.**

Because an initial flaw or crack size is assumed, most fracture mechanics analyses of the initiation and growth of delamination are difficult to apply [37]; however, it was notably shown that in a highly simplified isotropic axisymmetric analysis for the threshold force for growth of an internal circular delamination in the mid-plane, the mode II strain energy release rate is independent of delamination radius [7].

2.1.2-3 Delamination Growth

Delamination growth was attributed to interlaminar longitudinal shear stress (σ_{13}) and transverse in-plane stress (σ_{22}) in the layer below the delaminated interface and to the interlaminar transverse shear stress (σ_{12}) in the layer above the interface [26]. $\sigma_{13}, \sigma_{22}, \sigma_{12}$ can be drawn from **Figure 2.** Artificial delaminations were introduced by putting a thin foil between plies in the manufacturing stage to assess delamination growth from a known initial size [38]. The energy absorbed per unit area of delamination growth was calculated as (595 $J \cdot m^{-2}$) [39]. It was concluded that the interlaminar fracture toughness was independent of delamination size and that delamination area could be predicted from the peak impact force generated [10]. It was

also revealed that there was a linear relationship between the peak force and the delamination area and, by extrapolating from the results, a value of threshold force for the onset of delamination was found [25]. In a numerical simulation of impact-induced delamination growth, it was concluded that mode II was the dominant failure mode for propagation [40].

2.1.3. Fiber Failure

Fiber failure generally occurs much later in the fracture process than matrix cracking and delamination, and there is less information on this area since many researchers have concentrated on the low-energy modes of damage. Fiber failure occurs under the impactor due to locally high stresses and indentation effects governed by shear forces and on the non-impacted face due to high bending stresses. Fiber failure is a precursor to the catastrophic penetration mode [30].

2.1.4. Penetration

Penetration occurs when the fiber failure reaches a critical extent, enabling the impactor to completely penetrate the material and it is a macroscopic mode of failure [41]. Many studies into penetration impact have mainly concentrated on the ballistic range; however, some low-velocity impact work has been performed. It was shown that the impact energy penetration threshold rises rapidly with specimen thickness for carbon fiber reinforced plastic (CFRP) [12]. Penetration was also analyzed to calculate the energy absorbed by shear-out (i.e. removal of shear plug), delamination, and elastic flexure. This simplified analysis predicted shear-out as the major form of energy absorption (50-60% depending on plate thickness).

A variety of glass fiber-reinforced plastic (GFRP) composites at penetration loads was tested and it was concluded that the glass fiber treatment played a key role in determining the perforation load. While the matrix had little effect, polyester was more penetration-resistant than epoxy [42].

2.1.5. Failure Load

Failure load is the load level at which the failure modes such as delamination, matrix cracking, penetration etc... initiate. For instance, the results from two experimental investigations for three types of graphite/epoxy laminate specimens and five types of glass/epoxy laminate specimens are shown in **Table 1.**

Table 1: Delamination initiation load

Laminate	Stacking sequence	Delamination initiation load(N)	Reference
Graphite/epoxy	$[90_2/0_2/90_2]$	5338	[32]
Graphite/epoxy	$[90_6/0_2/90_6]$	2112	[32]
Graphite/epoxy	$[0/90_{12}/0]$	5115	[32]
Glass/epoxy	$[0_4/15_4/0_4]$	5300	[43]
Glass/epoxy	$[0_3/15_6/0_3]$	5711	[43]
Glass/epoxy	$[0_3/15_8/0_3]$	5914	[43]
Glass/epoxy	$[0_2/15_2/0/15]_s$	6368	[43]
Glass/epoxy	$[(0/15)_3]_s$	6696	[43]

From the **Table 1**, the delamination initiation load is lower for thicker 90° laminates. Also, placing 90° laminae on the outer faces of the laminate facilitate delamination by the reduction of delamination initiation loads [32,43,44]. Further, transverse matrix cracks in cross-plied laminates significantly reduce laminate strength. Also, it was noted that thicker 90°-plies with larger transverse matrix cracks cause higher stress concentration in the load-carrying 0°-plies and consequently result in further reductions in laminate strength [45].

For a sandwich structure there is a difference between top and bottom facesheet deflections due to indentation of the top facesheet associated with core crushing. The top facesheet deflection increases at a nearly linear rate versus impact force, a portion of which is recovered upon unloading. The portion of the top facesheet deflection that is not recovered is due largely to core crushing. Typical facesheet deflections and damage initiation are shown in **Figure 4** versus load versus displacement. From this graph, the total indentation can be estimated by subtracting the bottom facesheet deflection from the upper facesheet deflection.

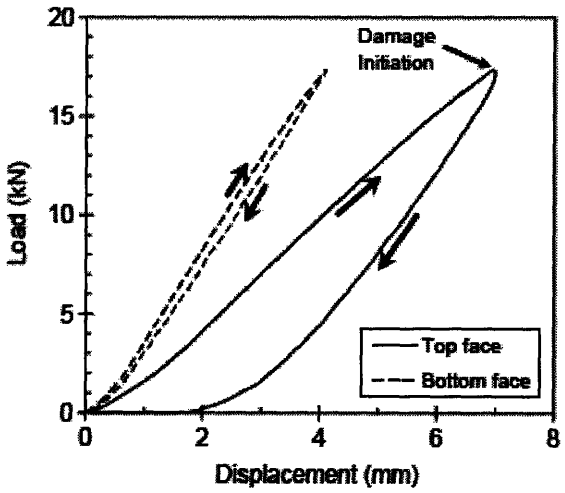

Figure 4: Load vs. displacement curves for upper and lower facesheets of sandwich panel [46].

The experimental results obtained from various investigations [32,44,45,46] on the failure loads of laminates and sandwich structures are shown in **Table 2.** In these studies two types of sandwich materials with similar types of polyvinyl chloride (PVC) foam and with unidirectional glass fiber fabric cross-ply laminate skins were investigated under low-velocity impact loading. In addition, thirteen different graphite epoxy and glass epoxy laminates with different resins and stacking sequences were investigated under low-velocity impact.

Table 2: Failure loads of laminates and sandwich structures

Material composition	Stacking sequence	Average thickness (mm)	Failure mode	Failure load(kN)	Displacement at failure(mm)	Ref.
AS4/3501-6	$[0_2]$	0.254	Fiber failure	16.013	*	45
AS4/3501-6	$[0_4]$	0.505	Fiber failure	28.91	*	45
AS4/3501-6	$[0_6]$	0.762	Fiber failure	43.014	*	45
AS4/3501-6	$[90_2/0_2/90_2]$	0.762	Fiber failure	13.7	*	32
AS4/3501-6	$[90_4/0_2/90_4]$	1.27	Fiber failure	11.12	*	32
AS4/3501-6	$[90_6/0_2/90_6]$	1.778	Fiber failure	10.49	*	32
AS4/3501-6	$[0/90_4/0]$	0.762	Fiber failure	13.84	*	32
AS4/3501-6	$[0/90_8/0]$	1.27	Fiber failure	12.54	*	32
AS4/3501-6	$[0/90_{12}/0]$	1.778	Fiber failure	12.45	*	32
SD1 C70 55	$[(0_2/90_2)_S]_S$	15	Delamination Between skins	1.051	11.6	46
SD2 C70 75	$[(0_2/90_2)_S]_S$	15	Delamination Between skins	1.4	11.51	46
SD3 C70 75	$[(0_2/90_2)_S]_S$	25	Delamination Between skins	1.929	12.22	46
AS4/3502	$[\pm45/0/90]_{3S}$	3.21	Fiber Breakage	11.77	0.64	44
AS4/3502	$[\pm45]_{24}$	6.52	Fiber Breakage	21.92	0.91	44
AS4/3502	$[\pm45/0_6/\pm45/0_6]_S$	4.22	Fiber Breakage	17.33	0.55	44
AS4/3502	$[90]_{48}$	6.22	Fiber Breakage	6.05	0.42	44
AS4/PEEK	$[(\pm45)_2/0_4/90/\pm45/0_2/90]_S$	3.86	Fiber Breakage	16.95	0.95	44
AS4/PEEK	$[\pm45/90_6/\pm45/90_6]_S$	4.27	Fiber Breakage	14.12	1.13	44
AS4/PEEK	$[\pm45/90_6/\pm45/90_6/0]_S$	4.61	Fiber Breakage	17.37	1.24	44

* Not evaluated

3. Characterization of Impact Damage

Many different sources can cause damage in composites, such as static and fatigue loading, environmental factors such as moisture absorption and corrosion, low energy impact during manufacture and in service. The low energy impact can be potentially dangerous as it can produce extensive subsurface delaminations that are not visible on the laminate surface. It has been proved that the presence of internal damage causes substantial losses in strength and stiffness of the composite components [47]. The damage induced by low-energy impact is often a complex mixture of three principal failure modes, namely, delaminations, matrix cracking, and fiber failure as mentioned in the impact properties section.

The delamination patterns at each interface are different in size, shape, and orientation. Matrix cracks also propagate in different manners in each layer. To fully understand the damage state, not only should the surface damage be evaluated, but also the location and spatial geometry of all delaminations and transverse matrix cracks within the composite must be accurately determined. Residual properties of a composite after impact are a complex function of the depth of the damage, so that, an accurate description of the impact damage state is a prerequisite to reliable assessment of residual mechanical properties [48].

To get an accurate damage assessment in composite materials, many experimental techniques that can be classified into destructive and nondestructive means were developed. The destructive techniques such as de-ply method and cross sectional fractography are designed to visualize the characteristic internal damage state. The nondestructive methods involve detection, measurements of the size and location of damage state based on visual inspection and optical microscopy, tap testing, bond testers, laser holography, shearography, ultrasonic testing, X-radiography, infrared termography, and eddy current testing.

The following study addresses nondestructive techniques which are mostly used in marine and aerospace industry and rating of these inspection techniques is shown in **Table 3.**

3.1. Current Inspection Methods

3.1.1. Visual Inspection and Optical Microscopy

Visual inspection is the original method of NDT with the naked eye or with optical aids such as microscopes, magnifying glasses, boroscopes, etc.. and it is still the first steps carried out in the inspection of components and is usually followed by more sophisticated NDT methods [49]. The visual inspection is particularly useful for moving components made from laminated composites and sandwich structures, such as water impellers, helicopter rotor blades, turbine compressor buckets [50]. Visual examination techniques are limited to the detection of surface-breaking defects and gross damages. Their main advantage is that result can be readily interpreted by an inspector. With visual equipment being continuously updated and coupled with image processing equipment, visual inspection still has an important place in NDT and should not be ignored [51,52].

An optical microphotograph of a glass woven fabric **vinyl ester** matrix composite taken with the aid of transmitted light is shown in **Figure 5.** In addition to the extensive delamination observed in the central impact area, minute interface debonding occurred along the warp and weft directions of woven fabric in the surrounding regions near the back surface of impact, which contributed considerably to the total damage area of the laminate. It was found that the total damage area varied significantly depending on the fiber-matrix interface bond strength which was affected by silane coupling agent applied onto the glass fiber surface [53,54].

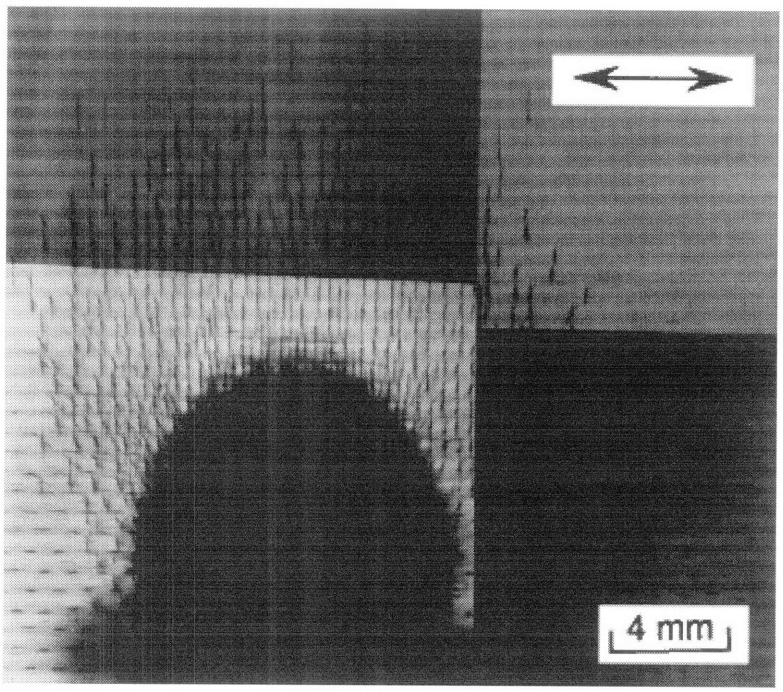

Figure 5: A magnified view of impact damage in a glass woven fabric vinyl ester matrix composite [53,54].

3.1.2. Tap Testing

This Technique has been commonly used for in service inspection because it does not require sophisticated, expensive equipment. This test involves tapping of thin composite laminate parts using a coin or a special tap hammer. The tap test relies on the different acoustic resonance of the loose upper layer compared to surrounding material, and thus is only sensitive to laminar-type flaws, including delaminations and debonds of fairly large area. Therefore, the disadvantages of this method are subjective interpretation, reduced sensitivity with flaw depth and complex flaw geometry, and an inability to calibrate effectively for either flaw size or depth. This means that the applications of thicker laminates and more highly loaded designs make this approach inadequate in many cases. Thus, it is considered not sufficient by itself for impact damage evaluation [50,55,56,57].

3.1.3. Ultrasonic Testing

Ultrasonic measurements are certainly the most commonly used inspection method to detect damage in composite structures. Ultrasonic testing methods use ultrasonic waves in the frequency range from 1 to 20 MHz. for material examination and internal flaw detection and sizing [51,52]. Ultrasonic systems benefited from visualization enhancing techniques which display results in a color coded C-scan format. Ultrasonic testing of composites with conventional equipment requires the use of a uniform layer of gel or water couplant between the probe and the material inspected.

Although this technique has many advantages, the inspection of honeycomb composites is difficult with ultrasound because the propagation of ultrasound is limited by the inconsistencies in the impedance between the air and solid walls of the cell, thus, causing high attenuation occurring in the material. Hence, non-conventional ultrasonic systems have been developed to try to overcome these limitations. Among these new systems we can find laser generated ultrasound [58,59,60] or fully automated equipment [61]. Even these expensive systems present some limitations in terms of portability and on-site inspection, the lowest reported impact energy detected in composites appears to be 12 J [61]. By the other studies the energies reported as 14 J and 15 J [62,63].

3.1.4. Radiography

X-Radiography is one of the most useful forms of NDE because it can be used effectively on very complicated structures, thus, it can provide detailed inspection especially where other methods are inapplicable [50,51,55,56,57]. X-Radiography is particularly useful for the detection of defects in bonded honeycomb core sandwich structures. The low density and

thin composite skins usually provide minimal interference so that X-rays can image the core material.

Because X-rays are weakly absorbed by graphite composites, low energy radiation has to be used. Using low kilo-voltage radiography for inspection of composites, the sensitivity and resolution of different film types were evaluated and the problems encountered were described [64]. Honeycomb core defects can be detected but radiographs are usually of poor resolution and image processing facilities are required to enhance the signal-to-noise ratio. Dye penetrants are often used and injected into the components inspected. The dye is detected by X-rays and is used to reveal the extent of delamination in honeycomb structures. However, it was shown that impact detection with X-rays, even with a dye penetrant, remains a difficult task [65]. In another research, very low detection rates were reported while using X-rays to inspect impacted composites [66].

3.1.5. Infrared Thermography

The physical basis of infrared thermography is well established as a standard non-destructive inspection technique. Important use of this technique is made in the aerospace industry of infrared thermographic systems to inspect composite materials [50,51,55,56,57]. Such systems present the advantage of portability and can be coupled to a computer for online automated signal interpretation. Infrared thermography is a non-contact method which measures and display variations in infrared radiation in real time allowing rapid scanning of large structures. Nevertheless, infrared thermography still remains an expensive technique when compared to the others. Moreover, it sometimes requires extensive image processing before a flaw can be accurately located due to poor signal to noise ratio. By the several experiments it

has revealed that the minimum energy of impact subject to change between 3.4 J and 13 J. A schematic diagram of a typical infrared thermographic inspection system is shown in **Figure 6** [67,68].

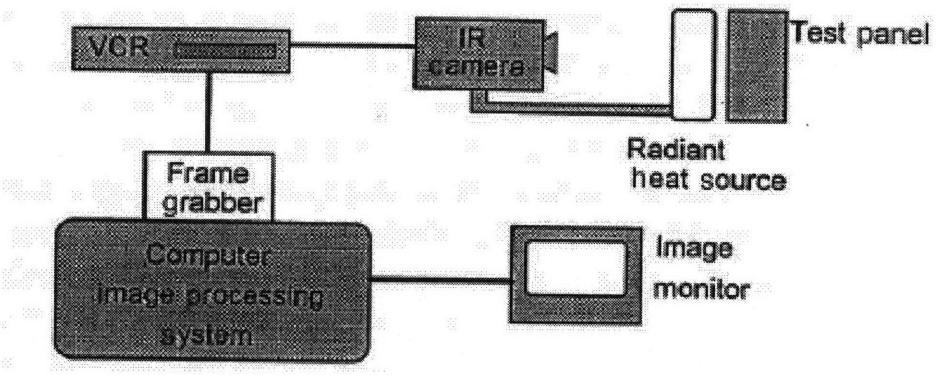

Figure 6: Schematic diagram of a typical thermographic inspection system [67,68].

3.1.6. Eddy Current Testing

Ultrasonic inspection was considered as the most reliable method until recently [58,59,60,61], however recent developments have shown that eddy current method can be used effectively and reliably as an inspection method for quantifying and detecting damages especially in carbon-reinforced composite materials. Using electromagnetic testing, cracks, disbonds, delaminations and variations in fiber orientation in graphite materials can be revealed. Some works on this field described the use of eddy currents to assess the structural integrity of conducting fibers in a non-conducting matrix [68,69]. Eddy current testing presents the advantage of being a reliable, low cost technique compared to othe techniques such as radiography, laser induced ultrasounds, infrared termography or shearography. In addition, there are no safety hazards associated to eddy current inspection.

Table 3: Rating of major inspection techniques [70,71].

Factor or Consideration	Visual Inspection	Acoustic Microscopy	Radiography	Infrared Thermography	Acoustic Emission	Laser Holography	Tap Test	Eddy Current Test
Damage Type Sensitivity:								
Delaminations	Good	Good	Fair	Fair	Poor	Fair	Fair	**
Fiber Breakage	Fair	Very Poor	Good	Poor	Poor	Poor	*	Good
Matrix Cracks	Fair	Very Poor	Good	Poor	Poor	Poor	*	Poor
Surface Defects	Very Poor	Poor	None	Poor	Very Poor	Poor	*	Poor
Skin-skin Disbond	Poor	*	Fair	Good	*	Good	Fair	*
Skin-core Disbond	*	*	Poor	Good	Poor	Good	Poor	*
Crushed Core	*	*	Good	Fair	*	Fair	*	*
Corroded Core	*	*	Fair	*	Poor	*	*	*
Damage Size Sensitivity	Fair	Good	Good	Fair	Very Poor	Poor	*	Fair
Damage Location Sensitivity :								
Distance from Surface	Fair	Good	Good	Poor	Very Poor	Very Poor	*	Poor

* Data not available

** According to [70] very poor, according to [71] fair

3.2. Nondestructive Testing of Marine Composites

Marine composites, as in the aerospace field require 100% inspection. Every method that is applied for aerospace composites is not applicable for marine composites. For instance, tap testing is not a good method for the evaluation of composite materials especially when the composite is thick [72]. The problems facing NDE inspection of composite marine structures are that large areas require to be inspected with 100% coverage, in a relatively short time frame, with a high degree of sensitivity. Traditional approaches to the non-destructive testing of marine composites have revolved around ultrasonics, however the low frequencies required to penetrate FRP have long wavelengths, which exclude the detailed sensitivity required [73].

3.3. Damage Assessment and Damage Tolerance

3.3.1. Damage Tolerance and Post Impact Residual Strength

Damage tolerance of composites can be defined as the ability of a structure to resist the formation of damage caused by certain forms of external load and the ability to sustain further service load. Dramatic loss in residual strength and structural integrity results due to the susceptibility of composite materials to impact damage. Even barely visible impact damage (BVID) can cause strength reductions of up to 50%, depending on the dominant damage mode residual strengths in tension, compression, bending and fatigue are reduced to varying degrees.

3.3.1-1. Residual Tensile Strength

Residual tensile strength normally follows a curve as shown in **Figure 7** [74]. In region I, no damage occurs as the impact energy is below the threshold value for damage initiation. In region II, once the threshold has been reached, the residual tensile strength reduces quickly to a minimum as the extent of damage increases. In region III residual strength has a constant value because the impact velocity has reached a point where clean perforation occurs, leaving a neat hole. In this region the tensile residual strength can be estimated by considering the damage to be equivalent to a hole, the size of the impactor. The minimum in region II is less than the constant value in region III because the damage spreads over a larger area than is produced at a higher velocity when the damage is more localized (resulting in a cleaner hole) [29]. As the fibers carry the majority of tensile load in the longitudinal direction, fiber damage is the critical damage mode.

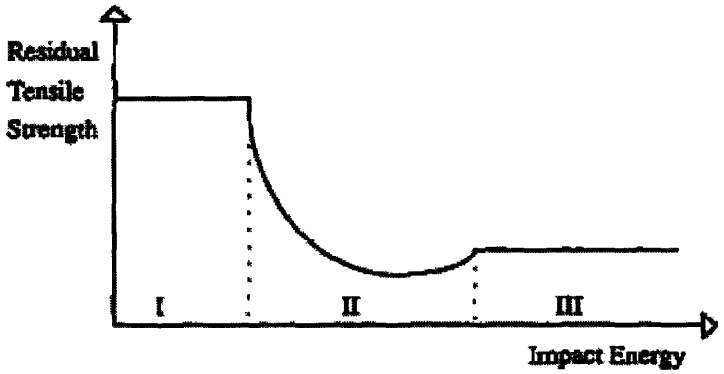

Figure 7: Residual tensile strength versus impact energy [74].

3.3.1-2. Residual Compressive Strength

Poor post-impact compressive strength (PICS) is the greatest weakness of composite laminates in terms of residual properties. This is mainly due to local instability resulting from delamination causing large reductions in compressive strength [29,75]. As delamination can be produced by low-energy impacts, large strength reductions in compression can occur for barely visible impact damage (BVID). Delamination divides the laminate into sub-laminates which have a lower bending stiffness than the original laminate and are less resistant to buckling loads [76]. Under a compressive load, a delamination can cause buckling in one of three modes [74]: global instability (buckling of the laminate), local instability (buckling of the thinner sub-laminate), or a combination of the above. The mode of failure generally changes from global, to local, to mixed mode as the delamination length increases.

PICS testing is often avoided due to the difficulty in providing a large enough gauge section to accommodate the damage. This necessitates the use of complex anti-buckling guides which must support the specimen to prevent global buckling, but at the same time must not prevent local instability [77].

3.3.1-3. Residual flexural strength

Less work has been done in this area, but it has been reported that both flexural modulus and strength decreased with increasing low-velocity impact energy for ductile specimens (glass/epoxy) while brittle graphite/epoxy exhibited no losses until complete failure occurred [74]. Flexural testing introduces a complex stress pattern in the specimen; therefore the effect of the damage on residual strength is less easy to analyze.

3.3.1-4. Residual fatigue life

It was reported that compression-compression and tension-compression are the critical fatigue loading cases, which would correspond to compression being the worst-case static loading condition [78]. The maximum residual compressive load divided by the static failure load (S) typically decreases from 1.0 to 0.6 in the range 1 to 10^6 cycles, depending on the initial damage size. The rate of degeneration is at its highest up to 100 cycles, and after 10^6 cycles no further degradation occurs; so S = 0.6 may be assumed to be the fatigue threshold. Therefore it is believed that fatigue loading is not a good way of characterizing residual properties.

3.3.2. Evaluation of Damage Tolerance

A precise definition of composite impact damage tolerance with the support of a standard test method is not available. Post-impact compressive strength has been adopted in the industry as a method to evaluate composite impact damage tolerance.

3.3.2-1. Compression After Impact

The compression after impact (CAI) is an empirical evaluation of the degradation of the compressive strength of the laminate due to out-of-plane impact. The CAI problem is considered to be one of the most important issues in the design of composite structures. It has been studied by many researchers, and several methods were used to determine the CAI [79,80,81,82,83,84]. CAI strength prediction methods are shown in **Table 4.**

Table 4: Prediction of CAI strength.

Composite Type	Approach	Model	Damage Zone	Reference
Laminate	Sublaminate Stability Method	Maximum Strain Criterion	Circular, Elliptical Sublaminate	[79],[80]
Laminate	Finite Element Method	Stress Redistribution and Failure Criterion	Circular Soft Inclusion	[81]
Laminate	Complex Potential Method	Point Stress Criterion	Elliptical Soft Inclusion	[82]
Sandwich Structure	Empirical Methods	Impact Region Stress Concentration	Elliptic Inclusion	[83]
Sandwich Structure	Semi-Empirical Methods	Impact Region Stress Concentration	Elliptic Inclusion	[84]

Among the above mentioned approaches, the most popular models are the sublaminate stability based methods although the details of the numerical modeling of impact damage in these studies may not fully agree with each other.

The accumulation of test data on many material systems from various researches has enabled some general conclusions as shown in **Table 5.**

Table 5: General conclusions.

Impact Type	Consideration	Conclusion	Related Figure	Reference
Low Energy	Compression and tension	Larger strength degradation in compression than tension	8	[85],[86]
Low Energy	Different resins similar fibers	Different resins showed significantly different characteristics in terms of impact energy	9	[87],[88], [89]
Low Energy	Resin toughness	Compressive strength correlates positively with maximum strain to failure of resin and interlaminar fracture energy	--	[88],[89]

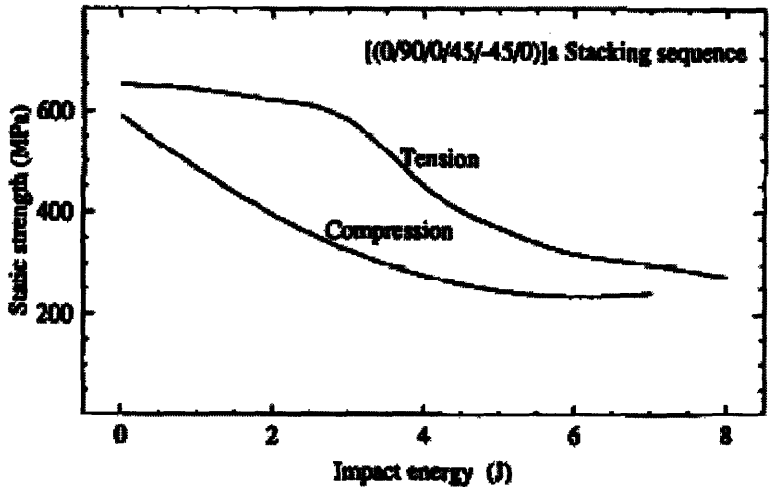

Figure 8: Post-impact tensile and compressive strength reductions of composite laminates [86].

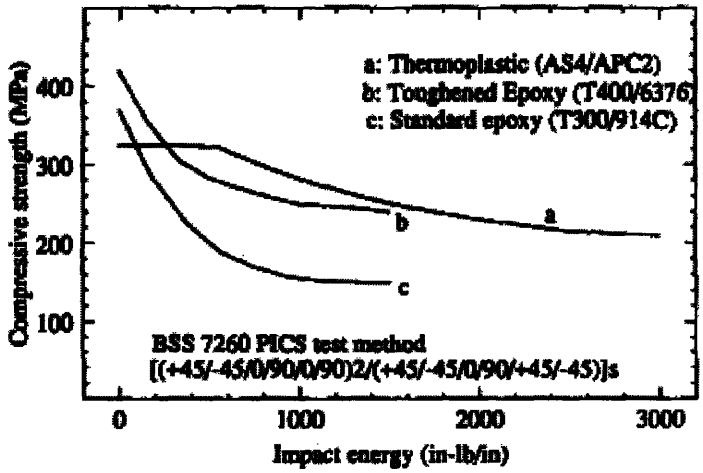

Figure 9: Dependence of compressive strength on resin systems [87].

3.3.2-2. Compression After Impact Tests for Laminates

Damage tolerance in laminates is usually studied by determining the effect of different impact energies on their residual strength and the compression after impact (CAI) test being the experimental test of components damaged by low energy impact. The damage tolerance of various lay-ups of thin carbon/epoxy laminates (1.6–2.2 mm thick) is examined by compression after impact (CAI) tests, using a testing device which adapts to the thicknesses of the specimens and does not require tabs nor any modification of the specimen geometry [90]. CAI tests must be carried out in a device that avoids global buckling of the impacted specimens, so that failure comes as the delamination progresses with the local buckling of the sublaminates produced by impact. Considering these requirements and trying to avoid the problems of other investigations, several devices were designed. One of the design is shown in **Figure 10 (a)** which is mostly used by aeronautical groups such as Composite Research Advisory Group in Great Britain (CRAG), NASA and Boeing [91][92],[93]. It is adapted to the geometry of the impacted specimens used in the studies. After the CAI test of the specimens, compression–shear failure in the free area between the supported and the clamped zones, near the top loading plate is observed. CRAG, NASA and Boeing Tests are compared in **Table 6.**

Table 6: Comparison of testing conditions for three post-impact CAI tests.

Test	Material : Thickness/Lay up	Impact: Indentor /Support Conditions	Compression: Specimen Size	Loading	Loading Rate	Ref.
CRAG	2 mm (+45/-45/0/90)	indentor—Φ 10 mm Mass—as required Drop height—1 m Energy—as required Support— Φ 100 mm ring Clamped— Φ 140 mm	h=180 mm w=50 mm	End tabs recommended but other suitable end grips acceptable	Adjust to achieve failure in 30-90 s	[92]
NASA	6.35 mm (+45/0/-45/90)	indentor —Φ 12.7 mm Mass—4.5 kg Drop height—0.63 m Energy—28 J Support— Φ 127 mm square Clamped	h=254-317 mm w=178 mm	End Loading	1.27	[91]
Boeing	4 to 5 mm (-45/0/+45/90)	indentor —Φ 15.75 mm Mass—4.6 to 6.8 kg Energy—as required Support— Φ 127 x 76 mm Clamped at four points	h=152 mm w=102 mm	End Loading	0.5	[93]

Abbreviations: CRAG, Composite Research Advisory Group.

Another set-up is shown in **Figure 10 (b)**. It used two anti-buckling plates with a square central opening [90,94]. Failure in the specimen is by compression–shear in one of the free zones, between the loading and the anti-buckling plates. A third set-up, is shown in **Figure 10 (c)**. Each of two anti-buckling plates is modified by splitting it into two parts, an upper and a lower plate. The two rear plates are welded to the loading plates. Both halves have a rectangular opening in the middle that leave the central surface of the specimen free and do not modify the surfaces damaged by the impact [90]. The positioning and alignment of the specimen in the loading direction is ensured in the test device when it is placed in the hydraulic machine, by the union of each part of the rear anti-buckling plate to the loading plates as shown in **Figure 11.**

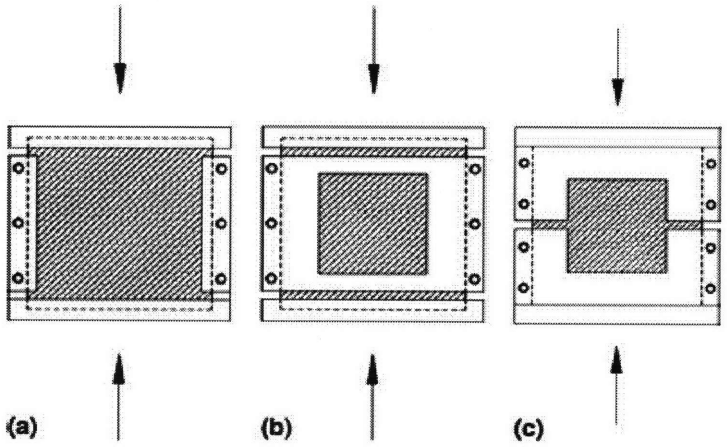

Figure 10: CAI devices [90].

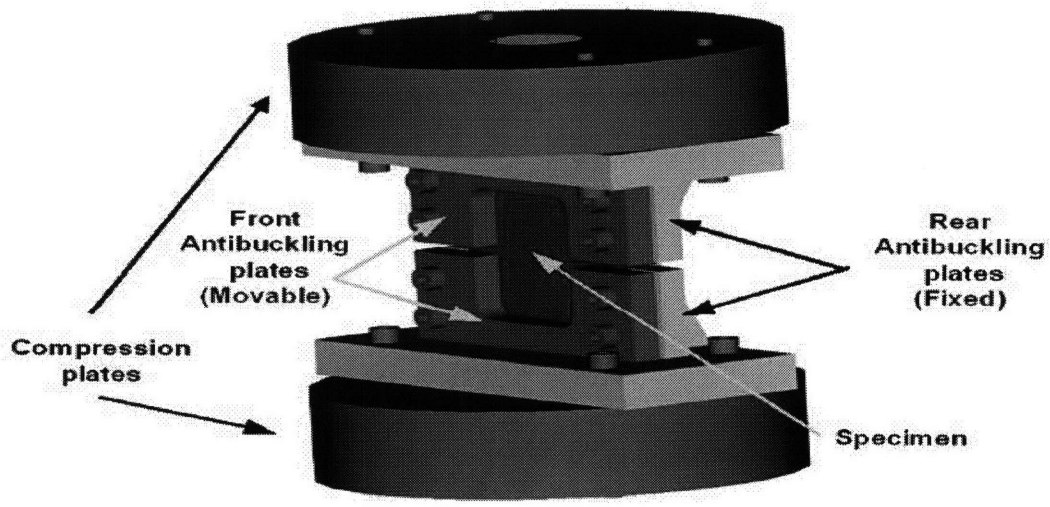

Figure 11: CAI set up [94].

3.3.3. Damage Assessment

3.3.3-1. Assessment of Impact Damage After CAI Tests

A toughened epoxy with Toroyca T800H carbon fibers (F924C) and PEEK with AS4 carbon fibers (APC2) were investigated for the damage assessment after compression after impact (CAI) test [87]. Delamination damage width plotted as a function of incident impact

energy as shown in **Figure 12 (a)**. The absorbed energy at damage initiation has been plotted on the energy axis to indicate the threshold below which delamination should not occur. The increase in damage width with increasing impact energy was much more rapid for F924C. 40 mm damage was reached at ~4 J for F924C , APC-2 has only reached 15 mm damage width for the same incident energy. The damage did not extend far outside the 40 mm diameter for F924C so that above 4 J the F924C curve leveled off. A similar response would be expected for the APC2 if the impact energy was further increased. It is clear that the scatter in the data is much greater for the APC2 than for the F924C.

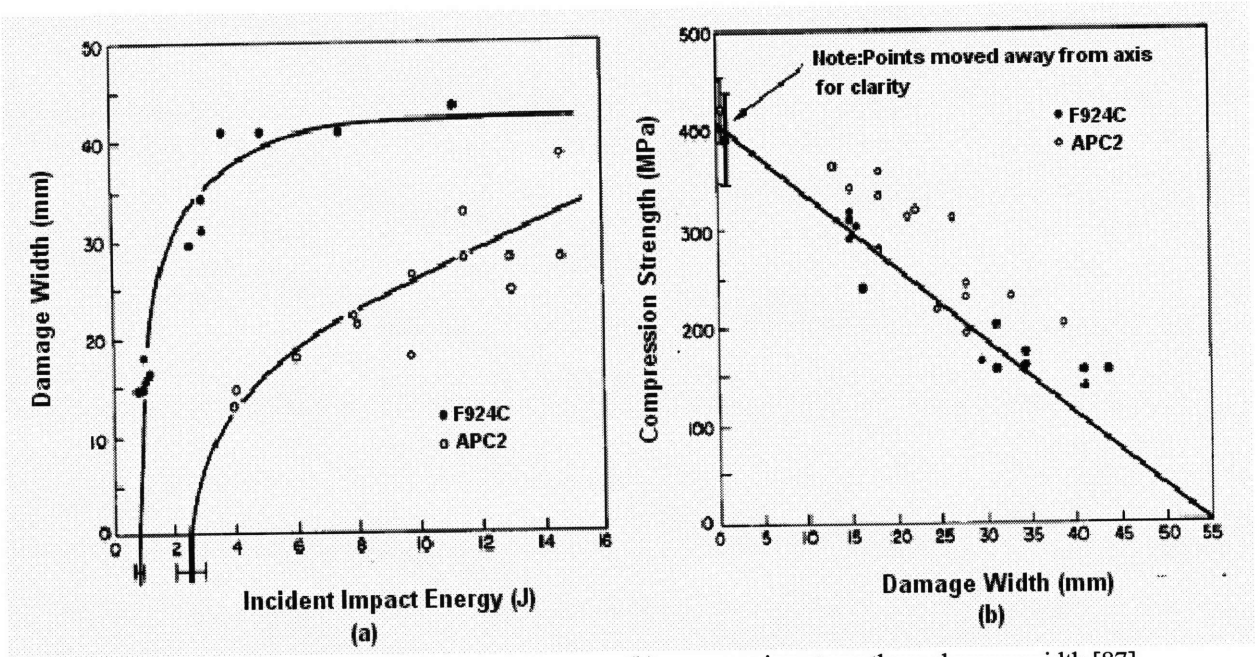

Figure 12: (a) Damage width vs. incident impact energy, (b) compression strength vs. damage width [87].

Figure 12 (b) showed the post impact compressive strength (PICS) of the two materials plotted against damage width as measured using the ultrasonic C-scan. Although the scatter was quite high there was a clear indication of a link between the residual strength and damage width. Furthermore, differences between the two materials were much reduced, the indication being that

APC2 performed only slightly better than F924C during the compression test. The diagonal line in **Figure 12 (b)** represented the strength reduction which would be expected if the loss in strength were simply due to a decrease in the cross-sectional area of the specimen able to carry load (the net section strength reduction line (NSRL)).

The triangular area formed by the axes and this line was regarded as a notch-sensitive zone while the area above the line represented a notch-insensitive zone. For the F924C material the points lay very close to the NSRL for damage widths up to 35 mm. For larger damage widths the points lay above the line indicating that the strength did not reduce to zero when the damage has spread all the way across the specimen. This was expected, as the material on either side of the delamination could still support load. The data points for APC-2 lay almost exclusively above the NSRL, indicating that the material was notch-insensitive in this loading mode for this type of damage.

3.3.3-2. Comparison of Low- and High-velocity Impact Loading

Carbon fiber reinforced plastics (CFRP) manufactured from XA-S fibers and epoxy resins were investigated under low- and high-velocity impact loading [1]. The variation of delaminated area (as measured from the C-scans) for both types of impact loading with energy for the 16 ply (0°, +45°) CFRP composite is shown in **Figure 13**. The overall level of damage increased rapidly with increasing energy, high velocity impact precipitating a greater level of impact damage for a given incident energy.

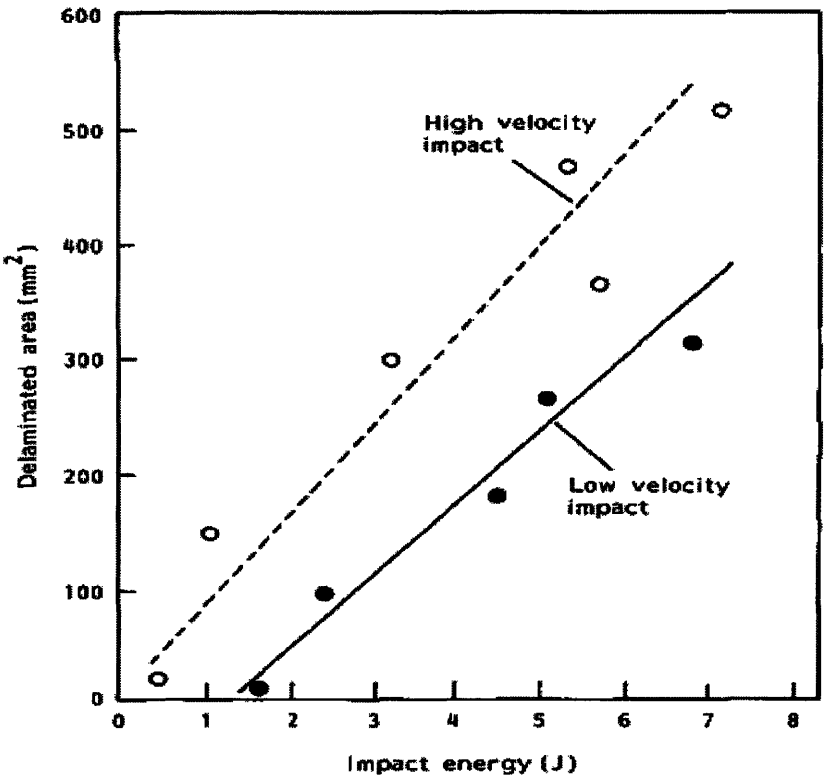

Figure 13: The variation of delaminated area with impact energy after high- and low-velocity impact loading [1].

After impact loading, residual strength analysis was done for the same composites. The variation of the normalized tensile strength after high- and low-velocity impact with incident energy for the eight and 16 ply (0°, +45°) composites is presented in **Figure 14 (a) and (b).** In all cases the curves exhibited the same general form. At low incident energies there appeared to be no reduction in the load-carrying capability of the composites. Measurable reductions in residual strength were first noted at the onset of fiber fracture; i.e., the destruction of the main load-carrying component of the material. The residual tensile strength then continued to drop rapidly until the target perforation threshold was reached at which point damage was extensive. At energies in excess of the perforation limit damage became more localized and the residual strength began to rise slowly.

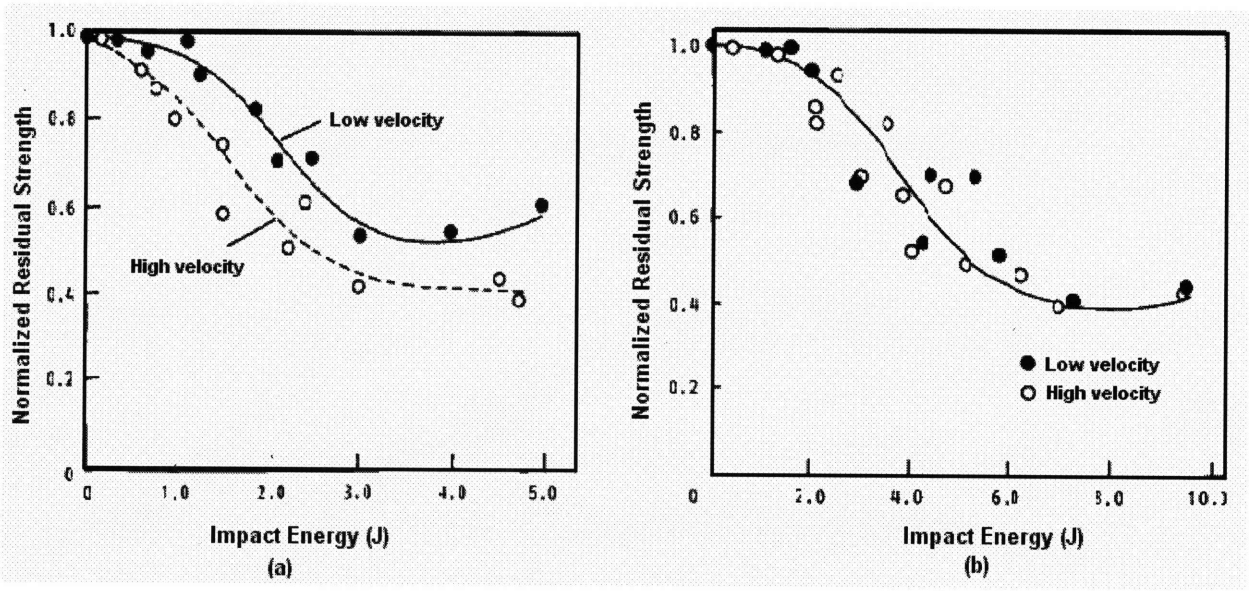

Figure 14: The variation of the normalized tensile strength after impact with impact energy, (a) for 8 ply (0°, +45°), (b) for 16 ply (0°, +45°), composites [1].

Considering first the eight ply laminate, **Figure 14 (a)**, it appeared that for a given incident energy, the residual strength after low-velocity impact was superior to that after high-velocity loading.

The data for the 16 ply laminate, **Figure 14 (b)**, indicated that the low- and high-velocity post-impact tensile properties were very similar. This effect was somewhat surprising since the overall level of damage detected after impact was greater in high-velocity loading. If similar tests were conducted on longer specimens where the elastic energy absorbing capability was greater it was believed that significant differences would be apparent between low- and high-velocity residual properties. Therefore, it was concluded that high-velocity impact loading is more detrimental to the tensile load-carrying capability than low-velocity impact.

3.3.4. Influence of Constituents on the Post-impact Residual Strength

3.3.4-1. Effect of Fiber Properties on Post-impact Residual Strength

In recent years a concerted effort has been made by the manufacturers of high performance fibers to improve both the short- and long-term mechanical properties of advanced composites. Much of this improvement has been achieved by increasing the strain to failure of the reinforcing fibers. The energy absorbing capacity of the fibers was identified as an important parameter in determining the level of damage incurred in a composite laminate. Often, materials that satisfy this condition also offer excellent residual properties. It was shown that this was the case for low and high strain carbon fiber composites [85]. An AS4 carbon fiber composite with a superior strain energy absorbing capacity than that of an XAS carbon fiber composite offered superior residual properties as seen in **Figure 15** [85]. This is not always the case, however. For example, if the stiffness of the fiber is very low and its strain to failure high, a composite containing these fibers will be capable of absorbing large amounts of energy but will exhibit poor residual compressive properties. In order to overcome this, hybrid composites are frequently used, combining the energy absorbing capability of low modulus fibers with stiffer fibers capable of resisting compressive loads [37]. As stated previously, many of the latest generation of composites are based on fibers with smaller diameters. Since the compressive strength of a composite depends upon the stability of the fibers, it would be expected that smaller diameter fibers would result in a material with poorer compressive properties. This indeed appears to be the case. However, reducing the fiber diameter increases the energy absorbing capability of the composite, resulting in lower levels of damage for a given incident energy. The reductions in plain compressive properties of the composite appear to be offset by the reduction in damage area.

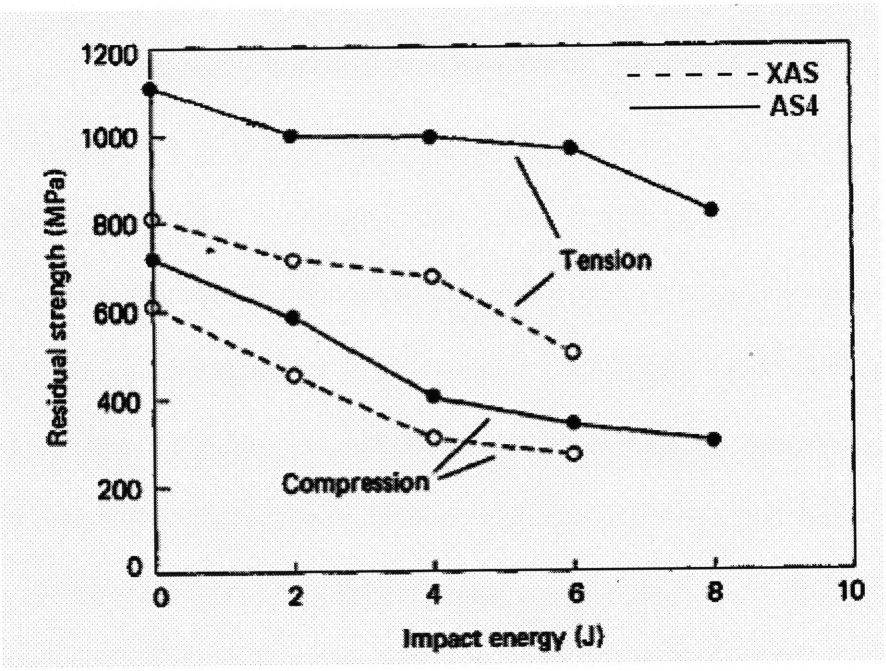

Figure 15: Variation of tensile and compressive residual strength with impact energy [85].

3.3.4-2. Effect of Matrix Properties on Post-impact Residual Strength

Impact-damaged composites are probably most sensitive to compressive loading since impact-generated delaminations tend to reduce the stability of the load-beating plies resulting in premature failure through buckling.

The residual tensile properties of toughened composites do not appear to be significantly better than those of standard epoxy systems as shown in **Figure 16** [86]. This results from the fact that composites with tougher matrices tend to be more notch-sensitive due to reduced splitting and delamination around stress concentrations such as notches or damage [95].

Toughening composites using elastomeric particles reduces the level of delamination and therefore enhances residual compressive properties as shown in **Figure 17** [86]. However, the presence of such inclusions often reduces the glass transition temperature of the matrix

material which in turn reduces the hot-wet properties of the composite. In many situations a compromise is therefore necessary.

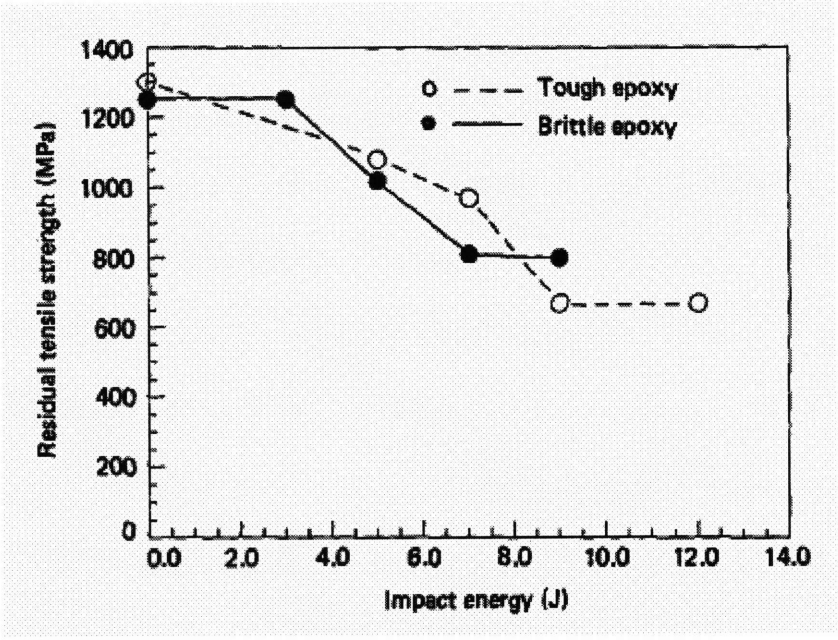

Figure 16: Variation of residual tensile strength with impact energy [86].

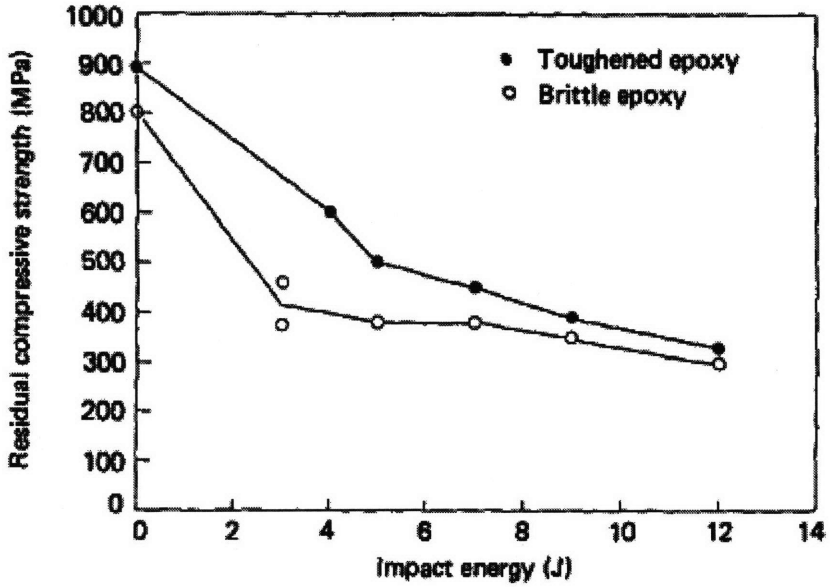

Figure 17: Residual compressive strength of toughened and brittle epoxy-based composites [86].

3.3.4-3. Effect of Interphase Properties on Post-impact Residual Strength

It has been shown that increasing the strength of the fiber/matrix bond increases the interlaminar shear strength (ILSS) of the composite until a plateau is reached beyond which point no significant increase is possible as shown in **Figure 18** [86]. Over this range of treatment levels the notched tensile strength falls dramatically. Increasing the ILSS in this way suppresses the formation of delaminated zones in the region of stress concentrations, rendering the material more notch-sensitive. Consequently, even though surface treatment of the fibers reduces the level of damage for a given energy, the increased notch-sensitivity of the laminate results in poorer residual tensile properties as shown in **Figure 19** [86]. Conversely, treating the fibers improves the post-impact compressive properties as shown in the lower part of **Figure 18**. Clearly, the level of surface treatment applied to the fibers in a multidirectional composite will depend upon the operational conditions the component will encounter. In general, a compromise is sought in which the fibers are given intermediate levels of treatment.

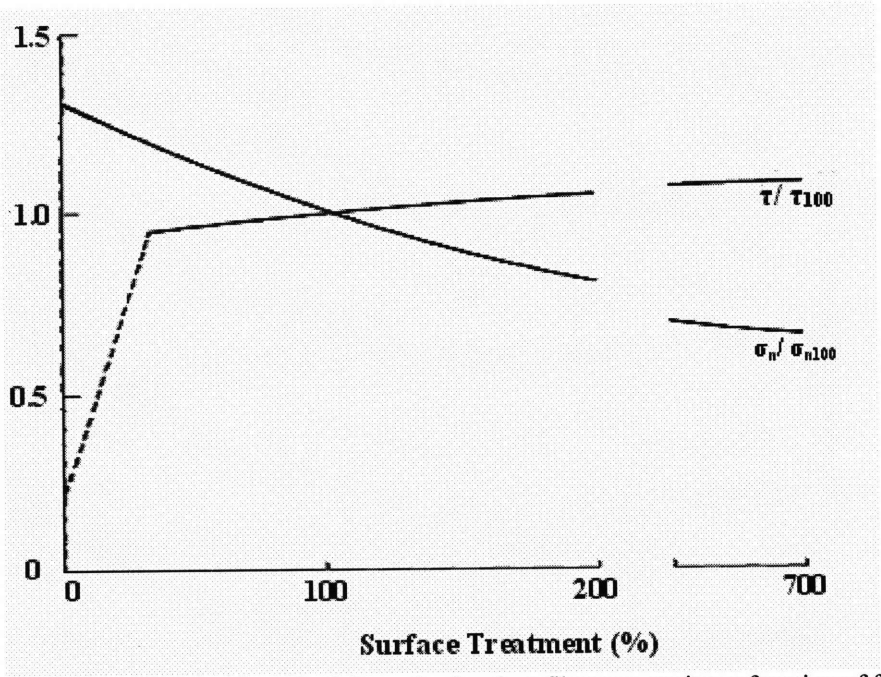

Figure 18: Variation of ILSS and notched strength of carbon fiber composites a function of fiber surface treatment [86].

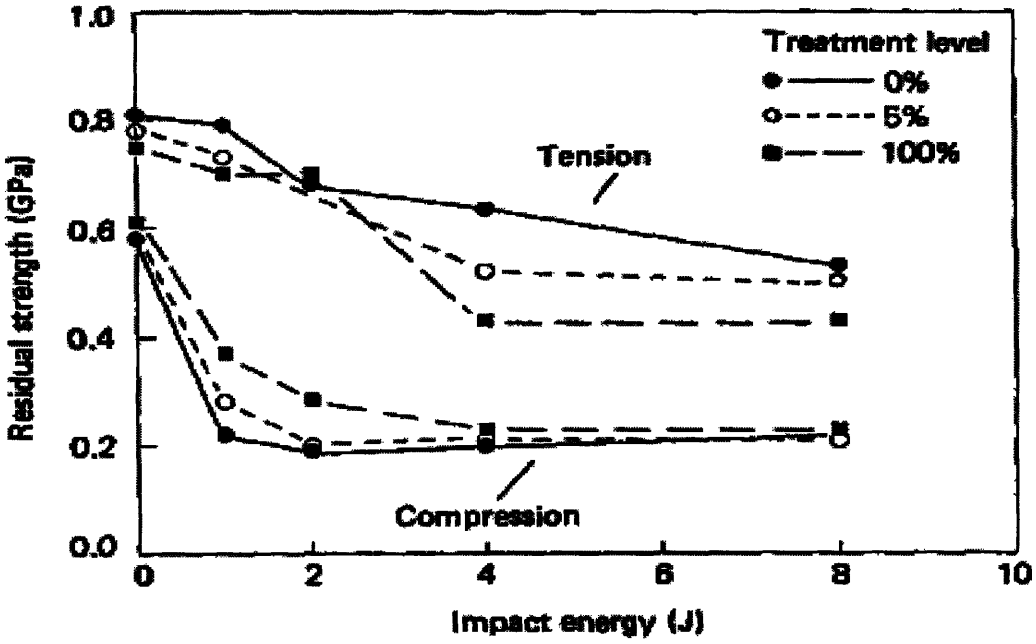

Figure 19: Residual strength of treated and untreated carbon fiber composites versus impact energy [86].

3.3.4-4. Effect of Specimen Width and Damage Size on Post-impact Residual Strength

The stress analysis indicated that interaction between finite specimen width and notch width influenced stress distribution around notch and finite width effect became significant for large ratio of notch width to specimen width. Moreover, for infinite laminate, the stress gradient was different for different notch sizes. Large stresses were localized more closely to the edge of a small notch than a large notch. Therefore, specimen and notch widths play critical roles in the compression and tension tests of notched laminates [96].

Compared with damage width, the dent diameter has little effect on CAI performance as it is within some range. This observation coincides with the test results of notched laminates. It was indicated that the residual strength of the notched laminates was hardly affected by notch shape [97,98]. This is believed to be due to damage zone near the edge of the notch.

Consequently, this damage zone significantly reduces the effect of the notch shape on stress distribution and, thus the notch size parallel to loading direction has no significant effect on notched laminate strength. For impact damaged laminates, a similar result can be expected.

Most of the previous investigations concerned the effect of various parameters, such as damage area, impact velocity and energy, impactor size and shape, and specimen support, etc. on residual strength. The recent studies show that all their effects on residual strength can be explained only by one parameter, i.e., damage width. The damage width is the most important factor governing CAI performance [99].

3.3.4-5. Effect of Fiber Stacking Sequence on Post-impact Residual Strength

The role of the fiber stacking sequence plays a significant role in determining the residual properties of impact damaged composites. Much of the work published in the literature concerns the residual compressive properties of damaged composites since this is considered to be the most critical form of loading condition. Certain conflicts may exist, when considering the optimum fiber stacking sequence for residual compressive strength. It was suggested that for improved post-impact residual strength the +/-45° fibers should be located on the outermost surface of the composite [100]. This may not be an ideal stacking sequence for stability in compression. Stiffer laminates, for example, those with surface 0° fibers, are better suited to in-plane compressive loading. Nevertheless, in another work [101], it has been shown that an APC2 $(0_2°, +/-45°)_{2S}$ laminate offers inferior properties to those of a $(+/-45°,0_3°,+/-45°,0°)_S$ plate, as shown in **Figure 20.**

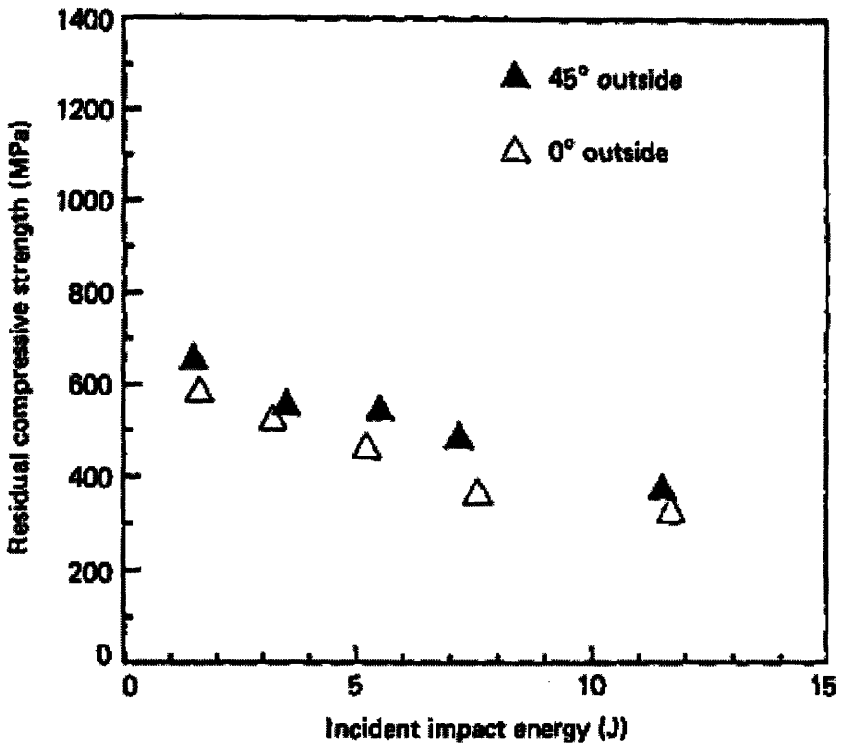

Figure 20: Effect of placing 45° plies on the outer surface of a 16-ply carbon fiber/peek laminate [101].

The use of woven +/-45° fabrics in (0°, +/-45°) laminates served to reduce the overall level of delamination under impact loading [102]. The subsequent residual strengths of the mixed-woven composites were superior to those of the standard material manufactured from unidirectional plies as shown in **Figure 21**.

Similar improvements in residual strength have been noted following impact on stitched carbon fiber composites [103]. Compression after impact tests on a number of AS4/3501-6 laminates [103] showed that stitched laminates offered residual strengths up to 100% greater than their unstitched counterparts. One of the disadvantages of this process is that the undamaged compressive strength of the material is reduced by up to 20% [103].

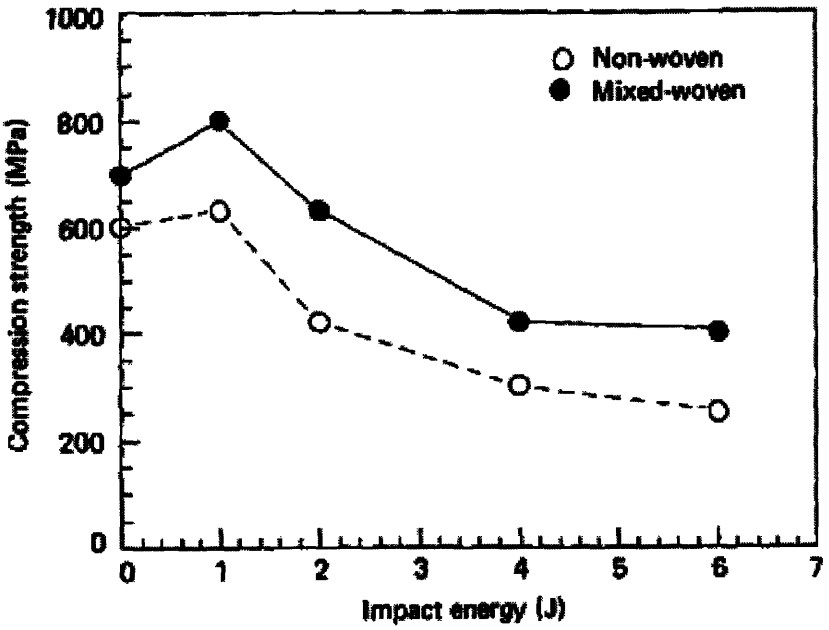

Figure 21: Effect of replacing the +/-45° plies in a 16-ply (0°, +/-45°) CFRP composite with a woven fabric [102].

4. Impact Resistance and Response

Impact resistance can be defined as the ability of a material to absorb energy during fracture. The total fracture energy absorbed by a material during impact should correspond to the amount of damage in one or more modes of rupture. The higher the energy absorption, the tougher the material. When dealing with laminated composites, this rule is complicated, since laminated plates have a unique failure mechanism of delamination.

If the measure of toughness is the compression strength or buckling load after impact, then delamination is probably the most devastating failure mode. Therefore, it is necessary to specify both the type of damage and the absorbed energy when considering impact resistance [3].

Failure modes that involve fracture of the matrix or interphase region result in low fracture energies, whereas failures involving fiber fracture result in significantly greater energy dissipation. The relative energy absorbing capability of these fracture modes depends upon the basic properties of the constituents as well as the loading mode. Typical fracture energies for a number of continuous fiber composites are given in **Table 7**.

Table 7: Fracture energy absorbing capability of various continuous fiber composites for different failure modes.

Failure mode	Material	Fracture energy ($kJ \cdot m^{-2}$)	Reference
Delamination	T300/epoxy	0.1	[104]
	IM6/PEEK	2.2	[105]
	E-glass/**vinyl ester**	0.43	[106]
Fiber pull-out	CF/polyester	26	[107]
	CF/bismaleimide	800	[108]
Debonding	CF/epoxy	6	[109]
Splitting	Type II CF/epoxy	0.1-1	[110]
	AS4/PEEK	3.8	[89]
Transverse fiber fracture	Treated CF/epoxy	20	[111]
	Untreated CF/epoxy	60	[111]
	AS4/PEEK	128	[89]

Abbreviations: CF, carbon fiber.

4.1. Methods for Improving Impact Damage Resistance

There are many methods to improve impact damage resistance of composite materials. The details of these techniques, and the resulting interlaminar fracture resistance and impact performance of the modified composites are discussed below.

4.1.1. Modification of Thermoset Resins

The low-velocity impact resistance of a resin composite is, to a great extent, controlled by the resin toughness. The ability of the resin to undergo large plastic deformation during an impact event is essential to achieving improved damage resistance of the composite. Better resistance to delamination and matrix cracking achieved with a tougher resin leads to improved impact resistance. It was demonstrated that, compared to more brittle carbon epoxy composites, carbon-PEEK composites exhibited significantly less extensive delaminations and, therefore, their compressive strengths after impact were much higher [110,112].

In general, improvement in interlaminar fracture toughness of CFRPs due to toughened resins is disappointing, although rubber modified epoxies display up to a twenty-fold improvement in fracture toughness of the bulk resin. Rubber modified epoxies and high performance thermoplastics have higher resistance to impact damage than unmodified thermoset resins [113]. Furthermore, the residual strength is substantially higher for the composites containing modified resins and thermoplastics than the unmodified counterparts for a given impact energy [113,114], as shown in **Figure 22**.

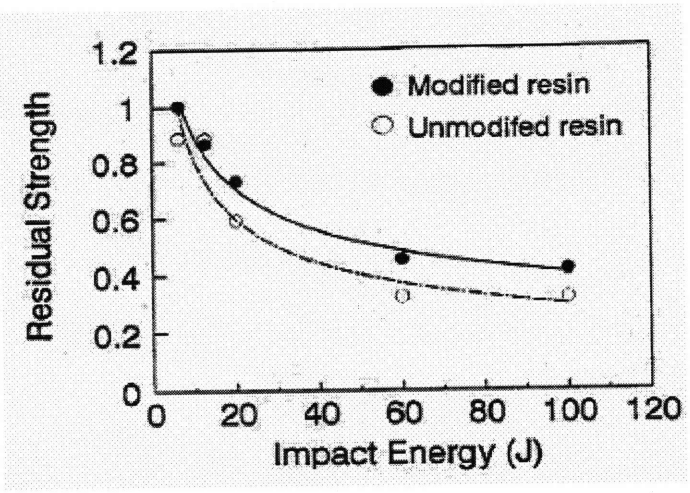

Figure 22: Normalized residual flexural strength as a function of impact energy [115].

4.1.2. Interleaving Technique

The interleaving technique is based on various crack arrest concepts where integral crack arrester strips were placed in damage-prone regions to enable the composite to sustain static and dynamic critical loads [116]. In subsequent studies, soft, ductile, and tough strips of adhesive layers were interleaved between delamination-prone layers to suppress the onset of free edge delamination of CFRPs due to in-plane axial loading [117, 118]. A configuration of a laminate with interleaved layers is shown in **Figure 23**.

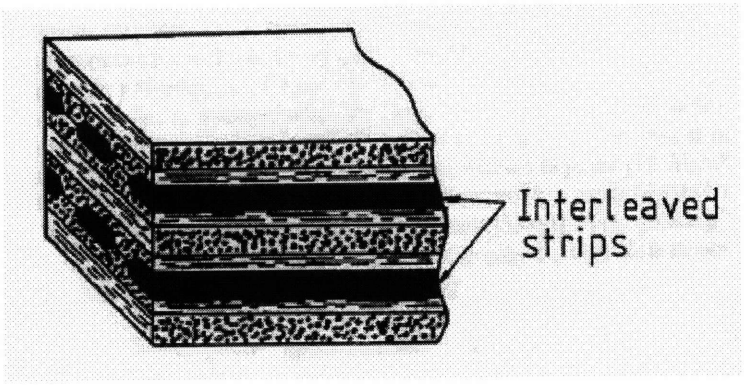

Figure 23: Configuration of a laminate with interleaved layers [117].

Interleaving has been shown to significantly improve the impact resistance of graphite epoxy and graphite bismaleimide composites [119,120], as manifested by an increase in residual compressive strength after impact. The shear failure strain of the interleaf resin has been identified as a key parameter in the impact damage tolerance improvement [119, 120,121]. The adhesive layers in composite laminates also effectively suppress delamination up to very high impact velocities and help reduce stress concentrations.

The role of the interleaves under impact loading is to alter the failure modes by allowing the transverse and delamination cracks to be arrested upon reaching the interleaved strips. The delamination area as a function of impact energy, as shown in **Figure 24**, demonstrates clearly the major advantage of the interleaved strips. These studies serve to demonstrate the advantages of utilizing the interleaving concept to improve composite toughness. However, the material variables that dictate the composite toughness need to be defined and optimized.

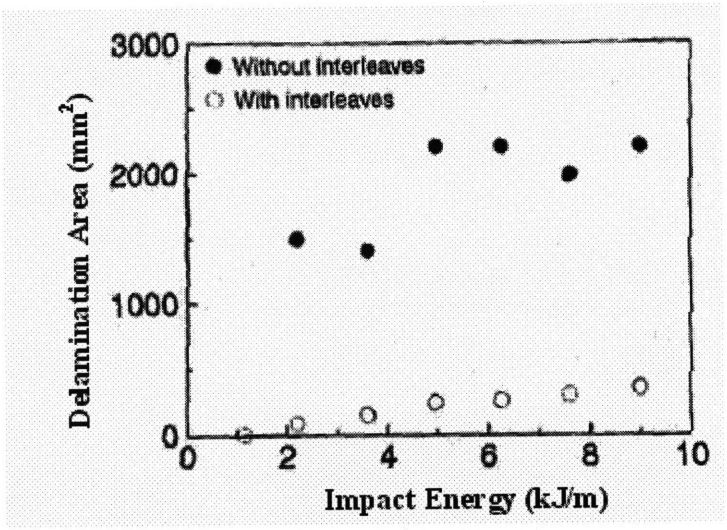

Figure 24: Delamination area as a function of impact energy for AS4/1808 CFRPs with and without interleaved strips [121].

Thermoplastic interleaves were found to be more effective than thermoset counterparts due to their higher energy absorption capability. Further, the interleaved strips made from ductile short fibers and an adhesive provided an additional energy absorption source during interlaminar fracture because of the toughening mechanisms associated with the fibers, such as interfacial debonding and subsequent fiber pull-out [122]. **Table 8** shows improved interlaminar fracture toughness due to interleaved adhesive layers.

Table 8: Mode I and Mode II interlaminar fracture toughness of CFRPs containing interleaved adhesive layers [122].

Types of Adhesive Layer	Adhesive Thickness (mm)	G_{IC}^{c} (kJ/m^2)	G_{IIC}^{c} (kJ/m^2)
Tuff-ply	0.04	0.444	1.15
Tuff-ply	0.08	0.575	1.7
Tuff-ply	0.11	0.754	2.61
FM® 73	0.12	0.975	1.84
FM® 300	0.1	1.14	1.77
FM® 300	0.26	1.47	2.23
FM® 300	0.3	1.27	2.01
FM® 300	0.68	1.48	2.32
FM® 300	1.1	1.78	1.65

4.1.3. Hybrid Fiber Composites

There are many studies regarding the improvement of impact performance of CFRPs by hybridizing with glass and aramid fibers [123,124]. Most of these studies are concerned with enhanced energy absorption capabilities mainly based on Charpy impact tests. Although widely accepted by relevant industries for easy specimen preparation and simple testing, these tests are not particularly suited to thorough characterization of impact performance of composite laminates as the loading geometry does not represent the end-use application of the composite structures [125,126].

In recent studies, with the development of ultra high molecular weight polyethylene (UHMWPE) fibers which have advantages of high ductility and light weight, the potential of incorporating polyethylene fibers into brittle carbon fibers has been extensively investigated. The strain energy absorption capacity of the fiber is one of the dominant parameters which dictate the impact damage resistance of a composite [1]. Significant improvement in damage resistance and damage tolerance was demonstrated in terms of the maximum load sustained, energy absorbed, and residual strength after impact [126,127,128]. The stacking sequence and the interfacial adhesion in hybrid laminates were found to play a critical role in controlling the plastic deformation and delamination under impact loading. The increase in energy absorbed and maximum load with increasing volume content of polyethylene fibers are shown in **Figure 25**.

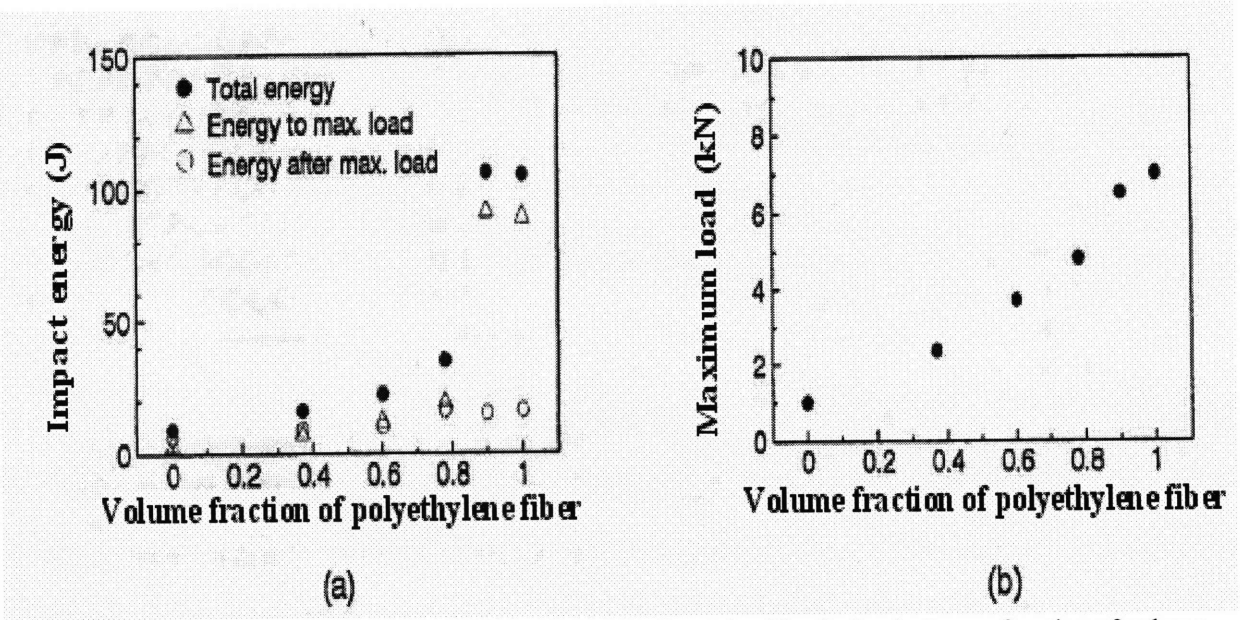

Figure 25: (a) Impact energy absorbed and (b) maximum load sustained by the laminate as a function of volume fraction of polyethylene fibers [128].

In these tests mentioned above, impact behavior was determined with a Dynatup model drop-weight facility and the specimens were impacted with an impactor nose tip of 1.27 cm in diameter and dropped through 1.5 m height. No penetration was observed in any laminates

containing more than three layers of polyethylene fabrics, except when they were loaded at relatively high rates and at low temperatures. The penetration resistance of hybrid laminates was found to be dictated by the strength and ductility of the polyethylene fibers [127]. Good adhesion at the polyethylene fiber-matrix interface was detrimental to the impact performance.

The residual flexural strength measured after controlled impact is presented in **Figure 26**. Composites containing polyethylene fibers treated with chromic acid resulted in a substantially greater reduction in strength than those with untreated fibers, especially at a high impact energy level. For a given damage area the residual strength of the composite with untreated polyethylene fibers was superior to that of treated fibers within the data scatter. The implication of these findings is that for a given impact energy level, the treated fibers were more susceptible to intensive local damage than the untreated fibers, which, in turn, had a harmful effect on the flexural load-carrying capacity of the laminates [126].

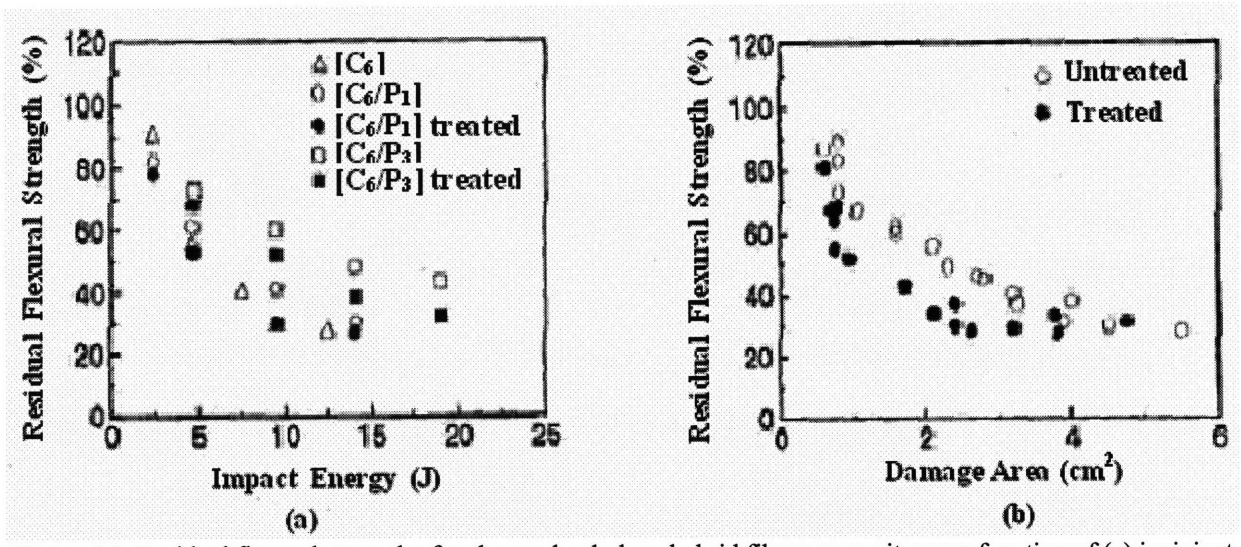

Figure 26: Residual flexural strength of carbon polyethylene hybrid fiber composites as a function of (a) incipient impact energy and (b) damage area [126].

4.1.4. Impact Performance of Woven Fabric Composites and Laminates Containing a Few Woven Fabric Laminae

Early studies of the impact of woven fabric composites involved the incorporation of woven fabrics at critical lamina interfaces such as [+/-45°] layers [1,102]. The woven fabric layers reduced the extent of impact damage by suppressing the initiation of delamination, and thus improved the residual strength. **Figure 27** presents a comparison of the residual compressive strength, indicating a marked reduction with increasing impact energy, the effect being greater for non-woven laminates than those with woven fabrics. **Incipient impact energy** is the energy required for damage initiation in the form of delamination, **incipient damage load** reflects the damage initiation in the form of delamination and the **maximum load** represents the peak load that a laminate can tolerate before undergoing major damage.

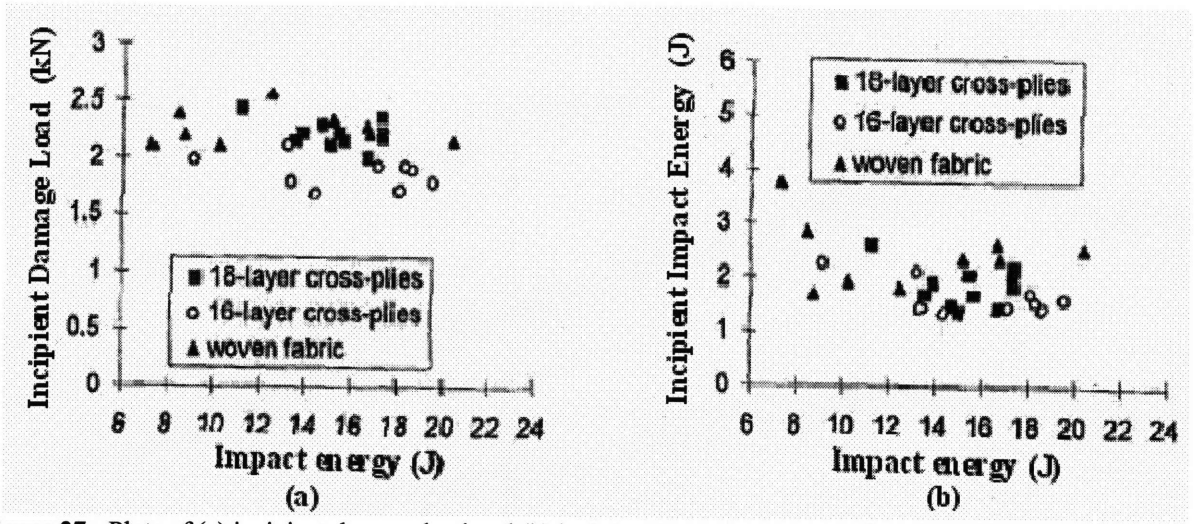

Figure 27: Plots of (a) incipient damage load and (b) incipient impact energy as a function of impact energy [129].

A comprehensive study was conducted using CFRPs made from woven fabrics and unidirectional cross-plies with two lay-up sequences [129]. These laminates of similar thickness should have similar static in-plane mechanical properties in the undamaged state. The load

displacement records obtained for a wide range of impact energy showed lower *maximum loads* [130] and larger total displacements for the woven fabric than for the cross-ply laminates. For the woven fabric laminates there were neither *incipient damage load* drops nor slope changes until the *maximum load* was reached, suggesting the initial damage occurred at the *maximum load*. There was no dramatic load drop after the maximum. In contrast, the cross-ply laminate exhibited a sudden small change in slope and clear *incipient damage load* drop in the ascending portion of the load, and the *maximum load* was followed by an instantaneous steep load drop toward zero for all energy levels studied. **Figure 27** depicts the relationship between the characteristic impact loads and energies generated from the load-displacement curves.

Maximum load was almost constant for the woven-fabric laminates, while for the laminates with cross-plies it increased consistently with increasing impact energy to a value much higher than that of the woven-fabric laminates at high impact energies, as shown in **Figure 28**. The lower maximum loads, but substantially higher plateau loads after the peak, along with the larger total displacement, were an indication of more ductile and compliant nature of the woven-fabric composites.

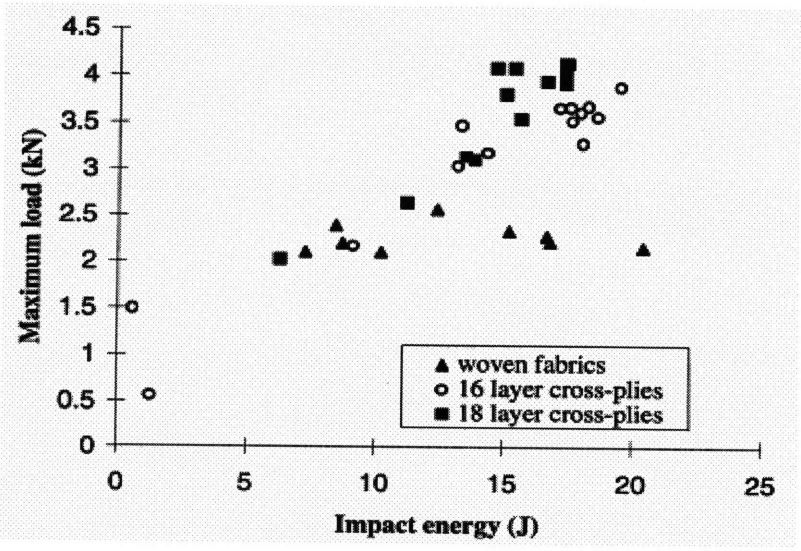

Figure 28: Plot of the maximum load as a function of impact energy [129]

The residual CAI strengths and the theoretical predictions based on a simple residual strength analysis are plotted in **Figure 29** [115,129] as a function of impact energy and total damage area on the surface, respectively. The residual CAI strengths were normalized by undamaged strengths measured before impact loading. Both the threshold energy and threshold damage that the material withstood without strength degradation were similar for the composites with two different fiber configurations, while the rates of strength degradation were much higher for the cross-ply laminates. This means that the reduction in CAI was much smaller for the woven fabric laminates than for those with cross-plies over the range of both impact energy and surface damage area.

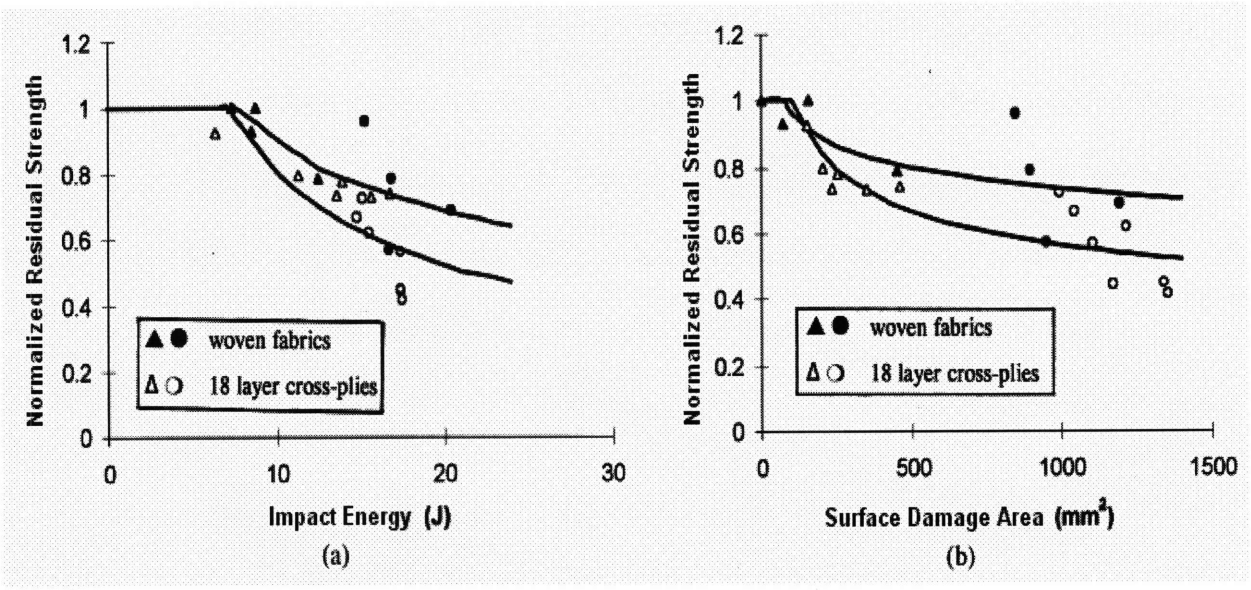

Figure 29: Plots of normalized residual compressive strength as a function of (a) impact energy and (b) surface damage area [115,129].

4.1.5. Stitched Composites

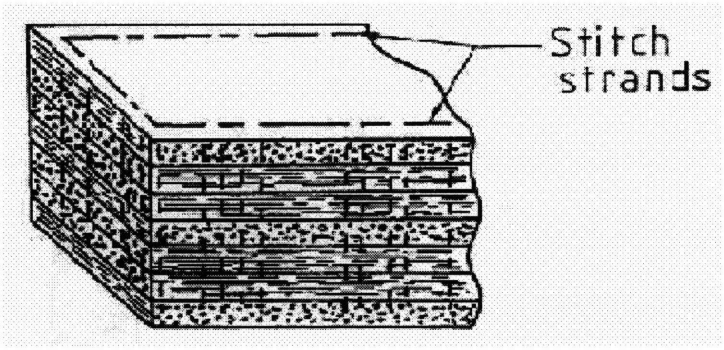

Figure 30: Schematic presentation of a stitched laminate [131].

The stitching technique has been widely accepted as a method to enhance the interlaminar fracture resistance and the impact damage tolerance of composites [131]. **Figure 30** shows schematically a stitched laminate. This technique was originally devised to reduce delamination using steel wires placed at ±45° angle through the laminate thickness. Later, aiming mainly at reducing the free-edge delamination and thus improving the in-plane tensile strength of CFRPs, aramid threads were stitched along the edges of the laminates. The stitches increased the mode I interlaminar fracture toughness by 85%, and at the same time enhanced the flexural strength by up to 30% for CFRPs fabricated from prepregs, as detailed in **Table 9**. The unstitched fiber composites normally failed by interlaminar shear, whereas the stitched counterparts failed predominantly by tension due to the high restriction of shear which was achieved by the through-thickness stitches [132].

Table 9: Effect of stitching on free-edge delamination in CFRP [132,133]

Stitching Details	Flexural Strength (MPa)	Mode I Interlaminar fracture Toughness (J/m^2)
No stitching	226	1880
6.35 mm at stitch free center zone	268	2150
11.1 mm at stitch free center zone	290	3450
14.3 mm at stitch free center zone	217	3250
19.05 mm at stitch free center zone	283	2170

Stitch density was found to be one of the most dominant parameters influencing the efficiency of stitching. There is a critical stitch density above which the improvement of interlaminar fracture toughness can be achieved. However, too high a stitch density is most often detrimental. The stitch density above an optimum value reduced significantly the in-plane strength and stiffness in compression and the interlaminar shear strength in bending [132,134].

A typical example is presented in **Figure 31** where the interlaminar shear strength decreases drastically above the optimal stitch density. The major reasons for these undesirable effects arise from the severe misalignment of longitudinal fibers due to the presence of stitch strands, the formation of a resin-rich region at the stitch holes, and localized in-plane fiber damage due to needle penetration [135].

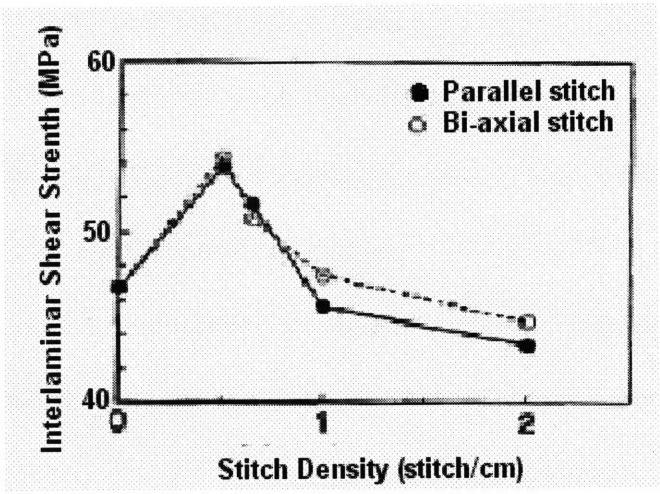

Figure 31: Interlaminar shear strength as a function of stitch density for glass fiber-epoxy matrix composites [132].

Impact data on stitched and unstitched CFRP composites containing varying constituent combinations showed that the damage area was less and the residual compression after impact

(CAI) strength was higher for the stitched CFRP composites. These results were valid only when the stitched density was below the optimum value, and the major damage mode due to low-velocity impact was delamination, but not when there was transverse fiber fracture. The damage area decreased continuously with increasing stitch density, before the optimum stitch density was reached as shown in **Figure 32** [136].

In some isolated cases, stitching had few beneficial effects, and even negative effects, on the impact resistance of CFRPs. The damage area and the residual CAI strength were more similar between the composites with and without stitches when orthotropic laminates were subjected to impact while loaded in axial tension. This disappointing result was mainly associated with excessive stitch density and unfavorable transverse shear failure of the stitched laminates.

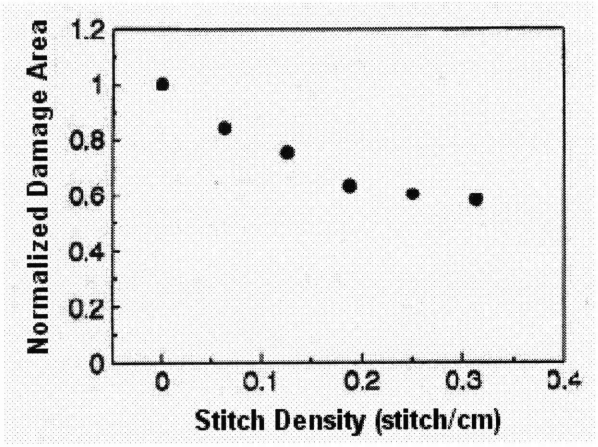

Figure 32: The relationship between damage area and stitch density [136].

The effectiveness of the individual techniques mentioned above is highlighted in **Table 10.**

Table 10: Comparison of methods of improving the impact damage tolerance of CFRPs.

Method	CFRP Composite System	% increase in G_{Ic}^{c} and/or G_{IIc}^{c}	% increase in CAI	References
Toughened Thermosets	IM7/X5255-3 AS4/907	45 (mode I&II) 250 (mode I), 95 (mode II)	55 90	[113] [137,138]
Interleaving Techniques	AS6/985 AS4/1808	20 (mode I) 20 (mode I), 140 (mode II)	50 100	[103] [121]
Hybrid Fibers	XA-S/LY556 Polyethylene	-	140	[126]
Woven Fabrics	T300/914 T300/913	- -	45 35	[102] [129]
Stitched Fibers	AS4/3501	150~2600 (mode I)	25~50	[139] [140]

4.2. Influence of Constituent Properties on Impact Resistance and Response of Composite Materials

4.2.1. Fiber

The role of the fibers in a composite structure is extremely important since they are responsible for bearing a significant percentage of the applied load. Many types of fiber are available. In aeronautical applications these mostly include carbon, glass, and Kevlar fibers. Within each of these categories, fibers exhibiting a wide range of mechanical properties are available. Unfortunately, it is often difficult to separate the effects of mechanical properties (such as strength and stiffness) from those arising from geometrical factors (such as fiber shape and diameter) and interfacial properties (such as the strength of the chemical bond between fiber and matrix).

In a study [141], in which the relative performance of a number of continuous fiber composites was examined, suggested that the Charpy impact resistance of S-glass and Kevlar fiber reinforced composites was over five times greater than that of a Modmor II carbon fiber-

reinforced composite. Charpy load/time traces of a number of materials was examined and it was shown that the curve corresponding to a high modulus strength (HMS) carbon composite was extremely brittle, failing catastrophically at maximum load [142]. E-glass and Kevlar 49 composites failed in a more progressive manner, indicative of energy dissipation through delamination, splitting, and other failure processes. Charpy load/time traces were quantified by defining a ductility index (DI), this being the ratio of the energies associated with the crack propagation phase (the area after maximum load) and the initiation phase (the area up to maximum load). The resulting ductility indices for the Kevlar-49, E-glass and HMS carbon/epoxy composites were 23, 0.4 and 0.0, respectively, clearly indicating the superior energy absorbing capability of the Kevlar fiber.

The low-velocity impact response of composites containing type I and II carbon fibers was compared [143,144]. In both cases it was demonstrated that the materials containing type II fibers (higher failure strength) offered superior impact resistance.

Izod impact tests were conducted on a wide range of systems to better understand the fundamental parameters controlling the processes of energy absorption and dissipation in composite materials [145]. It was concluded that flexure and interlaminar shear deformations were dominant energy-absorbing mechanisms in composites and that the area under the material's linear stress/strain diagram represented a useful approach for predicting the impact resistance of a composite. Essentially, composites with large areas under the stress/strain curve were more effective energy absorbers. **Figure 33** presented the experimental data plotted as a function of the energy absorbing capability of the fiber as determined by the energy under the static tensile stress/strain curve [146]. An examination of the data suggested a possible relationship between these two parameters, with materials containing fibers with a greater strain

energy absorbing capacity offering improved Izod energies. Therefore, it appeared that this technique formed a useful guide for assessing and evaluating the impact resistance of composite materials.

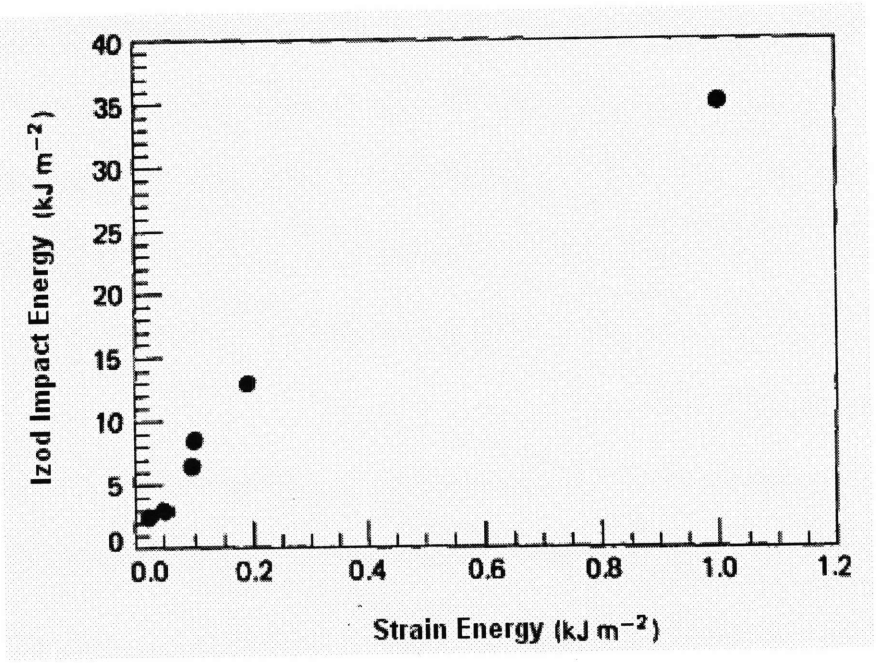

Figure 33: Variation of Izod impact energy with strain energy absorbing capacity of fibers [146].

Although the above approach was valuable for evaluating the impact resistance of a composite, a complete analysis should have taken energy dissipation into consideration in failure processes such as fiber/matrix debonding and fiber pull-out. Expressions were given for work associated with micro-mechanical fracture processes such as debonding and fiber pull-out [147]. The work for debonding was given as

$$W_d = \frac{\pi \cdot d^2 \cdot \sigma_f^{\,2} \cdot l_d}{24 \cdot E_f} \tag{1}$$

where d = fiber diameter, σ_f= failure strength of the fiber, l_d = length of the debonded zone and E_f= fiber modulus. The work to pull-out is given as

$$W_p = \frac{\pi \cdot d \cdot \tau \cdot l_c^2}{24} \quad (2)$$

where l_c = critical transfer length and τ=constant frictional shear stress.

It was concluded that post-debond fiber sliding is the primary energy absorbing mechanism in glass fiber composites, whereas fiber pull-out is responsible for much of the toughness in a carbon fiber composite. An examination of **Equation (2)** indicates a strong dependency of work to pull-out on fiber diameter. In theory, increasing the diameter of the reinforcing fiber should result in a composite with an improved resistance to pull-out and perhaps improved toughness [110]. Another study reported results that appear to support a fiber diameter dependence in continuous fiber reinforced composites [141]. However, the conclusions are based on differences between glass and boron fiber composites with different fiber volume fractions and are not, therefore, conclusive.

Fiber manufacturers have been improving the strain to failure of carbon fibers by reducing their diameter. Typically, the first generation of carbon fibers such as T300 and AS4 had diameters of 7-8 μm. Fibers such as IM6 have diameters of approximately 5 μm. By improving the strain to failure of the fibers in this way, the manufacturers have also improved the strain energy absorbing ability of composites and thereby improved their impact resistance. It was shown that the interlaminar fracture toughness of IM6/PEEK is superior to that AS4/PEEK [148]. Similar conclusions following low-velocity impact tests on these materials was drawn by Curson [149].

4.2.2. Matrix

The polymeric matrix in a fiber-reinforced composite serves to protect, align and stabilize the fibers as well as provide stress transfer from one fiber to another. In general, both

the stiffness and strength of the matrix are considerably below those of the reinforcing fiber. The fiber is therefore responsible for carrying most of the applied load in a composite component. The role of the matrix is nevertheless critical. For example, damage to the matrix such as impact-induced delamination can reduce the load-bearing capability of the composite by up to 50% [102]. As a result of this relatively poor behavior, much work has been undertaken in recent years in an attempt to identify the fundamental matrix properties that influence the impact resistance of composite materials. Since the first generation of matrix systems for advanced composites lacked toughness, a number of techniques have been developed to improve the toughness of these materials. These include:

- the use of plasticizing modifiers [110];
- the addition of rubber particles such as carboxyl-terminated butadiene-acrylonitrile (CTBN) [150,151] ;
- the addition of thermoplastic particles such as polyethersulphone (PES) and polyetherimide (PEI) [152];
- a reduction in the cross-linking density of thermosets such as epoxy resins [153,154];
- the use of thermoplastic matrices such as PEEK;
- the inclusion of thin, tough layers at ply interfaces [88,114].

Adding a plasticizer to Epikote 828 epoxy resin increased the Mode I fracture toughness by over two orders of magnitude [110]. When used as a matrix system in a carbon fiber composite, increases in toughness resulted; however, in this case the Izod impact energy was improved by only 25%. This disappointing transfer of toughness was explained by the fact that the Izod test induces crack propagation across fibers rather than between them.

High-velocity impact tests were conducted on a limited number of Modmor II carbon

fiber composites [155]. Their data suggested that the impact resistance of these materials did not depend upon the properties of the polymeric matrix.

In a more detailed analysis, the impact resistance of 24 modified and unmodified carbon fiber/epoxy composites was examined [151]. Their experimental analysis showed that both the level of damage incurred as well as the residual compressive properties of the laminates varied enormously. It was found that the brittle laminates tended to fail by extensive delamination, whereas the tougher systems failed in transverse shear near the impact location. It was concluded that the tensile performance of the neat matrix has a significant influence on the impact behavior of a composite structure. For improved impact resistance, the strength of the matrix should exceed 69 MPa and its strain to failure should be greater than 4%. Finally, in order to ensure adequate compressive strength, the shear modulus should be greater than 3.1 GPa.

To identify a link between matrix properties and composite fracture toughness, data from three sources were analyzed [150]. A definite correlation was identified between the resin Mode I fracture toughness and composite interlaminar fracture energy as measured by the double cantilever beam (DCB) specimen, as shown in Figure **34**.

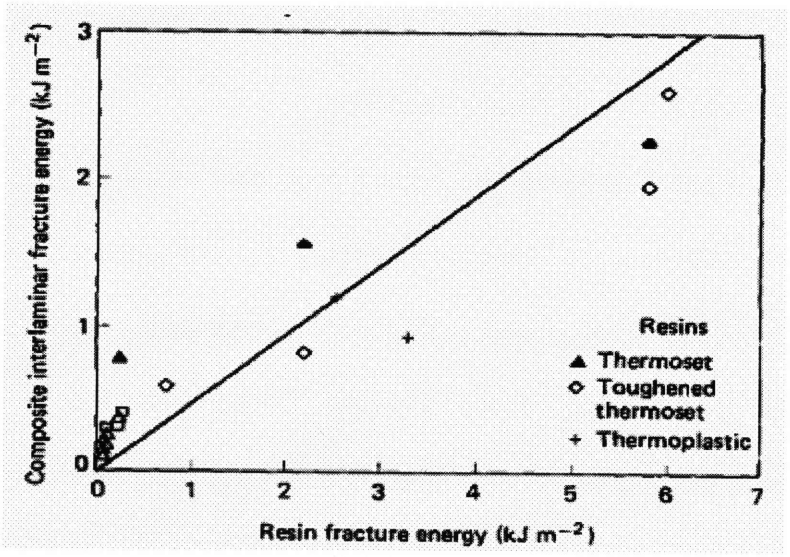

Figure 34: Variation of composite Mode I interlaminar fracture energy with resin fracture energy [150].

With brittle polymers, the resin toughness is fully transferred to the composite, whereas with tougher polymers the resin toughness is only partly transferred to the composite. In the latter it is proposed that the presence of the fibers restricts the crack-tip plastic zone size, thereby reducing the positive effect of the tougher matrices. This approach was extended by conducting Mode I, Mode II, and compression after impact (CAI) tests on a number of epoxy and bismaleimide-based carbon fiber composites [88,156]. It was demonstrated that no correlation existed between the Mode I interlaminar toughness and the CAI properties as shown in **Figure 35(a)**, whereas very good agreement was found between the Mode II resistance and residual compressive strength as shown **Figure 35(b)**. It is clear that the matrix in a flexurally loaded composite will be subjected to a large Mode II component and that the shear properties of the matrix will be important in determining the level of damage incurred. It is somewhat less clear why the residual compressive properties of the composite should be Mode II controlled since the failure process is undoubtedly complex, containing a significant Mode I component.

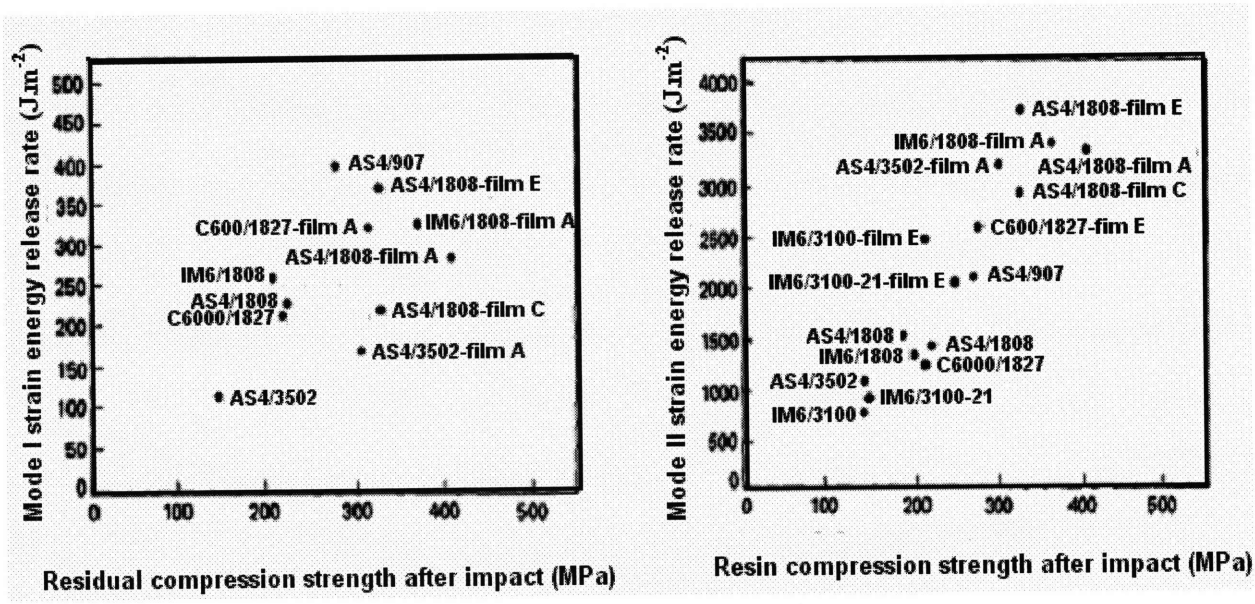

(a) (b)

Figure 35: Variation of residual compression strength after impact with (a) mode I and (b) mode II strain energy release rate [156].

Materials that satisfy the above condition and therefore offer superior impact properties include thermoplastic based composites and interleaved laminates. Considerable interest has been generated by carbon fiber-reinforced PEEK(APC2), a semi-crystalline thermoplastic composite [105,149,157,158]. Interlaminar fracture testing and impact loading have shown that this material offers excellent static and dynamic toughness and is capable of absorbing a considerable amount of energy while incurring only small amounts of damage [101,149,159]. Scanning electron micrographs of the fracture surfaces indicate extensive drawing and plastic flow [160]. Another advantage of this material is that its thermoplastic matrix allows rapid repair using fusion techniques such as the hot press technique [161]. Here, impact damage can be reduced or removed by simply heating the component to a temperature above the melting point of the matrix, reforming and cooling.

The high-velocity impact response of carbon fiber/PEEK has received very little attention.

Initial testing has suggested that its high velocity impact response is perhaps relatively poor. It was shown that beyond a certain velocity threshold, APC2 experienced a sudden drop in flexural strength [158]. Similar observations have been observed following ballistic impact tests on this material [101]. These observations suggest that care should be exercised when attempting to relate static properties such as interlaminar toughness and strength to characterize dynamic properties such as impact resistance.

Polymer interleaving involves the use of high toughness films or layers at ply interfaces in relatively brittle materials. The inclusion of such layers increases the laminate's interlaminar fracture toughness [156] as well as reduces the level of damage incurred for a given incident energy [162]. The load-bearing properties of damaged interleaved composites are significantly superior to those of conventional epoxy composites [162]. Interlayer technology is still in its infancy; however, early results are very favorable and the technique offers enormous potential.

4.2.3. Interphase

The strength of the bond between the matrix resin and the fiber reinforcement is a controlling factor in determining the mechanical performance of most polymer composites. In general, the surface of the fibers is treated by an oxidative process in order to improve the level of adhesion between matrix and fiber. Initially, this interfacial zone was considered as being a two dimensional surface with effectively zero thickness. However, studies have shown that this region is in fact three-dimensional, having its own distinct properties [163].

Studies have demonstrated that varying the level of surface treatment applied to a carbon fiber can change the mode of composite failure as well as many fundamental mechanical properties [110,163,164,165]. Composites with low levels of fiber surface treatment fail at

relatively low stresses when loaded transversely to the fibers, leaving smooth fibers on the fracture surface. Increasing the level of treatment applied to the fibers increases the transverse failure stress and failure occurs within the matrix; i.e., the interphase region is no longer the weakest link in the composite.

It was shown that improving the fiber/matrix bond strength in a carbon fiber-reinforced epoxy resulted in a four-fold increase in the incident impact energy required to initiate damage. At higher impact energies, the load-bearing properties of composites with surface-treated fibers drops dramatically until the perforation limit is reached [111]. In another study, it was demonstrated that the perforation threshold energy in a surface-treated composite is significantly lower than that of a similar untreated laminate [166].

This behavior has been explained by noting that the transverse fracture energy of a composite, a fundamental parameter for determining resistance to penetration and perforation, depends strongly upon the fiber/matrix bond strength [111]. **Penetration** is a macroscopic mode of failure enabling the impactor to completely penetrate the material. **Perforation** is the action of passing through the target structure of the projectile. Carbon fiber-reinforced epoxies with untreated fibers offer transverse fracture energies as high as 60 $kJ \cdot m^{-2}$ [111]. Transverse failure in composites with high levels of fiber surface treatment absorbs considerably less energy, with quoted transverse fracture energies being as low as 20 $kJ \cdot m^{-2}$ [111]. At energy levels above that required to achieve perforation, damage in a fiber-treated composite tends to be localized around the point of impact, often taking the form of a clean hole [165]. The post-perforation residual properties of treated composites are generally superior to those of untreated composites as shown in **Figure 36**.

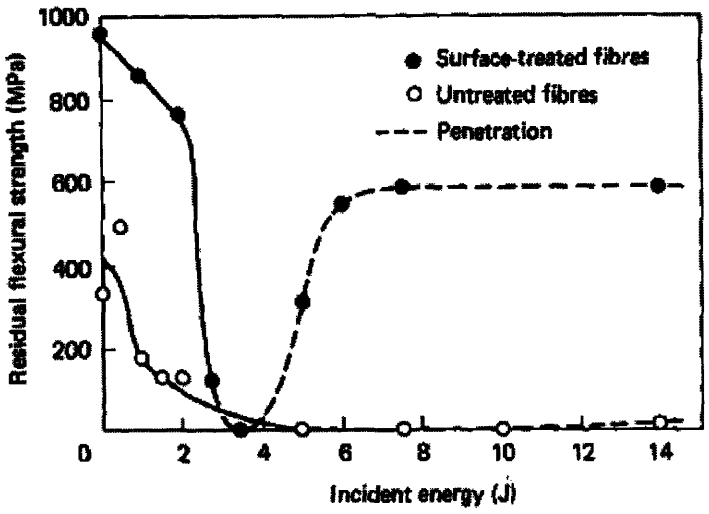

Figure 36: Residual flexural strength vs. impact energy for ballistically penetrated surface-treated and untreated carbon-fiber composites [111].

The impact resistance of T300/MY-720 carbon fiber/epoxy was enhanced by coating the surfaces of the fibers with a thin layer of CTBN rubber [167].

4.2.4. Fiber Stacking Sequence

Composite materials offer a unique advantage in that properties such as strength and stiffness can be tailored to meet specific design requirements through a careful selection of the fiber stacking sequence. It was shown that the impact resistance of composite materials also depends upon the specific order in which the plies are stacked [96,101,168,169,170]. For example, unidirectional composites having all their fibers aligned in one direction fail by splitting at very low energies and are therefore highly unsuitable for applications where impact loading might occur [110]. Following impact tests on a series of (0°, +/-45°) laminates, it was shown by several studies that composites having +/-45° surface plies offered a superior impact resistance and improved residual strengths [101,168]. It was suggested that the +/-45° plies increased the flexibility of the composite, thereby improving its ability to absorb energy

elastically [100]. Further, placing such plies on the surface of a composite serves to protect the load-bearing 0° plies against damage induced by the impinging projectile [100]. These ideas were supported by another study, in which instrumented Charpy tests on a series of multidirectional T300 carbon fiber composites were conducted [170]. It was demonstrated that (+/-45°) composites were capable of absorbing considerably more energy than (0°,90°), (0°,+/-45°) and (0°,90°,+/-45°) laminates.

The studies showed that damage initiation in a series of (+/-45°) laminates subjected to low-velocity impact depended upon the thickness and therefore the stiffness of the composite [12]. Initial failure in thin, flexible targets occurs in the innermost ply as a result of the tensile component of the flexural stress field. Damage in thicker, stiffer targets initiates at the top surface due to the contact stress field as shown in **Figure 37**.

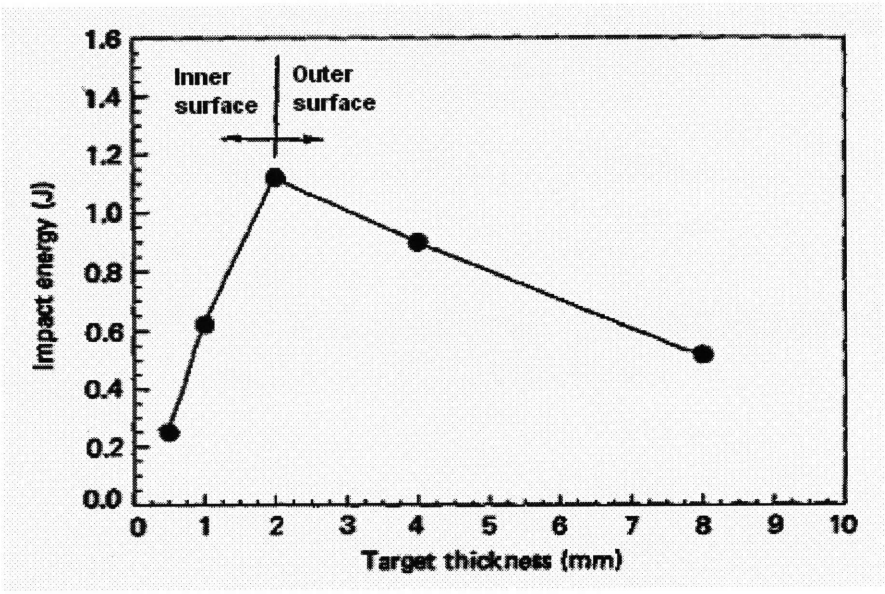

Figure 37: Low-velocity impact energy to initiate damage vs. target thickness for (+/-45°) CFRP composites [171].

Thus, increasing the flexural stiffness of a target, for example, by placing fibers on the surface of a laminate, can enhance its impact resistance [100]. This is true for the range of stiffnesses

where initial failure occurs at the top surface of the component. In more flexible targets, however, reducing the flexural stiffness may precipitate failure at a lower incident energy.

A detailed study identified fundamental aspects in the development of damage in glass fiber-reinforced plastic (GFRP) subjected to high-velocity impact loading (impactor speed>10 m/s) [172]. It was shown that increasing the angle q in a (0_5°,q°,0_5°) laminate resulted in greater delamination-type damage for a given incident energy as shown in **Figure 38**. Increasing q in this way also had the effect of reducing the first damage threshold energy. The studies also showed that for a given energy, increasing the thickness of the GFRP target resulted in an increase in the delaminated area. This increase in damage area may result from the reduction in the target's energy absorbing capability [100]. This work was extended by developing a simple model for predicting the likely delamination sites in a number of different composites [23]. It was suggested that delamination in multi-angle composites is more likely to occur at interfaces where the mismatch in bending stiffness is greatest, for example, between +/-45° plies. It was shown experimentally that the level of delamination in a glass/epoxy composite increased as the angle q in a (0°,q°) laminate increased; i.e., as the bending stiffness mismatch increased. This evidence suggests that if delamination needs to be suppressed, laminates with sudden large changes in fiber direction should be avoided.

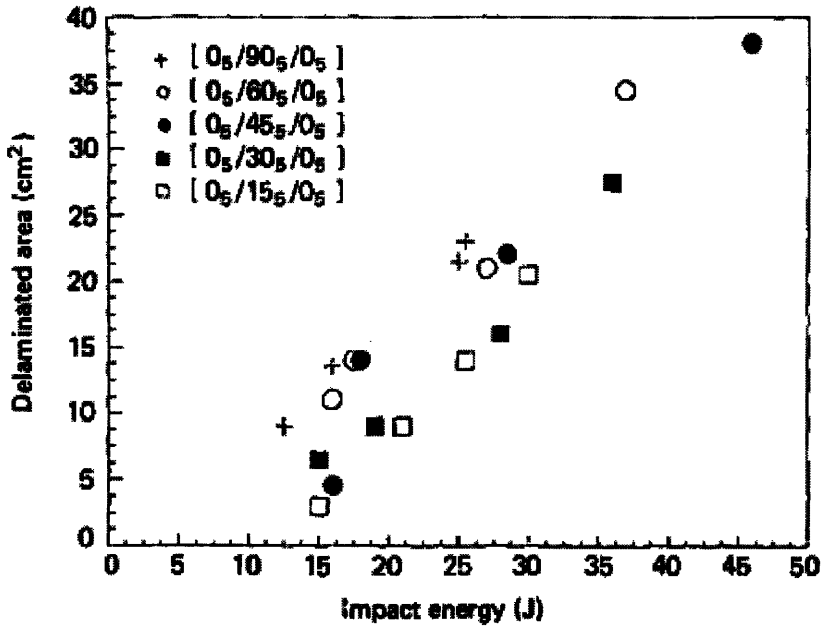

Figure 38: Delaminated area vs. impact energy for impacted GFRP laminates [172].

Other techniques to reduce impact-induced delamination include the use of woven fabrics [102,173], hybridization [174,175,176] (for example, carbon fibers with Kevlar fibers) and three-dimensional stitching [177,178]. The first of these techniques involves replacing the unidirectional +/-45° plies in a multidirectional composite by a +/-45° woven fabric. The three-dimensional nature of the fabric helps suppress the formation of delaminated zones at this critical interface.

The impact resistance of carbon fiber composites can be enhanced considerably by incorporating plies of lower modulus fibers [174,175,176]. In order to ensure compatibility, the matrix resin is usually the same in the two or more constituent materials. It was demonstrated that the Izod impact energy of a high tensile strength (HTS) carbon fiber composite could be increased by 500% through hybridization with E-glass fibers [175]. As well as reducing the basic price of the composite, the addition of the glass fibers was found to change the mode of fracture from a clean break to a delamination-type failure.

The high-velocity impact response of a number carbon-Kevlar hybrid laminates was assessed and it was concluded that the addition of the lower modulus Kevlar fibers increased the threshold energy for the onset of damage by up to four times [37].

4.2.5. Geometry

Geometry is a fundamental parameter in determining the impact response of a composite component [12,86,101,110,157,179]. Low-velocity impact tests on CFRP have shown that the mode of failure in a simple beam may vary depending upon its span-to-depth ratio. Short thick specimens tend to fail in an interlaminar mode, whereas as long thin beams failed in flexure [110].

High-velocity impact tests on CFRP indicated that the areal geometry of the target is less important at high rates of strain [180]. Ultrasonic C-scans of impacted specimens showed that the level of damage in a small, 50 mm long beam was the same as that in a 150 mm coupon. This suggests that high-velocity impact loading by a light projectile induces a localized form of target response in which much of the incident energy of the projectile is dissipated over a small zone immediate to the point of impact. Tests on large plates have substantiated this claim and it appears that under certain conditions, small simple coupons can be used to characterize the high velocity/low mass impact response of composite structures [180].

5. Energy Absorption Characteristics

The energy introduced into a composite specimen, i.e. the **impact energy**, is approximately equal to the kinetic energy of the impactor immediately before contact. During impact tests, energy absorbed by the specimens, i.e. the **absorbed energy**, can be calculated from the associated load–deflection curves. For an impact event having a closed load–deflection curve, the absorbed energy is equal to the area within the load–deflection curve. For an impact event having an open load- deflection curve, the absorbed energy is equal to the area bounded by the load–deflection curve and the deflection axis.

5.1. Energy Profiles

Impact energy versus absorbed energy of each impact event can be plotted and shown in a diagram called an *energy profile*. An example is illustrated in **Figure 39**, which gives the energy profile for a glass/epoxy composite laminate based on eleven tests [181].

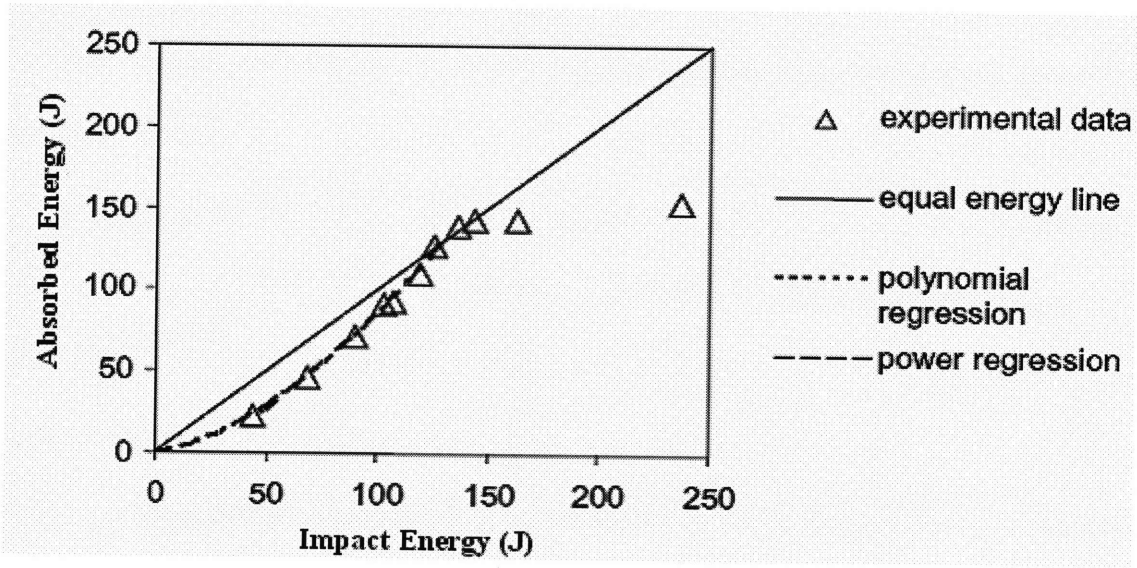

Figure 39: Energy profile based on eleven tests [181].

Thus, the energy profile is a diagram that shows the relationship between the impact energy and the absorbed energy.

In **Figure 39**, there are eleven data points designated by triangular symbols. The data points correspond to the eleven load–deflection curves in ascending energy order. As each data point is associated with a dropping height of the impactor, the impact energy increases with the height of the drop. Since a higher impact energy results in more severe damage to a composite specimen, the absorbed energy increases with the impact energy. A diagonal line representing the equal energy between impact and absorption is also shown on the diagram for comparison. As seen in **Figure 39**, the first six points are below the equal energy line, implying that there is an excessive impact energy in each test. The excessive energy is retained in the impactor and used to rebound the impactor from the specimen at the end of each contact–impact. Accordingly, all the lowest six cases, which have closed load–deflection curves, have either complete or partial rebounding in their unloading sections.

As shown in **Figure 39**, the excessive energy first increases, then decreases as the impact energy increases. At a higher impact energy level, the absorbed energy becomes equal to the impact energy. Points that are located very close to the diagonal line represent similarity, or equality, between the impact energy and the absorbed energy. Thus, they indicate that the energy used in impacting any of these composite specimens is almost completely, or completely, absorbed by the specimen. Hence, there is no excessive impact energy to rebound the impactor from the specimen. Penetration of the impactor into the specimens occurs in these cases. **Penetration** is a macroscopic mode of failure enabling the impactor to completely penetrate the material. The corresponding load–deflection curves of the penetrated cases are no longer closed. Points that are located on the diagonal line imply progress of penetration.

As the impact energy continues to increase, the impactor moves deeper and deeper into the composite specimens. That is, the penetration process continues to progress. Once the impact energy is high enough, perforation eventually takes place in the composite specimens. **Perforation** is the action of passing through the target structure of the projectile. In the last two cases, far away from diagonal line, the composite specimens are perforated. The impact energies in these two cases are again higher than the absorbed energies and the excessive energies are retained in the impactor for post-perforation motions.

5.1.1. Penetration Threshold

Based on the energy viewpoint, penetration should take place the first time the absorbed energy reaches the level of the impact energy when a single impact occurs. In order to better define the *penetration threshold* and to account for experimental variation, second-order polynomial regression and power regression based on the least-squares method are used to represent the experimental data points. These two curves are shown in **Figure 39** for comparison. The polynomial regression is represented by a dotted line while the power regression by a dashed line. The polynomial regression intersects with the equal energy line at 127.9 J. The power regression intersects with the equal-energy line at 131.3 J. These intersection points are called *penetration thresholds*. The *penetration thresholds* based on these two regression methods seem to agree with each other [181].

During an impact test the size of the impactor significantly affects *penetration threshold. Penetration threshold* is approximately linearly proportional to the size of the impactor.

5.1.2. Perforation Threshold

Perforation is another important impact property of composite laminates. It can also be identified from the energy profile. Once a perforation takes place, the excessive impact energy will be used to move the impactor through the damaged composite specimen continuously. Based on **Figure 39**, the *perforation threshold* of the composite laminate must be near the first point coming off the equal-energy line. Thus, the *perforation threshold* of the glass/epoxy composite laminates is identified as 143J. However, if such a convenient point is not available for determining the *perforation threshold*, the least-squares method for finding the penetration threshold can be used to determine the *perforation threshold* from all points coming off the equal-energy line. The *perforation threshold* is a material constant because it represents the energy required to perforate the composite laminates of interest. However, the absorbed energies of the data points beyond the *perforation threshold* are not constant because friction and strain-rate effects are involved in the post-perforation process [181].

During an impact test the size of the impactor significantly affects *perforation threshold. Perforation threshold* is approximately linearly proportional to the size of the impactor.

5.1.3. Range for Penetration Process

The equal energy points in **Figure 39**, represent different stages of the penetration process. As the impactor moves deeper into the composite specimen, more energy is required for the penetration process to advance. Based on the penetration and perforation thresholds of glass/epoxy composite laminates, there exists a range in which the impact energy and the absorbed energy are equal to each other. This range is called the *range of the penetration process*. The range of the penetration process is expected to be proportional to the thickness of

the composite laminates [181].

5.2. Ballistic Impact

5.2.1. Ballistic Impact Test

Ballistic impact tests are often performed using a helium or air gas gun which allows a variation of striking velocity from 100 to 500 m/s. The composite is placed between two clamping (constraining) plates with different diameter holes (so-called apertures) in the center, and firmly tightened. The composite clamped by plates is placed in the center of the ballistic impact test apparatus and subjected to fragment-simulating projectiles (FSP) of different weights and diameters. The striking velocity and residual velocity are estimated from an electronic timer [182,183].

5.2.2. Ballistic Limit Velocity

The *ballistic limit velocity*, V_{BL}, is defined as the highest *striking velocity*, V_s, where the *residual* or *rebound velocity*, V_r, equals zero (i.e. no full penetration) [184,185]. For a better understanding, **Figure 40** shows 23-ply laminates of Spectra 900® fabric-reinforced **vinyl ester** resin composite (6.71 mm thick) and 31-ply laminates of Kevlar KM2® fabric-reinforced phenolic-polyvinylbutyral resin composite subjected to the ballistic impact of a tungsten carbide ball (16 g, 12.7 mm diameter) at various levels of *striking velocity*, which led to either full perforation or no/partial perforation with rebound action. This plot allows the estimation of the *ballistic limit velocity*.

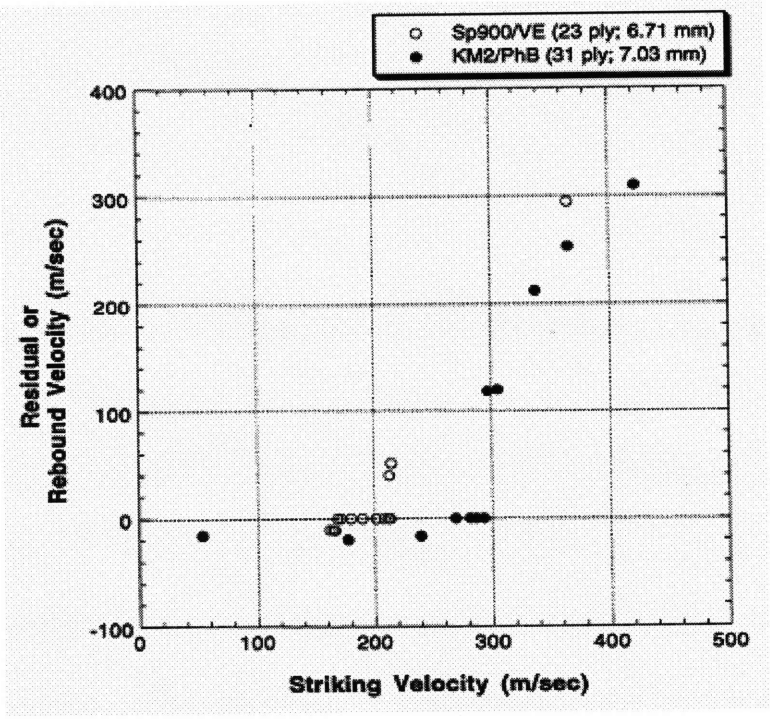

Figure 40: Relationship between the residual or rebound velocity and striking velocity [183].

For fully perforated specimens, the following relationship can be used to estimate the *ballistic limit velocity*.

$$V_{BL}=(V_s^2-V_r^2)^{1/2} \text{ for } V_r>0 \quad (1)$$

where V_s is *the striking velocity*, V_r is the *residual* or *rebound velocity*, and V_{BL} is the *ballistic limit velocity*. The relationship in **Equation 1** is based on the assumption of a nondeformable penetrator and the conservation of energy [183].

5.2.3. Factors Affecting Ballistic Impact

5.2.3-1. Effect of Resin Addition on Penetration Characteristics

Single ply specimens of dry Spectra fabric as well as Spectra fabric-reinforced laminate (25% by weight of resin) were compared in both the static puncture mode and drop-weight impact loading mode [183] to examine how the addition of a matrix resin alters the penetration characteristics. **Figure 41(a)** shows the load-deflection response of Spectra fabric/**vinyl ester** resin and Spectra fabric/polyurethane resin composite laminates, while **Figure 41(b)** shows that of spectra dry fabrics. The difference between the dry fabric and composite laminate was noted in the final failure mode. The composite laminate showed a sudden failure with one large drop of load. On the other hand, the failure of the woven dry fabric was associated with several load drops. Detailed observation during and after testing of the dry fabric revealed that the numerous load drops in **Figure 41(b)** corresponded to successive breaking of individual yarns along the periphery of the penetrating head, and the movement of yarns slipping off from the penetrator. Both of these events led to load drops in a sequential manner, since they resulted in a decrease in the number of yarns imparting force onto the penetrator.

In contrast to the case of dry fabric, the principal yarns in the composite, which face the penetrating head, failed to carry the load mostly through fracture due to their constraint by the resin matrix. The composites failed at a higher load than the dry fabric, because they required more force to break many yarns simultaneously than to break them one or two at a time. Therefore, the effect of the resin addition appeared to be a coupling of the yarns so as to make the stress state across all fibers more uniform, resulting in a failure process that was more sudden compared with the dry fabric.

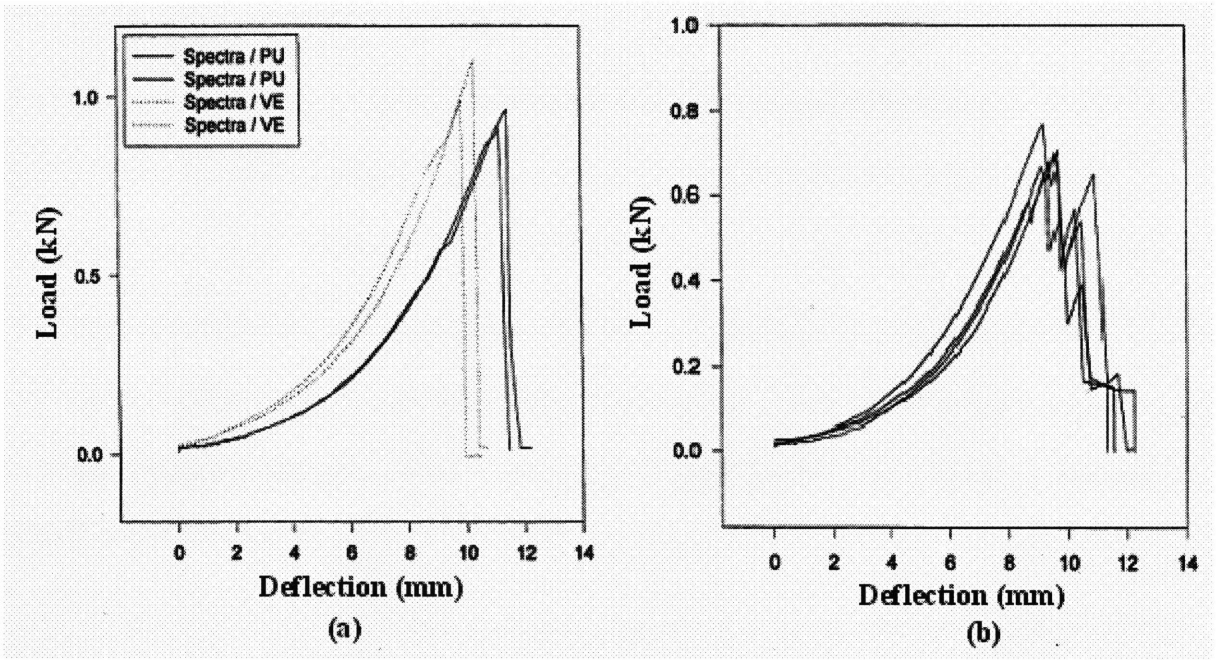

Figure 41: Load-deflection curves for (a) single-ply composite laminate of Spectra 900® fabric-reinforced **vinyl ester** (VE) resin composite vs. spectra 900® fabric-reinforced polyurethane (PU) resin composite (b) single ply of spectra 900® dry fabric; all under quasi-static penetration loading at 0.000254 m/s [183].

5.2.3-2. Effect of Multi-ply Composite Laminates with Different Resin Matrices

In **Table 11,** Spectra 900 fabric-reinforced 5-ply composite laminates with **vinyl ester** and polyurethane resin matrices were compared in the following loading modes: low-velocity drop-weight impact (impact energy=87 J) and ballistic impact (impact energy=37 J) [183]. S2-glass/epoxy 5-ply and 10-ply laminates were also compared as unstitched, stitched with Kevlar threads with a stitched density of 2 stitches/cm and 12.7 mm and 25.4 mm spacing configurations in the following loading modes: low-velocity drop-weight impact (impact energy=80 J) and ballistic impact (impact energy=4700 J) [186].

Table 11: Energy absorption for full perforation of 5 and 10 ply laminates.

Laminate Type	Number of plies	Impact Energy(J)	D.W.I. Energy Absorption (J)	Impact Energy(J)	B.I. Energy Absorption (J)	Reference
Spectra 900/**Vinyl ester**	5	87	16.4	37	30.07	[183]
Spectra 900/Polyurethane	5	87	14.3	37	25.95	[183]
S2-Glass/Epoxy Unstitched	5/10	80	16.72	4700	592	[186]
S2-Glass/Epoxy 12.7 mm stitched	5/10	80	31.61	4700	655	[186]
S2-Glass/Epoxy 25.4 mm stitched	5/10	80	18.55	4700	613	[186]

Abbreviations: D.W.I., drop-weight impact; B.I., ballistic impact

As seen from **Table 11,** for the same impact energies, Spectra 900/**vinyl ester** has better drop weight and ballistic impact performance than Spectra 900/polyurethane. Absorbed energy of Spectra 900/**vinyl ester** was observed %14 and %16 higher in drop-weight impact and ballistic impact, respectively [183]. Further, absorbed energy for unstitched S2-glass/epoxy laminates was less compared to stitched S2-glass/epoxy ; among stitched laminates, absorbed energy was more for the 12.7 mm stitch spacing laminates in both drop-weight and ballistic impacts. Thus, one can conclude that 12.7 mm stitched S2-glass/epoxy has better impact performance than that of the 25.4 mm stitched and unstitched S2-glass/epoxy.

5.2.3-3. Effect of Laminate Thickness on Ballistic Limit Velocity

Effect of Laminate thickness on *ballistic limit velocity* was assessed between the angle-plied unidirectional fiber-reinforced laminates and fabric-reinforced laminates [182,187]. The

data of ballistic limit were plotted as a function of areal density (mass per unit area). Higher areal density largely means thicker composite systems. An empirical relationship was obtained as follows:

$$BL = a(AD)^b \quad (2)$$

where BL is the *ballistic limit velocity*, AD is the *areal density*, and a and b are *material-dependent constants* [182,187]. **Table 12** shows the data obtained in these studies [182,187].

Table 12: Comparison of the different fiber compositions based on empirical data.

Resin Matrix	Fiber Composition	Reinforcement Geometry	a $m^3/(kg.s)$	b	Ref.
Vinyl ester	Spectra 1000	Angle-plied web	205.36	0.65	[182]
Vinyl ester	Spectra 900	Plain-weave fabric	226.36	0.51	[182]
Vinyl ester	Kevlar-29	Basket-weave fabric	157.69	0.56	[187]
Vinyl ester	S-2 glass	Plain-weave fabric	98.81	0.64	[187]

According to data presented in **Table12,** at a given areal density, the ballistic limit velocities of spectra fiber-reinforced laminates are apparently higher than those of Kevlar-29 and S-2 glass fiber-reinforced laminates. To understand the difference between the two spectra fiber-based laminates, ballistic limits of both laminates were plotted as a function of areal density as shown in **Figure 42.**

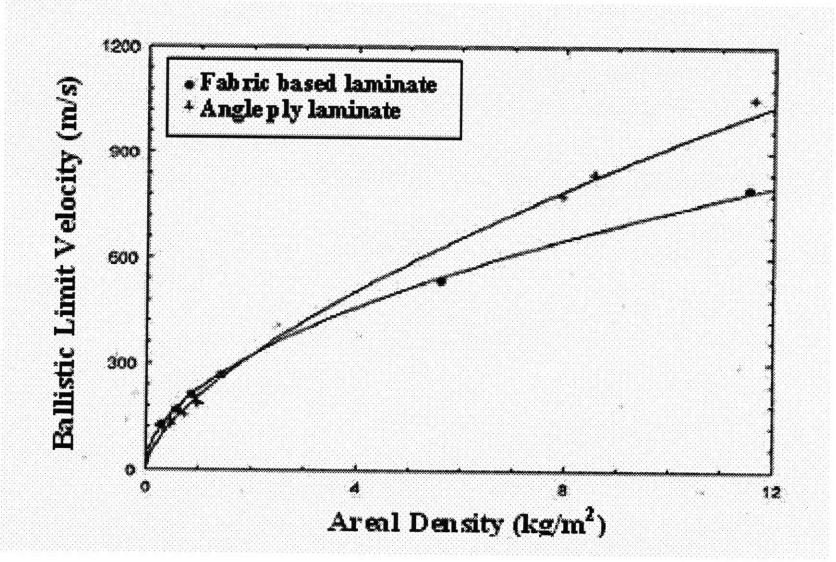

Figure 42: Ballistic limit velocities of spectra fiber- and spectra fabric-reinforced laminates vs. areal density [182].

At low areal density, both spectra fiber-based laminates demonstrate similar ballistic limits. However, as areal density increases, differences in ballistic limit become more apparent, with the angle-plied spectra fiber-reinforced laminate showing higher values.

In another study [188] plain and satin weave carbon/epoxy laminates were investigated and the *ballistic limit velocity* was plotted as a function of number of layers as it is shown in **Figure 43.**

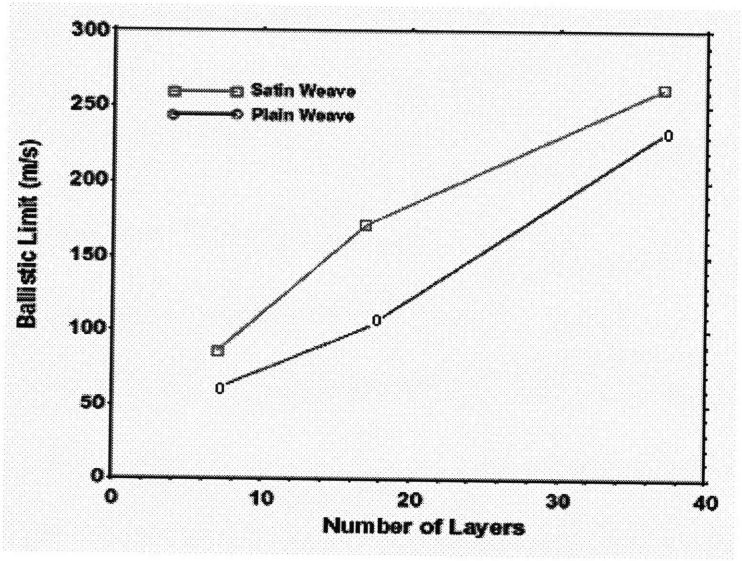

Figure 43: Variation of ballistic limit velocity with number of layers [188].

From **Figure 43** it can be seen that the *ballistic limit velocity* for satin weave laminates is much higher than the corresponding plain weave laminates for the same number of layers. This characteristic was attributed to satin weave laminates are slightly thicker than plain weave laminates.

5.3. Influence of Constituents on Energy Absorption Capability

Specific energy absorption, E_S, is defined as the energy absorbed per unit mass of laminate material. Total absorbed energy can be calculated from the area under the load-displacement curves obtained from impact tests [181]. The energy absorption characteristics of composites can be adjusted by controlling various parameters such as the fiber type, matrix type, fiber architecture, specimen geometry, fiber volume fraction, and testing speed.

5.3.1. The Effect of the Matrix on the Energy Absorption Capability

Carbon fiber-reinforced composites with the same fiber orientation and impact rate but different thermoplastic matrices were investigated. Among all types of composites investigated, carbon fiber/PEEK laminates exhibited the highest specific energy compared to carbon fiber/polyetherimide (PEI) and carbon fiber/polyimide (PI) composite materials, and carbon fiber/polyarylsulfone (PAS) polyimide laminate displayed the lowest energy absorption capability [189,190,191]. Based on these three studies, the specific energy absorption of thermoplastic composites follow the order PAS<PI<PEI< PEEK. The specific energy absorption and interlaminar fracture toughness of these matrices are shown in **Table 13**. From data in the table, it was concluded that higher interlaminar fracture toughness of the thermoplastic matrix

materials produced the corresponding increases in energy absorption capability of the composite material.

Table 13: Effect of matrix on specific energy absorption.

Fiber Composition	Matrix Material	Specific Energy Absorption, E_S (kJ/kg)	Interlaminar Fracture Tougness (kJ/m^2)	Reference
Carbon fiber	Polyetheretherketone (PEEK)	194	1.6	[189]
Carbon fiber	Polyetherimide (PEI)	155	1.2	[190,191]
Carbon fiber	Polyimide (PI)	131	0.9	[190,191]
Carbon fiber	Polyarylsulfone (PAS)	128	0.4	[189]

In a similar study, the energy absorption of carbon/PEI (C/PEI), carbon/polyimide (C/PI), carbon/polyarylsulfore (C/PAS), and carbon/PEEK (C/PEEK) were investigated and compared with that of carbon/epoxy and glass/polyester. Carbon/thermoplastic composites demonstrated superior energy absorbing capabilities (E_S=128–194 kJ/kg) than carbon/epoxy (E_S =110 kJ/kg) or glass/polyester (E_S=80 kJ/kg) composites [192].

In another study, the energy absorption capability of carbon/epoxy and carbon/PEEK composites made from unidirectional prepreg materials was investigated by conducting axial compressive tests [193]. The superior energy absorption capability of carbon fiber/PEEK composites (180 kJ/kg) was attributed to the higher interlaminar fracture toughness of the thermoplastic PEEK matrix composite (1.56–2.4 kJ/m^2). The carbon/epoxy composite having an interlaminar fracture toughness in the range 0.12–0.18 kJ/ m^2 absorbed only 53 kJ/kg specific energy.

In a different study, based upon observation and a general understanding of the impact process, it was concluded that the energy absorption of materials that fail by transverse shearing or brittle fracturing was little affected by matrix stiffness. However, materials that fail by lamina

bending could be more significantly affected by matrix stiffness. A change in matrix stiffness could cause brittle fiber composites to fail in a different mode. However, changes in matrix stiffness had very little effect on the energy absorption of ductile fiber reinforcements [194].

5.3.2. The Effect of Fiber on the Energy Absorption Capability

The type of reinforcing fiber used in a composite material determines to a very large extent its energy absorption characteristics. A decrease in the density of fiber causes an increase in specific energy absorption capability of the corresponding fiber-reinforced composites [195,196]. Energy absorption capacity of graphite/epoxy, Kevlar/epoxy and glass/epoxy composites having similar ply constructions was compared and it was seen that graphite/epoxy composite had E_S values greater than that of Kevlar/epoxy and glass/epoxy composites. This was attributed to the lower density of carbon fibers compared to glass and Kevlar fibers [195].

In another study, PEEK matrix composite tubes reinforced with AS4 carbon fiber, IM7 carbon fiber, and S2 glass fiber were investigated, respectively [196]. The fibers were aligned parallel to the tube axis. S2/PEEK tubes displayed approximately 20% lower E_S than the AS4/PEEK and IM7/PEEK tubes. It was concluded that this was a direct result of the lower density of the carbon fiber reinforcing materials compared with the glass reinforcing material. Despite AS4 carbon fibers being more ductile than IM7 carbon fibers, both AS4/PEEK and IM7/PEEK tubes displayed similar specific energies.

Epoxy composite tubes reinforced with Thornel-300 carbon fibers which have low failure strain and Hercules AS-4 carbon fibers which have intermediate failure strain were investigated and it was observed that the tubes having greater energy absorption properties were the ones reinforced with fibers having higher strain to failure [197]. **Table 14** summarizes effects of fiber

on specific energy absorption.

Table 14: Effect of fiber on specific energy absorption E_S

Fiber Material	Matrix Resin	Fiber Orientation	Specific Energy Absorption, E_S (kJ/kg)	Reference
AS4 Carbon	Polyetheretherketone	[±0]	194	[196]
IM7 Carbon	Polyetheretherketone	[±0]	202	[196]
S2 Glass	Polyetheretherketone	[±0]	143	[196]
Kevlar	Epoxy	[0±45]	32	[197]
Graphite	Epoxy	[0±45]	45	[197]

5.3.3. The Effect of Fiber Orientation on the Energy Absorption Capability

Fiber orientation also plays an important role on the energy absorption of composite laminates and tubes. Five glass/epoxy composite laminates having different stacking sequences of $[0_5/\theta_5/0_5]$ where θ= 0, 15, 30, 45, and 90, were investigated [181]. They were all 3.83 mm thick. These laminates were subjected to drop-weight impact test by a cylindrical impactor that had a hemispherical head of 12.5 mm in diameter and a mass of 24 kg. It was concluded that the $[0_5/90_5/0_5]$ laminate had the highest energy absorption followed by in decreasing energy absorption by laminates with $[0_5/45_5/0_5]$, $[0_5/30_5/0_5]$, $[0_5/15_5/0_5]$ fiber orientation.

Further, among the five composite laminates investigated, it was obtained that $[0_5/0_5/0_5]$ had the lowest penetration threshold and perforation threshold; the composite laminate $[0_5/15_5/0_5]$ had the highest penetration and perforation thresholds; the *penetration* and *perforation thresholds* of the composite laminates $[0_5/\theta_5/0_5]$ decreased as the fiber orientation of the middle lamina increased from 15° to 90°, with θ=0 being the exception.

To understand the effect of fiber orientation on energy absorption characteristics of

composite tubes, glass/epoxy, carbon/epoxy and Kevlar/epoxy composite tubes with fiber orientation $[0\pm\theta]_4$ where θ varied from 0 to 90 were investigated [198]. The specific energy of the glass/epoxy and Kevlar/epoxy tubes remained constant with increasing θ up to 45, and above this value they increased. This increase in energy was attributed to the increased lateral support to the axial fibers with increasing θ. On the other hand, the specific energy of the carbon/epoxy tubes initially decreased with increasing θ up to 45° and then remained constant. This initial decrease in the energy absorption was attributed to the reduction in axial stiffness of the composite material with increasing θ.

In a different study [189] carbon fiber-reinforced composite tubes with different thermoplastic matrices such as PEEK, PEI, PI, and PAS were investigated under quasi-static loading. The tubes had fiber orientation of [0°], [±5°], [±10°], [±15°], [±20°], [±25°] with respect to the axis of the tube. **Table 15** summarizes the effects of fiber orientation on specific energy absorption for various composite tubes investigated in this study .

Table 15: Effects of fiber orientation on specific energy absorption

Fiber Orientation	Fiber Composition	Matrix Resin	E_S (kJ/kg)	Matrix Resin	E_S (kJ/kg)	Matrix Resin	E_S (kJ/kg)	Ref.
[0°]	Carbon	PEEK	194.1	PEI	155.4	PI	131.4	[189]
[±5°]	Carbon	PEEK	205.3	PEI	162.4	PI	151.1	[189]
[±10°]	Carbon	PEEK	225.3	PEI	187.9	PI	160.7	[189]
[±15°]	Carbon	PEEK	226.8	PEI	167.5	PI	162.3	[189]
[±20°]	Carbon	PEEK	202.3	PEI	162.4	PI	167.9	[189]
[±25°]	Carbon	PEEK	181.1	PEI	135.6	PI	*	[189]

* Not evaluated. Abbreviations: PEEK, polyetheretherketone;PEI, polyetherimide; PI, polyimide

5.3.4. The Effect of Geometry on the Energy Absorption Capability

Increasing thickness is the most direct way to increase the energy absorption capacity of a material. **Figure 44** shows the penetration and perforation thresholds of cross-ply glass/ epoxy composite laminates for various thicknesses. The *penetration threshold* (solid circles) and the *perforation threshold* (open circles) increase with thickness, and so does the difference between the penetration and perforation thresholds.

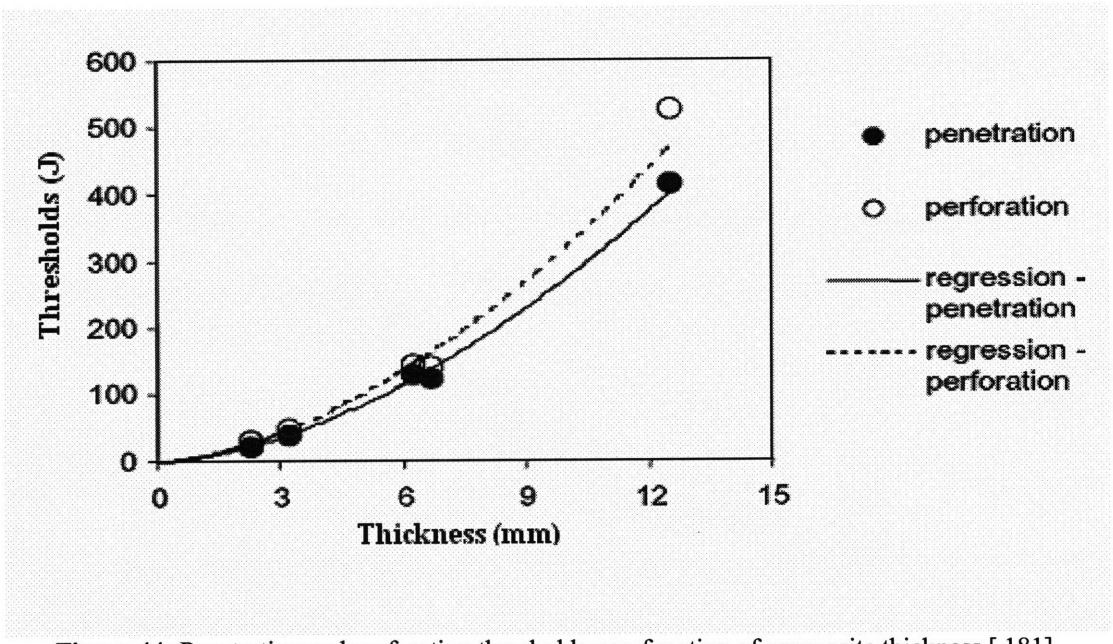

Figure 44: Penetration and perforation thresholds as a function of composite thickness [181].

From the regression curves of penetration and perforation, the following ratio was obtained

$$\frac{P_n}{P_r} \approx 0.8 \cdot t \tag{3}$$

where P_n is penetration threshold, P_r is perforation threshold, and t is thickness.

A study was conducted to investigate the geometrical effects in energy absorption of circular, square, and rectangular cross section tubes. Graphite, Kevlar and glass-reinforced epoxy tubes were tested under quasi-static loading and it was concluded that for a given fiber lay-up

and tube geometry, the specific energy follows the order, circular > square > rectangle [199]. Further, it was found that the tube inside diameter to wall thickness (D/t) ratio was determined to significantly affect the energy absorption capability of the composite materials [200,201,202,203]. Energy absorption was found to be a decreasing nonlinear function of tube (D/t) ratio. That is, a reduction in D/t ratio resulted in an increase in the specific energy absorption. It was reported that carbon/epoxy and Kevlar/epoxy tubes with elliptical cross sections exhibit similar trends, where the energy absorption capability was determined to be a decreasing nonlinear function of the ratio of tube internal diameter to wall thickness (D/t) [201].

Another study investigated the effect of tube dimensions. It was found that carbon/epoxy exhibited large changes in energy absorption characteristics with a range of values of tube diameter (D), tube wall thickness (t) and (D/t) ratio [202]. **Table 16** shows how specific energy absorption changed with (D/t) ratio.

Table 16: Effect of (D/t) ratio on specific energy absorption.

Fiber Composition	Matrix Resin	Diameter ,D (mm)	Thickness, t (mm)	(D/t) Ratio	Specific Energy Absorption,E_S,(kJ/kg)	Reference
Carbon Fiber	PEEK	35.5	0.8	44.375	171.7	[203]
Carbon Fiber	PEEK	35.5	1.04	34.134	172.3	[203]
Carbon Fiber	PEEK	35.5	2.2	16.136	205.9	[203]
Carbon Fiber	PEEK	55	1.09	50.458	189	[203]
Carbon Fiber	PEEK	55	2.09	26.315	218.4	[203]
Carbon Fiber	PEEK	55	2.66	20.676	228.3	[203]
Carbon Fiber	PEEK	96	1.64	58.536	194	[203]
Carbon Fiber	PEEK	96	1.91	50.261	215.2	[203]

.

5.3.5. The Effect of Fiber Volume Fraction on the Energy Absorption Capability

E_S capability of knitted carbon fiber-fabric/ epoxy and knitted glass fiber-fabric/epoxy composites was investigated [204,205]. It was found that the specific energy absorption capability increased with fiber content. Contrary to the above finding, a decrease was reported in

specific energy absorption of carbon fiber/epoxy composite material with an increase in fiber volume fraction from 40 to 70% [198]. The decrease in specific energy absorption was attributed to the decrease in interlaminar shear strength of the composite with increasing fiber content.

In another study, carbon/epoxy composites with fiber volume fractions in the range 40–55% were investigated [206]. It was concluded that some specimens exhibit a large decrease in energy absorption capability with increasing fiber volume fraction, whereas other specimens exhibit a slight decrease. Glass fiber/**vinyl ester** composites were studied with fiber volume fractions in the range 10–50% and an increase in specific energy absorption with an increase in fiber volume fraction was reported [207]. E-glass fiber/epoxy laminates were studied with different fiber volume fractions as shown in **Figure 45** and it was concluded that the amount of energy absorbed increases with fiber volume fraction [208].

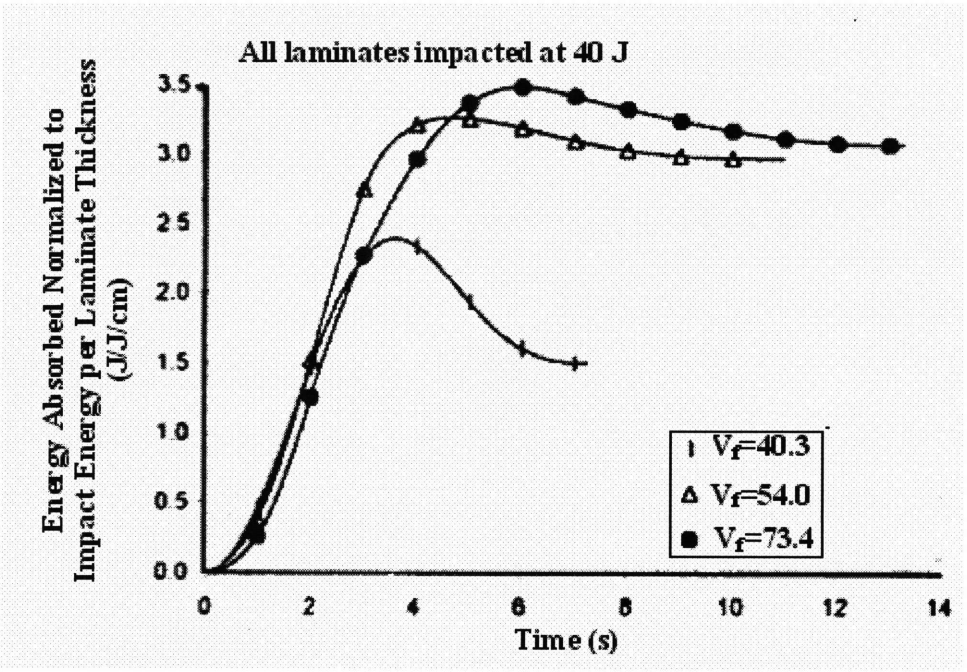

Figure 45: Effect of fiber volume fraction-energy absorption versus time [208].

Therefore, it should be concluded that an increase in the fiber volume fraction does not always improve the composite energy absorption capability.

5.3.6. The Effect of Impactor Speed on the Energy Absorption Capability

Carbon/epoxy and Kevlar/epoxy composites were studied and an increase was reported in energy absorption with impactor speed increase [209]. Contrarily, graphite/epoxy, Kevlar/epoxy, and glass/epoxy composites were investigated and very little change in the energy absorption was reported with testing speed change [210]. In another study [211], the energy absorption behavior of glass/polyester and glass/**vinyl ester** composites were investigated in the impactor speed range from $2.1x10^{-4}$ to 15 m/s. In the case of glass/**vinyl ester** composites, a 10% decrease was reported in energy absorption with increasing test speed, however, in the case of glass/polyester, a 20% increase was reported in energy absorption with increasing test speed. This result was attributed to the higher tensile strength and modulus of the **vinyl ester**. These data are shown in **Table 17.**

Table 17: Effect of impactor speed on specific energy absorption.

Fiber Composition	Matrix Resin	Initial Velocity (m/s)	Specific Energy Absorption, E_S (kJ/kg)	Reference
Glass	Vinyl ester	$2.1x10^{-4}$	57.5	[211]
Glass	Vinyl ester	12	53.5	[211]
Glass	Polyester	$2.1x10^{-4}$	40.5	[211]
Glass	Polyester	12	47.5	[211]

6. Conclusions and Recommendations

6.1. Modes of Failure [See Tables 1 and 2.]

Conclusions

The modes of impact damage range from matrix cracking and delamination to fiber failure and penetration. Matrix cracking is the lowest level of failure induced by low-velocity impact. A matrix crack often extends across the entire lamina with the crack tip touching the interlaminar interface. Such a crack may turn into a delamination along the interface during subsequent loading. Delamination is an important damage mode because the level of impact energy to initiate delamination is often low. Although delamination does not provide high energy absorption during the impact process, it represents significant degradation to composite materials. Placing 90° laminae on the outer faces of the laminate further decreases energy absorption by the reduction of delamination initiation loads. Thus, a stacking sequence of [45°,0°,...] would have a higher delamination load than a stacking sequence of [90°,0°,...]. Delamination crack length can be found using the linear relationship between peak contact force and delamination crack length. Fiber failure generally occurs much later in the fracture process than matrix cracking and delamination. Penetration is the worst damage mode and is often investigated in ballistic loading.

Recommendations

Damage mode interaction should be better understood for predicting initiation and propagation of a particular form of damage. The current literature contains relatively little information on fiber failure due to impact. Studies should be conducted to better understand these issues.

6.2. Damage Tolerance and Post-impact Residual Strength [See Table 5.]

Conclusions

Post-impact performance is dictated by the existing damage modes, therefore a combination of tension and compression residual strength testing is required to characterize damaged laminates. Often, there is a larger strength degradation in compression than in tension in low- energy impact loadings.

Recommendations

Compared with tension and compression, relatively less work has been conducted on the residual flexural strength of laminates. Future studies should be conducted to better understand residual flexural strength.

6.3. Evaluation of Damage Tolerance

Conclusions

The compression after impact (CAI) test is an important characterization in the design of composite structures. Although there are many methods to predict damage tolerance, compression after impact testing is one of the best ways to evaluate damage tolerance.

Recommendations

There is no standard testing machine for CAI tests. These tests are conducted using purpose-built machines for convenient specimen geometries. Standardized testing procedures could enhance the understanding and expand the applicability of these tests.

6.4. Effect of Fiber on the Post-impact Residual Strength

Conclusions

Often fibers having high energy absorbing capacity offer excellent residual properties unless the stiffness of the fiber is very low. Further, reducing the fiber diameter will result in a degradation in residual strength. However, reducing the fiber diameter increases the energy absorbing capability of the composite, resulting in lower levels of damage for a given impact energy. These conclusions are all for a fixed fiber volume fraction.

Recommendations

An improvement in the post-impact residual strength of a laminate can be achieved by increasing the strain to failure of the reinforcing fiber. This concept suggests a set of tests.

6.5. Effect of Matrix Properties on Post-impact Residual Strength

Conclusions

The post-impact residual strength of toughened composites does not appear to be significantly better than those of untoughened composites . This results from the ironic fact that composites with tougher matrices tend to be more notch-sensitive due to reduced splitting and delamination around stress concentrations such as notches.

6.6. Effect of Interphase Properties on Post-impact Residual Strength

Conclusions

Treating the fibers improves the post-impact compressive properties. Even though surface treatment of the fibers reduces the level of damage for a given energy, the increased

notch-sensitivity of the laminate may result in poorer residual tensile properties.

Recommendations

The level of surface treatment applied to fibers in a multidirectional composite should depend upon the operational conditions the component will encounter. Therefore, a compromise should be sought in which the fibers are given intermediate levels of treatment.

6.7. Effect of Fiber Stacking Sequence on Post-impact Residual Strength

Conclusions

The role of the fiber stacking sequence plays a significant role in determining the residual properties of impact damaged composites. For improved post-impact residual strength the laminate's +/-45° fibers should be located on the outermost surface of the composite [100].

6.8. Modification of Thermoset Resins [See Table 10.]

Conclusions

The low-velocity impact resistance of a resin composite is, to a great extent, controlled by the resin toughness. Rubber modified epoxies have higher resistance to impact damage and have higher residual strength than unmodified thermoset resins. Modified thermosets have an interlaminar fracture toughness ---up to 95%--- and a residual strength ---up to 90%--- greater than their unmodified counterparts. However, a modified matrix resin imparts improved impact damage resistance, with a concomitant reduction in stiffness and compressive strength in hot-wet conditions.

Recommendations

Care should be taken and a compromise should be sought when modifying composite thermosets as there are optimal conditions that provide balanced properties of the composites.

6.9. Interleaving Technique [See Tables 8 and 10.]

Conclusions

Interleaved strips placed at delamination-prone laminar interfaces are a variant of the method based on a tough matrix material. Thermoplastic interleaves are found to be more effective than their thermoset counterparts due to their higher energy absorption capability. Further, interleaved strips made from ductile short fibers with an adhesive provide an additional energy absorption source during interlaminar fracture. Interleaving techniques offer greater residual strength ---up to 100%--- and greater interlaminar fracture toughness ---up to 20%.

Recommendations

Although the interleaving technique is well-established to suppress the onset of delamination at free-edges, its success for damage tolerance design requires further research.

6.10. Hybrid Fiber Composites [See Table 10.]

Conclusions

Hybridization of low-modulus tough fibers into brittle carbon fibers is based on the fact that the strain energy absorption capacity of the fiber is the most dominant parameter dictating the impact damage resistance of composites. Hybridization offers increased residual strengths up to 140%. Among the many candidate fibers studied in the open literature, the addition of

polyethylene fibers is frequently recommended for superior damage tolerance and penetration resistance.

6.11. Woven Fabric Composites [See Table 10.]

Conclusions

The use of woven fabrics in place of cross plies has the beneficial effects of improving the interlaminar fracture toughness and the impact damage resistance. The propagation of delamination and shear cracks is also severely hindered by the weave structure in woven fabric laminates. Woven laminates have residual strengths up to 45% greater than their unwoven counterparts.

6.12. Stitched Composites [See Tables 9 and 10.]

Conclusions

Through-thickness stitches present an opportunity for the development of composites with greatly improved resistance to delamination and impact damage. Stitched laminates offer residual strengths up to 50% and interlaminar fracture toughness up to 150% greater than their unstitched counterparts. One of the disadvantages of this process is that the undamaged compressive strength of the material is reduced by up to 20%. Stitch density is a dominant parameter in determining the efficiency of stitching.

Recommendations

Excessive stitching should be avoided since it is detrimental to damage resistance and CAI strength due to misalignment and localized disruption of longitudinal fibers.

6.13. Influence of Fiber on Impact Resistance

Conclusions

The properties of the fibers in a continuous fiber laminate have a significant effect on the impact resistance and subsequent load-bearing capacity. During low-velocity impact, the ability of the fibers to store energy elastically appears to be the fundamental parameter in determining impact resistance. Strain to failure improvement of fibers can be achieved by reducing the fiber diameter. Impact resistance of S-glass and Kevlar fiber reinforced composites is more than five times greater than that of a Modmor II carbon fiber reinforced composite. Kevlar fibers, which have large areas under their stress/strain curves, offer excellent impact resistance.

Recommendations

The role of the fiber diameter on impact resistance is not completely clear in the current literature. A simple model suggests that composites with larger diameter fibers should be inherently tougher [110]. Current trends are, however, towards smaller diameter fibers offering higher strains to failure. Further investigation should be conducted in this area.

6.14. Influence of Matrix on Impact Resistance

Conclusions

It is clear that matrix properties play a significant role in determining the impact resistance and subsequent load-bearing capability of a fiber reinforced composite. For improved impact resistance of carbon fiber reinforced epoxy laminates, the strength of the matrix should exceed 69 MPa and its strain to failure should be greater than 4% [151]. It appears that materials with high Mode II interlaminar fracture toughness offer superior post-impact compression strengths.

Recommendations

It is somewhat unclear why the residual compressive properties of a composite should be Mode II controlled since the failure process is undoubtedly complex, containing a significant Mode I component. Further research should be done on this question.

6.15. Influence of Interphase on Impact Resistance

Conclusions

The level of treatment applied to the surface of the fibers in a composite has a significant effect upon both its impact resistance as well as its residual load-carrying capability. Improving the fiber-matrix bond strength in a carbon fiber reinforced epoxy can result in a four-fold increase in the impact energy required to initiate damage. In general, impact on composites with low levels of fiber surface treatment may generate large areas of splitting and delamination with severe effects on the compressive properties of the material. Localized impact loading on highly treated fiber composites results in a smaller, more localized damage zone, a higher perforation threshold, and improved residual compressive properties. However, the increased notch sensitivity associated with fiber surface treatments results in a reduction in the post-impact tensile strength of the composite.

Recommendations

The level of treatment applied to the surface of the fibers should be determined very carefully, depending upon the desired application.

6.16. Influence of Fiber Stacking Sequence on Impact Resistance

Conclusions

The impact resistance of a multidirectional laminate is strongly dependent upon the specific orientation of the plies. Further, impact damage appears to be greatest where ply orientation changes of 90° occur. The mismatch in bending stiffness between two such adjacent plies whether on the surface or internal to the laminate appears to have a significant effect upon the level of damage incurred at that interface. Increasing the angle q° from 0° to 90° in a $(0_5°,q°,0_5°)$ laminate decreases the delamination strength for a given incident impact energy.

Recommendations

These conclusions suggest that for containment of damage in laminates (1) unidirectional laminates should be avoided since they split and fail at relatively low energies and (2) 90° fiber direction changes in adjacent lamina should be avoided, if feasible.

6.17. The Effect of the Matrix on the Energy Absorption Capability [See Table 13.]

Conclusions

A higher fracture toughness of thermoplastic matrix materials would increase the energy absorption capability of the composite material. Among all types of composites investigated in this thesis, carbon fiber/PEEK laminates exhibited the highest specific energy absorption and this is attributed to the higher interlaminar fracture toughness of the PEEK matrix.

Recommendations

The question of whether there is a role for thermoplastic composites in the U.S. Navy could be explored.

6.18. The Effect of the Fiber on the Energy Absorption Capability [See Table 14.]

Conclusions

Composites reinforced with fibers having higher strain to failure result in greater energy absorption properties. And, composites reinforced with fibers having lower stiffness result in greater energy absorption properties.

Recommendation

Changes in fiber stiffness affect energy absorption capability less than changes in fiber failure strain. This should be considered in the fiber selection process for each task.

6.19. The Effect of the Fiber Orientation on the Energy Absorption Capability [See Table 15.]

Conclusions

Regarding the effects of fiber orientation on the energy absorption capability of a composite material, the fiber orientations that enhance the energy absorption capability of the composite also increase the number of fractured fibers, increase the material deformation, and increase the axial stiffness of the composite material. Thus, for example, glass epoxy laminates having $[0_5/90_5/0_5]_S$ fiber orientations display the highest energy absorption followed, in decreasing energy absorption, by laminates having $[0_5/45_5/0_5]_S$, $[0_5/30_5/0_5]_S$, $[0_5/15_5/0_5]_S$ fiber orientations. While this is true for energy absorption, it is counter to the initial delamination load, as noted in Conclusion 6.16.

6.20. The Effect of Fiber Volume Fraction on the Energy Absorption Capability

Conclusions

An increase in the fiber volume content may not always improve the energy absorption capability of a composite. As the fiber volume fraction increases, the volume of the matrix between the fibers decreases. This can cause the interlaminar strength of the composite to decrease. As the interlaminar strength decreases, interlaminar cracks may form at lower loads, resulting in a reduction in the energy absorption capability. For glass fiber **vinyl ester** composites with a fiber volume fraction in the range of 10-50%, an increase in fiber volume fraction results in an increase in energy absorption.

Recommendations

There has been no systematic study reported in the open literature on the effect of fiber volume fraction on the energy absorption of composites. Such a study could be rewarding.

6.21. The Effect of Impactor Speed on the Energy Absorption Capability [See Table 17.]

Conclusions

It is known that energy absorption capability is a function of impactor speed. The strain energy absorbing capabilities of a composite and its geometrical configuration affect the impact resistance of the structure at low rates of strain. However, the strain energy absorbing capabilities of the composite and its geometrical configuration are less influential at very high rates of strain.

Recommendations

There seems to be a lack of consensus about the influence of the impactor speed on energy absorption. Further investigations are necessary for a potential consensus on this topic.

References

1 W.J. Cantwell and J.Morton, "Comparison of the Low- and High-velocity Impact Response of CFRP", Composites, Vol.20, No.6, pp.545-5551, 1989.

2 K.N. Shivakumar, W. Elber, and W. Illg, "Prediction of Low-velocity Impact Damage in Thin Circular Laminates", American Institute of Aeronautics and Astronautics Journal, Vol.23, No.3, pp.442-449, 1985.

3 P.O. Sjoblom, J.T. Hartness, and T.M. Cordell, "On Low-velocity Impact Testing of Composite Materials", Journal of Composite Materials, Vol. 22, pp.30-52, 1988.

4 D. Liu, and L.E. Malvern, "Matrix Cracking in Impacted Glass/epoxy Plates", Journal of Composite Materials, Vol.21, pp.594-609, 1987.

5 S.P. Joshi, and C.T. Sun, "Impact-induced Fracture Initiation and Detailed Dynamic Stress Field in the Vicinity of Impact", Proceedings American Society of Composites 2nd Technical Conference, pp.177-185, 23-25 September 1987.

6 P. Robinson and G.A.O. Davies, "Impactor Mass and Specimen Geometry Effects in Low-velocity Impact of Laminated Composites", International Journal of Impact Engineering, Vol.12, No.2, pp.189-207, 1992.

7 G.A.O. Davies, and P. Robinson, "Predicting Failure by Debonding/delamination", AGARD:74th Structures and Materials Meeting, 1992.

8 S.P. Joshi, and C.T. Sun, "Impact Induced Fracture in a Laminated Composite", Journal of Composite Materials, Vol.19, pp.51-66 ,1985.

9 H.Y.Choi, H.Y.T. Wu, and F.K. Chang, "A New Approach Toward Understanding Damage Mechanisms and Mechanics of Laminated Composites Due to Low-velocity Impact: Part II Analysis", Journal of Composite Materials, Vol.25, pp.1012-1038, 1991.

10 C.J. Jihand and C.T. Sun, "Prediction of Delamination in Composite Laminates Subjected to Low-velocity Impact", Journal of Composite Materials, Vol.27, No.7, pp.684-701, 1993.

11 S.W.R Lee, and C.T. Sun, "A Quasi-static Penetration Model for Composite Laminates", Journal of Composite Materials,Vol.27,No.3, pp.251-271, 1993.

12 W.J. Cantwell, and J. Morton, "Geometrical Effects in the Low Velocity Impact Response of CFRP", Composite Structures,Vol.12, pp.39-59, 1989.

13 H.Y.T. Wu, and G.S. Springer, "Measurements of Matrix Cracking and Delamination Caused by Impact on Composite Plates", Journal of Composite Materials, Vol.22, pp.518-532, 1988.

14 H.Y. Choi, H.S. Wang, and F.-K. Chang, "Effect of Laminate Configuration and Impactor's Mass on the Initial Impact Damage of Graphite/epoxy Composite Plates due to Line Loading Impact" , Journal of Composite Materials, Vol.26, No.6, pp.804-827 1992.

15 F.K Chang, H.Y. Choi, and S.-T. Jeng, "Study on Impact Damage in Laminated Composites", Mechanics of Materials, Vol.10, pp.83-95, 1990.

16 H.Y. Choi, and F.-Y. Chang, "Impact Damage Threshold of Laminated Composites", ASME Applied Mechanics Division Vol. 107, pp. 31-35, November 1990.

17 F.K. Chang, and K.Y. Chang, "A Progressive Damage Model for Laminated Composites Containing Stress Concentrations", Journal of Composite Materials, Vol.21, pp.834-855, 1987.

18 H.Y.Choi, H.Y.T. Wu, and F.K. Chang, "A New Approach Toward Understanding Damage Mechanisms and Mechanics of Laminated Composites Due to Low-velocity Impact: Part I-Experiments", Journal of Composite Materials, Vol.25, pp.992-1011, 1991.

19 Z.Guan and C.Yang, "Low Velocity Impact and Damage Process of Composite Laminates", Journal of Composite Materials, Vol.36, No.7, pp.851-871, 2002.

20 P.A. Lagace, "On Delamination Failures in Composite Laminates", Composite Structures, pp. 111-132, 1992.

21 W. Cui, and M.R Wisnom, "A Combined Stress-based and Fracture-mechanics-based Model for Predicting Delamination in Composites" ,Composites, Vol.24, No.6, pp.467-474, 1993.

22 S.S. Wang, "Delamination Crack Growth in Unidirectional Fiber-reinforced Composites Under Static and Cyclic Loading", Composite Materials: Testing and Design (Fifth Conference) ASTM STP 674, pp. 642-663, 1979.

23 D. Liu, "Impact-induced Delamination-a View of Bending Stiffness Mismatching", Journal of Composite Materials, Vol.22, pp.674-692, 1988.

24 F.J. Guild, P.J. Hogg, and J.C. Prichard, "A Model for the Reduction in Compression Strength of Continuous Fiber Composites After Impact Damage", Composites, Vol.24, No.4, pp.333-339,1993.

25 E. Wu, and K. Shyu, "Response of Composite Laminates to Contact Loads and Relationship to Low-velocity Impact", Journal of Composite Materials, Vol.27, No.15, pp.1443-1464, 1993.

26 H.T. Choi, and F.K. Chang, "A Model for Predicting Damage in Graphite/epoxy Laminated Composites Resulting from Low-velocity Point Impact", Journal of Composite Materials, Vol. 26, No.14, pp.2134-2169 , 1992.

27 G.A.O Davies, X. Zhang, and A. Edlund, "Predicting Damage in Composite Aircraft Structures due to Low Velocity Impact", Aero-tech Conference, Birmingham, UK, January 1994.

28 S.R. Finn, Y.F. He, and G.S. Springer, "Delaminations in Composite Plates under Transverse Impact Loads-experimental Results", Composite Structures, Vol.23, pp.191-204,1993.

29 G. Dorey, "Impact Damage Tolerance and Assessment in Advanced Composite Materials", Seminar on Advanced Composites, Cranfield Institute of Technology, Cranfield, UK, 1986.

30 G. Dorey, "Impact Damage in Composites-development, Consequences, and Prevention", 6th International Conference on Composite Materials and 2nd European Conference on Composite Materials, Imperial College, London, Vol. 3, pp. 3.1-3.26, 1988.

31 G. Dorey, P. Sigety, K. Stellbrink, "Impact Damage Tolerance of Carbon Fiber and Hybrid Laminates", RAE Technical Report 87 057, Royal Aerospace Establishment, Farnborough, UK, 1987.

32 K.C Jen and C.T.Sun "Matrix Cracking and Delamination Prediction in Graphite/Epoxy Laminates", Journal of Reinforced Plastics and Composites, Vol.11, pp.1163-1175,1992.

33 N. Takeda, R.L. Sierakowski, and L.E. Malvern, "Microscopic Observations of Cross Sections of Impacted Composite Laminates", Journal of Composite Technology and Research, Vol4, No.2, pp.40-44, 1982.

34 S. Liu, Z. Kutlu, and F.K. Chang, "Matrix Cracking and Delamination in Laminated Composite Beams Subjected to a Transverse Concentrated Line Load", Journal of Composite Materials,Vol.27,No.5, pp.436-470, 1993.

35 AC. Garg, "Delamination-a Damage Mode in Composite Structures", Engineering Fracture Mechanics, Vol.29, No.5, pp.557-584, 1988.

36 S.R. Finn, and G.S. Springer, "Delaminations in Composite Plates Under Transverse Static or Impact Loads-a Model", Composite Structures,Vol.23, pp.177-190, 1993.

37 Dorey, G.R. Sidey, and J. Hutchings, "Impact Properties of Carbon fiber/Kevlar 49 Fiber Hybrid Composites", Composites,Vol.9, pp.25-32, 1978.

38 M.P. Clarke, and M.J. Pavier, "Artificial Damage Techniques for Low Velocity Impact in Carbon Fiber Composites", Composite Structures,Vol.25, pp.113-120, 1993.

39 L.E Doxsee, P. Rubbrecht, L. Li, I. Verpoest, and M. Scholle, "Delamination Growth in Composite Plates Subjected to Transverse Loads", Journal of Composite Materials, Vol.27, No.8, pp.764-781, 1993.

40 H. Razi, and A.S. Kobayashi, "Delamination in Cross-ply Laminated Composite Subjected to Low-velocity Impact", American Institute of Aeronautics and Astronautics Journal,Vol.31, No.8, pp.1498-1502,1993.

41 S. Leeand, P. Zahuta, "Instrumented Impact and Static Indentation of composites", Journal of Composite Materials, Vol. 25, pp.204-222,1995.

42 A.M. El-Habak, "Effect of Impact Perforation Load on GFRP Composites", Composites, Vol.24, No.4, pp.341-345 , 1993.

43 D.Liu and T.Uchiyama, "Characterization of Energy Absorption Capability of Composite Materials Subjected to Impact Loading", Proceedings of the American Society for Composites, Technical Conference, Vol.20, pp.107, 2005.

44 Robeson, "Study of Impact Damage of Composite Laminates Using Five-Point Bending", Journal of Reinforced Plastics and Composites, Vol.17, No.2, pp.109-121,1998.

45 K.C Jen and C.T. Sun "On the Effect of Matrix Cracks on Laminate Strength", Journal of Reinforced Plastics and Composites, Vol.6, pp.208-222, 1987.

46 A.Bezazi, A.El Mahi and J.M.Berthelot, "Experimental Analysis of Behavior and Damage of Sandwich Composite Materials in Three-point Bending", Strength of Materials, Vol.39, No.2, 2007.

47 J.K. Kim, D.B. Mackay and Y.W. Mai, "Drop Weight Impact Damage Tolerance of CFRP with Rubber Modified Epoxy Matrix", Composites,Vol.24, pp.485-491, 1991.

48 K.I. McRae, A.G. McGray, and A.J.Russel, "Ultrasonic Imaging of Delamination Damage Around Fastener Holes in a Graphite/Epoxy Composite", Damage Detection in Composite Materials, ASTM STP 1128, pp. 163-179, 1992.

49 M.W. Allgaier, "Visual Testing: Method with a Future", Materials Evaluation, Vol.49, No.9, pp.1186-1187, 1991.

50 S.R. Reid and G. Zhou, "Impact Behavior of Fiber-Reinforced Composite Materials and Structures", Woodhead Publishing Limited, Cambridge England, 2000.

51 X.E. Gross, "Characterization of Low Energy Impact Damages in Composites", Journal of Reinforced Plastics and Composites, Vol.15, pp.266-281, 1996.

52 C.A. Ross and R.L. Sierakowski, "Studies on the Impact Resistance of Composite Plates", Composites, Vol.4, pp.157-161, 1973.

53 Y. Hirai, H. Hamada and J.K. Kim, "Impact Response of Glass Woven Fabric Laminates.Part-1:Effect of Silane Coupling Agents", Composites Science and Technology, Vol.58, pp.91-104, 1998.

54 Y. Hirai, H.Hamada and J.K. Kim, "Impact Response of Glass Woven Fabric Laminates. Part-2:Effect of Temperature", Composites Science and Technology, Vol.58, pp.119-128, 1998.

55 D.E. Bray and D. McGride, "Non-destructive Testing Techniques", New York ,Wiley , 1992.

56 S.K Burke, S.M. Cousland and C.M. Scala, "Nondestructive Characterization of Advanced Composite Materials", Material Forum, Vol.18 , pp. 85-109, 1994.

57 J. Summerscales, "Non-destructive Testing of Fiber-reinforced Plastics Composites, New York, Elsevier Applied Science, 1987.

58 R.J. Dewhurst, R.He, Q.Shan, "Defect Visualization in Carbon Fiber Composite Using Laser Ultrasound", Materials Evaluation, Vol.51, No.8, pp.935-940, 1993.

59 J.P. Monchalin, "Laser Ultrasonics", Flight-Vehicle Materials, Structures, and Dynamics Assessments and Future Directions, Vol.4, ASME, Chapter 4.

60 R.C Addison, H.A Ryden, " Laser Based Ultrasonics for the Inspection of Large Area Graphite/Epoxy Composites", Review of Progress in QNDE, New York: Plenum Press, pp.485-492.

61 T.S. Jones, "Inspection of Composites Using the Automated Ultrasonic Scanning System", Materials Evaluation, Vol.43, No.5, pp.746-753, 1985.

62 C.F. Buynak, T.J. Moran and R.W.Martin, "Delamination and Crack Imaging in Graphite-Epoxy Composites", Materials Evaluation, Vol.47, No.4, pp.438-441, 1989.

63 K.V. Steiner , "Defect Classification in Composites Using Ultrasonic NDE Techniques", Damage Detection in Composite Materials, ASTM, pp.72-84, 1992.

64 R.H. Fassbender and D.J. Hagemaier, "Low Kilovoltage Radiography of Composites", Materials Evaluation, Vol.41.No.6, pp.831-838, 1983.

65 S.Girshovich, T.Gottesmann, H. Rosenthal and E. Drukker, "Impact Damage Assessment of Composites", Damage Detection in Composite Materials, ASTM, pp.183-199, 1992.

66 W.H. Sheldon, "Comparative Evaluation of Potential NDE Techniques for Inspection of Advanced Composite Structures", Materials Evaluation, pp.41-46, 1978.

67 T.S.Jones and H.Berger, "Non-destructive Evaluation Methods for Composites", International Encyclopedia of Composites, Vol.4, pp.37-49, 1991.

68 S.N. Vernon and P.M. Gammell, "Eddy Current Inspection of Broken Fiber Flaws in Non-metallic Fiber Composites", Review of Progress in QNDE, Vol4B, pp.1229-1237, 1985.

69 C.N. Owston, "Eddy Current Methods for the Examination of Carbon Fiber Reinforced Epoxy Resins", Materials Evaluation, Vol.34,No.11, pp.237-244, 1976.

70 S.L. Gao and J.K. Kim, "Scanning Acoustic Microscopy as a Tool for Quantitative Characterization of Damage in CFRPs", Composite Science and Technology, Vol.59, pp.345-354, 1999.

71 T.S.Jones and H.Berger, "Application of Nondestructive Inspection Methods to Composites".

72 J.R. Weitzenbock, A.T. Echtermeyer, "Nondestructive Inspection and Evaluation Methods for Composites Used in the Marine Industry", International Conference on Composite Materials, Paris, July,1999.

73 R.Gregory, "Rapid, Sensitive Inspection of Marine Composites Using Laser Shearography", Society for the Advancement of Material and Process Engineering,2004 .

74 S. Abrate, "Impact on Laminated Composite Materials", Applied Mechanics Reviews, Vol.44, No.4, pp.155-190, 1991.

75 H.Y.T Wu and G.S.Springer, "Impact Induced Stresses, Strains and Delaminations in Composite Plates", Journal of Composite Materials, Vol.22, pp.533-560, 1988.

76 N.Sela and O.Ishai, "Interlaminar Fracture Toughness and Toughening of Laminated Composite Materials", Composites, Vol.20, No.5, pp.423-435, 1989.

77 A.T.Nettles and A.J.Hodge, "Compression after Impact Testing of Thin Composite Materials, 23 rd International Sampe Technical Conference, pp.177-183, 21-24 October 1991.

78 R.Jones, J.Paul, T.E.Tay, "Assessment of the Effect of Impact Damage in Composites", Composite Structures, Vol.10, No.1, pp.51-73, 1988 .

79 F.E. Dost, L.B. Ilcewicz, and J. H. Goos, "Sublaminate Stability Based Modeling of Impact Damaged Composite Laminates", 3rd Technical Conference of America Society for Composite, Seattle Washington, September 1988.

80 W. B. Avery, "Semi-Discrete Approach to Modeling Post-impact Compression Strength of Composite Laminates", 21st International SAMPE Technical Conference, pp.141–151, September 1989.

81 F. J. Guild, P. J. Hogg, and J. C. Pritchard, "A Model for the Reduction in Compression Strength of Continuous Fiber Composites After Impact Damage", Composites, Vol.24, No.4, pp.333–339, 1993.

82 Y. Xiong, and C. Poon, "Prediction of Residual Compressive Strength of Impact-Damage Composite Laminates", ICCM 9, Madrid, 1993.

83 E. Armanios, and G.A. Kardomates, "Damage Tolerance Analysis for Composite Rotor-craft Structures", Contract S2536612, Status Report,1993.

84 C. Kassapoglu, "Compression Strength of Composite Sandwich Structures After Barely Visible Impact Damage", Journal of Composite Technology and Research, Vol.18, No.4, 274–284,1996.

85 W.J Cantwell, P.T. Curtis, "An Assessment of the Impact Performance of CFRP with High Strain Carbon Fibers", Composite Science and Technology, Vol.25, pp.133-148, 1986.

86 G. Dorey, "Damage Tolerance and Damage Assessment in Advanced Composites", Advanced Composites, Vol.11, 1989.

87 J. C. Prichard and P. J. Hogg, "The Role of Impact Damage in Post-impact Compression Testing", Composites, Vol.21, pp.503-11, 1990.

88 R. E. Evan and J. E. Masters, "A New Generation of Epoxy Composites for Primary Structural Applications", Toughened Composites, ASTM STP 937, pp. 413-36, 1987.

89 J. Brandt, and J. Warnecke, "Influence of Material Parameters on the Impact Performance of Carbon Fiber Reinforced Polymers", In High-Tech Elsevier Science Publishers B. V., Amsterdam, pp. 251-60, 1986.

90 S.Sanchez, E.Barbero and C.Navarro, "Compression After Impact of Thin Composite Laminates", Composite Science and Technology, pp.1911-1919, 2005.

91 Anon, "Standard Tests for Toughened Resin Composites", NASA Reference Publication, pp.1092, 1982.

92 P.T. Curtis, "CRAG Test Methods for the Measurement Engineering Properties of the FRP", Royal Aerospace Establishment, UK, 1988.

93 Anon, "Advanced Composite Compression Tests", Boeing Specification Support Standards 7620, 1982.

94 PO Sjoblom, B.Hwang, "Compression After Impact", International SAMPE Symposium and Exhibition, Vol. 34, p.1411–1421,1989.

95 F. Griffin, "Damage Tolerance of Toughened Resin Graphite Composites", Toughened Composites, pp.23-33.

96 F.E., Dost, L.B. Ilcewicz, "A Model for Compression After Impact Strength Evaluation", 21st International SAMPE Technical Conference, pp.130-140, 1989.

97 T.R. Porter, "Compression and Compression Fatigue Testing of Composite Laminates", NASA CR-168023, 1982.

98 T.B. Irvine, and C.A. Ginty, "Progressive Fracture of Fiber Composites", Journal of Composite Materials, Vol.20, 1986.

99 C.Puhui and S. Zhen, "A New Method for Compression After Impact Strength Prediction of Composite Laminates", Journal of Composite Materials, Vol.36, No.5, pp.589-610, 2002.

100 G. Dorey, "Fracture of Composites and Damage Tolerance", Fabrication and Tests for Composite Materials, A GARD Lecture Series 124, 1982.

101 J. Morton, and E.W. Godwin, "Impact Response of Tough Carbon Fiber Composites", Composite Structures, Vol.13, pp.1-19, 1989.

102 W.J. Cantwell, P.T. Curtis, and J. Morton, "Low Velocity Impact Damage Tolerance in CFRP Laminates Containing Woven and non-woven Layers", Composites, Vol.14, pp.301-305, 1983.

103 M.B. Dow, and D.L. Smith, "Damage-tolerant Composite Materials Produced by Stitching Carbon Fabrics", 21st International SAMPE Technical Conference, September 1989.

104 P. Beguelin and M. Barbezat, "Caracterisation Mecanique des Polymres et Composites", Proceedings 5th Journee Nationale DYMAT, Bordeaux, France, 1989.

105 P.Davies, W.J. Cantwell, and H.H. Kamch, 'Measurement of Initiation Values of G_{IC} in IM6/PEEK Composites', Composites Science and Technology, Vol.35, pp.301-313, 1989.

106 P.Compston and P-Y.B.Jar, "Comparison of Interlaminar Fracture Toughness in Unidirectional and Woven Roving Marine Composites", Applied Composite Materials, Vol.5, pp.189-206, 1998.

107 B. Harris, P.W.R Beaumont, and E. Monennin de Ferran, "Strength and Fracture Toughness of Carbon Fiber Polyester Composites", Journal of Material Science, Vol.6, pp. 238-251, 1971.

108 S. Bandyopadhyay, E.P Gellert, and V.M. Silva, "Microscopic Aspects of Failure and Fracture Toughness in Advanced Composite Materials", Journal of Composite Materials, Vol. 23, pp. 1216-1231, 1989.

109 J.N. Kirk, M. Munro,and P.W.R. Beaumont, 'The Fracture Energy of Hybrid Carbon Fiber and Glass Fiber Composites' , Journal of Material Science, Vol.13, pp. 2197-2204, 1978.

110 F.J. Bradshaw, G. Dorey, and G.R. Skley, "Impact Resistance of Carbon Reinforced Plastics", RAE TR 72240, 1972.

111 G. Dorey, 'Relationship Between Impact Resistance and Fracture Toughness in Advanced Composite Materials', Effect of Service Environment on Composite Materials, AGARD CP 288,1980.

112 B.Z. Jang and W.C. Chung, "Structure Property Relationships in Three Dimensionally Reinforced Fiberous Composites", Advanced Composites, ASM International, pp.183-192, 1986.

113 H.G.Recker AND V.Altstadt, " Toughened Thermosets for Damage Tolerant Carbon Fiber Reinforced Composites", SAMPE Journal, Vol. 26, pp.73-78, 1990.

114 K.R.Hirschbuehler, "A Comparison of Several Mechanical Tests Used to Evaluate the Toughness of Composites", Toughnened Composites, ASTM STP 937, pp.61-73, 1987.

115 G.Caprino, "On the Prediction of Residual Strength for Notched Laminates", Journal of Material Science, Vol.18, pp.2269-2273,1983.

116 T.E. Hess, S.L Huang and H.Rubin, "Influence of Temperature Change on Optimum Laminate Design", Journal of Aircraft ,Vol.14, pp. 994-999, 1977.

117 C.T. Sun and J.Luo , "Enhancing Compressive Strength of Unidirectional Polymeric Composites Using Nanoclay", Composite Science and Technology, Vol.22, pp.121-133, 1988.

118 W.S. Chan, C.Rogers and A.Aker, "Improvement of Edge Delamination Strength of Composite Laminates Using Adhesive Layers", Composite Materials: Testing and Design, ASTM, pp. 266-285, 1986.

119 K.R. Hirschbuehler, "An Improved 270 F Performance Interleaf System Having Extremely High Impact Resistance", Sampe Quartely, Vol. 17, pp. 46-49, 1985.

120 G.L Dolan, J.E. Masters, "Characterization of Carbon/Bismaleimide Interleafed for Improved Resistance to Delamination and Impact", 20th International Sampe Technical Conference, pp. 34-45, 1988.

121 J.E. Masters, "Improved Impact and Delamination Resistance Through Interleafing", Key Engineering Materials, Vol.37, pp.317-348, 1989.

122 N.Sela , O.Ishai, "Interlaminar Fracture Toughness and Toughening of Laminated Composite Materials", Composites. Vol.20, pp.257-264, 1989.

123 B.Harris and A.R.Bunsell, " Impact Properties of Glass Fiber/Carbon Fiber Hybrid Composites", Composites,Vol.6, pp.197-201, 1975.

124 J.L. Perry and D.F. Adams, "Charpy Impact Experiments on Graphite/epoxy Hybrid Composites", Composites, Vol.6, pp.166-172, 1975.

125 D.R Ireland, "Physical Testing of Plastics-Correlation with End-use Performance", ASTM-STP 736, pp. 45-58, 1981.

126 A.A.J.M Peijs, R.M. Venderbosch, "Hybrid Composites Based on Polyethylene and Carbon Fibers", Composites, Vol.21, pp. 522-530, 1990.

127 B.Z.Jang, L.C. Chen, "Impact Resistance and Energy Absorption Mechanisms in Hybrid Composites", Composite Science and Technology, Vol.34, pp.305-335, 1989.

128 B.Z.Jang, L.C. Chen, "The Response of Fibrous Composites to Impact Loading", Polymer Composites, Vol.11, pp.144-157, 1990.

129 J.K.Kim, L.M.Leung and Y.Hirai, "Impact Performance of a Woven Fabric CFRP Laminate", Polymers and Polymer Composites, Vol.4, pp.549-561, 1996.

130 L.H. Strait, M.L. Karasek, "Effects of Stacking Sequence on the Impact Resistance of Carbon Fiber Reinforced Thermoplastic Toughened Epoxy Laminate", Journal of Composite Materials, Vol.26, pp.1725-1740, 1992.

131 K.Dransfield, C.A. Baillie and Y.W.Mai, "On the Effects of Stitching in CFRPs", Composites Science and Technology, Vol.50, pp.305-317, 1995.

132 S.Adanur and Y.P.Tsao, "Improving Fracture Resistance of Laminar Textile Composites by Third Direction Reinforcement", Composite Engineering, Vol.5, pp.1149-1158, 1995.

133 W.C. Chung, B.Z. Jang and T.C. Chang, "Fracture Behavior in Stitched Multidirectional Composites", Material Science and Engineering, Vol.A112, pp.157.173, 1989.

134 A.P. Mouritz, "The Damage to Stitched GRP Laminates by Underwater Explosion Shock Loading", Composites Science Technology, Vol.55, pp.365-374, 1995.

135 T.J.Kang and S.H.Lee, "Effect of Stitching on the Mechanical and Impact Properties of Woven Laminate Composite", Journal of Composite Materials, Vol.28, pp.1574-1587, 1994.

136 D.Liu, "Delamination Resistance in Stitched and Unstitched Composite Plates Subjected to Impact Loading", Journal of Reinforced Plastics Composites, Vol.9, pp.59-69, 1990.

137 J.E.Masters, "Mechanical Performance of Carbon-fiber and Glass-fiber-reinforced Epoxy", Proceeding 6th Internatonal Conference of Composite Materials, pp.96-107, 1987.

138 W.L.Bradley, "How to Improve the Toughness of Polymers and Composites", Proceeding "Benibana" International Symposium, pp.221-230, 1990.

139 A.Morales,"Thermal Degradation of the Mode I Interlaminar Fracture Properties of Stitched Glass Fiber/vinyl Ester Composites", Proceeding 22nd International SAMPE Technical Conference, pp.1217-1230, 1990.

140 G.L. Farley, B.T.Smith, "Compression Response of Thick Layer Composite Laminates with Through-the-Thickness Reinforcement", Journal of Reinforced Plastics and Composites, Vol.11, pp.787-810.

141 A.W.H. Morris, and R.S. Smith, "Some Aspects of the Evaluation of the Impact Behavior of Low-temperature Fiber Composites", Fiber Science and Technogy, Vol. 3, pp. 219-242, 1971.

142 P.W.R. Beaumont, P.G. Riewald, and C. Zweben, "Methods for Improving the Impact Resistance of Composite Materials",IBID, pp.134-145.

143 M.G. Bader, and R.M Ellis,"The Effect of Notches and Specimen Geometry on the Pendulum Impact Strength of Uniaxial CFRP", Composites, Vol.5, pp.253-258, 1974.

144 N.L. Hancox, "Izod Impact Testing of Carbon Fiber-reinforced Plastics", Composites, Vol. 2, pp. 41-45, 1971.

145 C.C Chamis, M.P. Hanson, and T.T. Serafini, "Impact Resistance of Unidirectional Fiber Composites", Composite Materials, pp.324-349.

146 C.C Chamis,. and J.H. Sinclair, "Impact Resistance of Fiber Composites: Energy Absorbing Mechanisms and Environmental Effects", ASTM STP 864, pp.326-345, 1985.

147 P.W.R. Beaumont, "Fracture Mechanisms in Fibrous Composites", Fracture Mechanics, pp. 211-233, 1979.

148 P. Davies and W.J. Cantwell, "Interlaminar Fracture Testing of Carbon fiber/ PEEK Composites Validity and Applications", Developments in the Science and Technology of Composite Materials, pp. 747-755, 1989.

149 A.D. Curson, D.C. Leach, and D.R. Moore, "Impact Failure Mechanisms in Carbon Fiber/PEEK Composites", Journal of Thermoplastic Composite Materials, Vol.3, pp 24-31, 1990.

150 D.L Hunston, "Composite Interlaminar Fracture: Effect of Matrix Fracture Energy, Composites Technology Review, Vol 6, pp. 176-180, 1984.

151 J.G. Williams, and M.D. Rhodes, "Effect of Resin on Impact Damage Tolerance of Graphite/epoxy Laminates", Composite Materials: Testing and Design (Sixth Conference), ASTM STP 787, pp. 450-480, 1982.

152 C.B. Bucknall, and I.K. Partridge, "Phase Separation in Epoxy Resins Containing Polyethersulphone", Polymer , Vol.24, pp. 639-644, 1983.

153 L.D. Bravene, A.G. Filippov, and K.C. Dewhirst, "New Concepts in Damage to Tolerant Composites", Proceeding 34th lnternational SAMPE Symposium, pp. 714-725 ,1989.

154 G.F. Sykes, and D.M. Steakley, "Impact Penetration Studies of Graphite/epoxy Laminates", Proceeding 12th SAMPE Technology Conference, pp. 482-493, 1980.

155 G.E.Husman, J.M. Whitney, and J.C. Halpin, "Residual Strength Characterization of Laminated Composites Subjected to Impact loading", Foreign Object Impact Damage to Composites, pp.92-113.

156 J.E. Masters, 'Correlation of Impact and Interleaf Delamination Resistance in Intefleafed Laminates", Proceeding 6th lnternational Conference on Composite Materials, pp. 3.96-3.107, 1987.

157 K.K.U. Stellbrink, "Improved Impact Damage Tolerance", Proceedings European Symposium on Damage Development and Failure Processes in Composite Materials, Belgium, 1987.

158 E.Dan-Jumbo, A.R. Leewood, and C.T. San, "Impact Damage Characteristics of Bismaleimides and Thermoplastic Composite Laminates", Composite Materials: Fatigue and Fracture, ASTM STP 1012. Vol.2, pp.356-372, 1989.

159 D.R. Moore, and R.S. Predlger, "A Study of Low-energy Impact of Continuous Carbon Fiber Reinforced Composites", 8th NRCC/IMRI Symposium, Composites 87,1987.

160 P. Davies, "Delamination Behaviour of Thermoplastic Matrix Composites", PhD Thesis, University of Compiegne, France, 1987.

161 W.J. Cantwell, P.Davies, and P. Jar, "Joining and Repair of Carbon fiber PEEK Composites", Plastics Metals-Ceramics SAMPE, pp 411-426, 1990.

162 R.E Evans, J.E. Masters, and J.L. Courter, Toughened Interleafed Composites", Advanced Composites, pp. 249-257, 1985.

163 S. Lchmam, C. Megerdiglan, and R. Papalla, "Carbon Fiber/resin Matrix Interphase: Effect of Carbon Fiber Surface Treatment on Composite Performance", SAMPE Quarterly, Vol.16, pp.7-13, 1985.

164 L.T. Drzal, and M.J. Rich, "Effect of Graphite Fiber/epoxy Matrix Adhesion on Composite Fracture Behavior", Recent Advances in Composites, pp.16-26.

165 K.F. Rogers, G.R. Sidey, and D.M. Kinston-Lee, "Ballistic Impact Resistance of Carbon-fiber Laminates", Composites, Vol. 2, pp. 237-241, 1971.

166 S.J. Bless, and D.R. Hartman, "Ballistic Penetration of S-2 Glass Laminates", Proceeding 2lst International SAMPE Conference, pp.852-866, 1989.

167 F.J. McGarry, J.F Manden,. and J. Knwamoto, "Impact Resistance of Rubber Modified Carbon Fiber Composite", Advanced Composites, pp.195-205.

168 G. Dorey, "Fracture Behavior and Residual Strength of Carbon Fiber Composites Subjected to Impact Loads", Failure Modes of Composite Materials with Organic Matrices and Their Consequences in Design, AGARD CP 163, paper 8, 1975.

169 C.Y. Kam, and J.V. Walker, "Toughened Composites Selection Criteria", Toughened Composites, pp.9-22.

170 M. Stevanovic , M. Kostic, T. Stecenko, and D. Briski, "Impact Behavior of CFRP Composites of Different Stacking Geometry", Composites Evaluation, pp.78-83.

171 W.J. Cantwell, "Impact Damage in Carbon Fiber Composites", PhD thesis, University of London, UK, 1985.

172 S. Hong, and D. Liu, "On the Relationship Between Impact Energy and Delamination Area", Experimental Mechanics, Vol.13, pp.115-120, 1989.

173 M. Vedula, and M.J. Koczak, "Impact Resistance of Cross-plied Polyphenylene Sulfide Composites", Journal of Thermoplastic Composite Materials, pp.154-163, 1989.

174 P.K. Malllek, and L.J. Broutman, "Static and Impact Properties of Laminated Hybrid Composites", Journal of Testing and Evaluation, Vol.5, pp.190-200, 1977.

175 N.L. Hancex, and H. Wells, "Izod Impact Properties of Carbon Fiber/glass Fiber Sandwich Structures", Composites, Vol. 4, pp. 26-29, 1973.

176 D.F. Adams, and J.L. Perry, "Static and Impact Behavior of Graphite/epoxy Composite Laminates Containing Third-phase Reinforcement materials", Journal of Testing and Evaluation, Vol.5, pp.114-123, 1977.

177 F.K. Ko, and D. Hartman, "Impact Behavior of 2-D and 3-D Glass/epoxy Composites", SAMPE Journal, Vol. 22, No. 4, pp. 26-30, 1986.

178 J.W. Herrick, "Impact Resistant Multidimensional Composites",Proceeding 12th National SAMPE Technology Conference, pp. 845-856, 1980.

179 L.J. Broutman, A. Rotem, "Impact Strength and Toughness of Fiber Composite Materials", Foreign Object Impact Damage to Composites, ASTM STP 568, pp.114-133, 1975.

180 W.J. Cantwell, "The Influence of Target Geometry on the High-velocity Impact Response of CFRP", Composite Structures, Vol.10, pp.247-265, 1988.

181 D. Liu, "Characterization of Impact Properties and Damage Process of Glass/Epoxy Composite Laminates", Journal of Composite Materials, Vol.38,No.16, pp.1425-1442, 2004.

182 B.L.Lee, "Failure of Spectra Polyethylene Fiber-Reinforced Composites under Ballistic Impact Loading", Journal of Composite Materials, Vol.28, No.13, pp.1202-1226, 2004.

183 B.L.Lee, T.F.Walsh and A.H.Mayer, "Penetration Failure Mechanism of Armor-Grade Fiber Composites under Impact", Journal of Composite Materials, Vol.35, pp.1605-1633, 2001.

184 L.C.Lin and H.W Chang, "Ballistic Energy Absorption of Composites", Proceeding of the 22nd SAMPE International Technical Conference, pp.1-13, 1990.

185 P.M.Cuniff, "An analysis of the System Effects in Woven Fabric under Ballistic Impact", Textile Research Journal, Vol62, No.9, pp.495-509, 1992.

186 M.V.Hosur and M.R.Karim, "Studies on Stitched Woven S2 Glass/Epoxy Laminates under Low-velocity and Ballistic Impact Loading", Journal of Reinforced Plastics and Composites, Vol.23, pp.1313-1323, 2004.

187 J.W.Song and G.T.Egglestone, "Investigation of the PVB/PF Ratios on the Crosslinking and Ballistic Properties in Glass and Aramid Fiber Laminate Systems", Proceeding of the 19th SAMPE International Technical Conference, pp.108-119, 1987.

188 M.V.Hosur, U.K.Vaidya and C.Ulven, "Performance of Stitched/unstitched Woven Carbon/epoxy Composites under High-velocity Impact Loading", Composite Structures, Vol.64, pp.455-466, 2004.

189 S. Ramakrishna, H.Hamada, and H. Sato, "Energy Absorption Behavior of Carbon Fiber Reinforced Thermoplastic Composite Tubes.",Journal of Thermoplastic Composite Materials, Vol.8, pp. 323–344, 1995.

190 I.Y. Chang, J.K. and Lees, "Recent Development in Thermoplastic Composites.", Journal of Thermoplastic Composite Materials , Vol.1, pp.277–295, 1998.

191 I.Y. Chang, "Thermoplastic Matrix Continuous Filament Composites of Kevlar, Aramid or Graphite Fiber", Composite Science and Technology, Vol.24, pp.61–79,1985.

192 H.Satoh, H.Hirakawa, and D.Hull, "Comparison of Energy Absorption Among Carbon/Thermoplastic Tubes", 38th International SAMPE Symposium, Science of Advanced Materials and Process Engineering Series, Vol. 38, pp.10–13, 1993.

193 H.Hamada, J.C.Coppola, and D.Hull, "Comparison of Energy Absorption of Carbon/E and Carbon/PEEK Composite Tubes", Composites, Vol.23, No.4, pp. 245–252, 1992.

194 G.L. Farley, "Energy Absorption in Composite Materials for Crashworthy Structures", Proceedings of the ICCM 6. London: Elsevier Science Publishers Limited. pp. 3.57–3.66, 1987.

195 G.L. Farley, "Effect of Fiber and Matrix Maximum Strain on the Energy Absorption of Composite Materials", Journal of Composite Materials, Vol.20, pp.322–334, 1986.

196 H. Hamada, and S. Ramakrishna, "Effect of Fiber Material on the Energy Absorption Behavior of Thermoplastic Composite Tubes", Journal of Thermoplastic Composite Materials, Vol. 9, No.3, pp. 259–279, 1996.

197 G.L.Farley, "Energy Absorption of Composite Materials.", Journal of Composite Materials, Vol.17, pp. 267–279, 1983.

198 G.L. Farley, "Energy Absorption of Composite Material and Structures", Proceedings of the 43rd American Helicopter Society Annual Forum, pp. 613–627,1987.

199 P.H. Thornton, and P.J.Edwards, "Energy Absorption in Composite Tubes", Journal of Composite Materials, Vol.16, pp.521–545, 1982.

200 G.L. Farley, "Effect of Specimen Geometry on the Energy Absorption Capability of Composite Materials.", Journal of Composite Materials, Vol.20, pp.390–400,1986.

201 G.L. Farley, and R.M. Jones, "Crushing Characteristics of Composite Tubes with Near-elliptical Cross Sections.", Journal of Composite Materials, Vol.26, No.12, pp.1741 1751, 1992.

202 Thornton, J.J.Harwood, and, P. Beardmore, "Fiber Reinforced Plastic Composites for Energy Absorption Purposes", Composite Science and Technology, Vol,24, pp.275–298,

1985.

203 S. Ramakrishna, and H. Hamada, "Energy Absorption Characteristic of Crashworthy Structural Composite Materials", Key Engineering Materials, pp.141–143, 1998.

204 S. Ramakrishna, and D. Hull, "Energy Absorption Capability of Epoxy Composite Tubes with Knitted Carbon Fiber Fabric Reinforcement", Composite Science and Technology, Vol.49,pp.349–356, 1993.

205 S. Ramakrishna, "Energy Absorption Characteristics of Knitted Fabric Reinforced Composite Tubes", Journal of Reinforced Plastics and Composites, Vol.14, pp.1121–141,1995.

206 G.L. Farley, and R.M. Jones, "Energy Absorption Capability of Composite Tubes and Beams", NASA TM-101634, AVSCOM TR-89-B-003, 1989.

207 P.H. Thornton, W.H. Tao, and R.E. Robertson, "Crash Energy Management: Axial Crush of Unidirectional Fiber Composite Rods", Advanced Composite Materials: New Development and Applications Conference Proceedings, pp. 489–496, 1991.

208 L.A.Ruhala and R.S.Engel, "An Investigation of the Effects of Fiber Volume Fraction on he Impact Properties of Fiber-reinforced Composite Laminated Plates", Journal of Reinforced Plastics and Composites, Vol.19, pp.449-464,2000.

209 D.C. Bannerman, and C.M. Kindervater, "Crash Energy Absorption Properties of Composite Structural Elements", Proceedings of the 4th International SAMPE, pp. 155-167.

210 P.H. Thornton, "Energy Absorption in Composite Structures", Journal of Composite Materials, Vol.13, pp.247–262,1979.

211 P.H. Thornton, "The Crush Behavior of Pultruded Tubes at High Strain Rate", Journal of Composite Materials, Vol.24, pp.594–615, 1990.

212 J G Williams, T K Obrien, A.J. Chapman, "Comparison of Toughened Composite Laminates Using NASA Standard Damage Tolerance Tests", Composite Structure Technology, pp.51-74,1984.

213 P.W. Manders, and W.C. Harris, "A parametric Study of Composite Performance in Compression-after-impact Testing", SAMPE Journal, Vol.22, pp 47-51,1986.

214 M. Akay, "Post Damage Capability of Carbon Fibre Reinforced Matrices", Proceeding lnternational Conference on Polymers for Composites, London, UK, pp 11.1-11.10,1987.

215 C.A. Rea, and R.L. Sierakowski,"Studies on the Impact Resistance of Composite Plates", Composites, Vol.4, pp.157-161,1973.

216 J.D. Helfinstine, "Charpy Impact of Unidirectional Graphite/Aramid/epoxy Hybrid Composites", Composite Materials:Testing and Design (Fourth Conference), ASTM STP 617, pp.375-388,1977.

217 S.N. Kakarala, and J.L. Roche, "Experimental Comparison of Several Impact Test Methods", Instrumented Impact Testing of Plastics and Composite Materials, pp.144-162.

218 H.Ku, Y.M. Cheng, C.Snook and D.Baddeley, "Drop Weight Impact Test Fracture of Vinyl Ester Composites", Journal of Composite Materials, Vol.39, No.18, pp.1607-1620,2005.

219 M.C. Cheresh, and S. McMichael, "Instrumented Impact Test Data Interpretation", Instrumented Impact Testing of Plastics and Composite Materials, ASTM STP 936, pp.9-23, 1987.

220 R.C. Novak, and M.A. de Crescente,Composite Materials: Testing and Design (Second Conference), ASTM STP 497, pp.311-323, 1972.

221 J.W. Gilllespie Jr, L.A. Carlsson and , A.J. Smiley, "Rate Dependent Mode I Interlaminar Crack Growth Mechanisms in Graphite/epoxy and Graphite/PEEK", Composites Science and Technology, Vol.28, pp.1-15, 1987.

222 M.D. Rhodes, J.G. Williams, and J.H. Starnes Jr., "Low-velocity Impact Damage in Graphite-fiber Reinforced Epoxy Laminates", Proceedings 34th Annual Technical Conference, section 20-D, pp.1-10, 1979.

223 J. Degrieck, and R. Dechaene, "Real Time Recording of Transverse Impact Experiments on Composite Laminates", Composites Evaluation, Proceedings 2nd International Conference on Testing, Evaluation and Quality Control of Composites,London, UK,pp.61-68, 1987.

224 J. Harding, "Impact Damage in Composite Materials", Science and Engineering of Composite Materials I, pp.41-68, 1989.

225 S. AmiJima, and T. Fujii, "Compressive Strength and Fracture Characteristics of Fiber Composites under Impact Loading"', Progress in Science and Engineering of Composites, Proceedings 4th International Conference on Composite Materials, pp 399-413,1982.

226 Y. Bai, and J. Harding, "Fracture Initiation in Glass Reinforced Plastics under Impact Compression", Structural Impact and Crashworthiness, Vol. 2, pp.482-493, 1984.

227 J. Harding, and L. Welsh, "A Tensile Testing Technique for Fibre-reinforced Composites at Impact Rates of Strain", Journal of Material Science, Vol.18,pp.1810-1826, 1983.

Appendix

Impact Test Techniques for Composite Materials

Most impact tests, at least the final confirming tests of a component, are performed on the real structure, with a real projectile. This reflects the problem of comparing or extrapolating results from one test situation to another. Ideally, the impact test fixture should be designed to simulate the loading conditions to which a composite component is subjected during operational service and the failure modes that are likely to occur. Without claims to thoroughness, there are at least two typical test methods. One is a drop weight method and the other a relatively high-velocity impact test [212]. In simple terms, the impact problem can be divided into two separate conditions: low velocity impact by a large mass (dropped tool) and high velocity impact by a small mass (runway debris, small arms fire, etc.). The low velocity impact test is generally simulated using a falling weight or a swinging pendulum and the high velocity impact test using a gas gun or some other ballistic launcher. However, as stated previously, a wide variety of non-standard testing techniques is presently being employed in order to assess the dynamic response of reinforced plastics [149,155,157,179,213,214,215,216] making direct comparison difficult.

For materials evaluation and characterization, both types of tests have some disadvantages. Substantial amount of materials maybe required to conduct a complete set of tests. This is often a very severe problem when trying to characterize new materials available only in small quantities. In addition, there is the problem of subsequent testing to determine residual properties after impact. Large, thick panels may require a very large test machine. Therefore, a major concern in the design of a standard test must be the test specimen size.

Low-velocity Impact

Charpy and izod pendulums, falling weight fixtures such as the Gardner and drop dart tests, and hydraulic machines designed to perform both in-plane and out-of-plane testing at velocities up to 10 $m{\cdot}s^{-1}$, are used for simulating the low-velocity impact response of composite materials.

Drop-weight Impact Test

In the drop-weight impact test a weight is allowed to fall from a pre-determined height to strike the test specimen or plate supported in the horizontal plane. The method of using the drop-weight impact includes the use of a falling weight that impacts the specimen. A schematic and a photograph of a drop-weight test are shown in **Figure A1**.

In testing composite materials, the constant weight and varying height method has to be used because the composite material is strain rate sensitive [217,218,219]. Sometimes, the impact event does not cause complete rupture of the test specimen but rebounds, enabling a residual energy to be determined if necessary. The incident velocity of the impactor can be determined by using optical sensors located just above the target or from dynamic equations of motion. Frequently, the impactor is instrumented, enabling the force/time characteristics to be determined, and may also contain a displacement transducer to permit the determination of energy dissipation during the impact event.

The most important advantage of this test compared to the Charpy and Izod tests is that a wider range of test geometries can be tested, thereby enabling more complex components to be tested. Although testing is generally undertaken using a hemi-spherical impactor, it is possible to

use other impactor shapes such as blunt cylinders or sharp points. Variations on the drop-weight theme include the Gardner test where a hemi-spherical impactor strikes a small-diameter circular plate, and the driven dart test where a hemi-spherical probe is driven into the specimen at a predetermined rate [217].

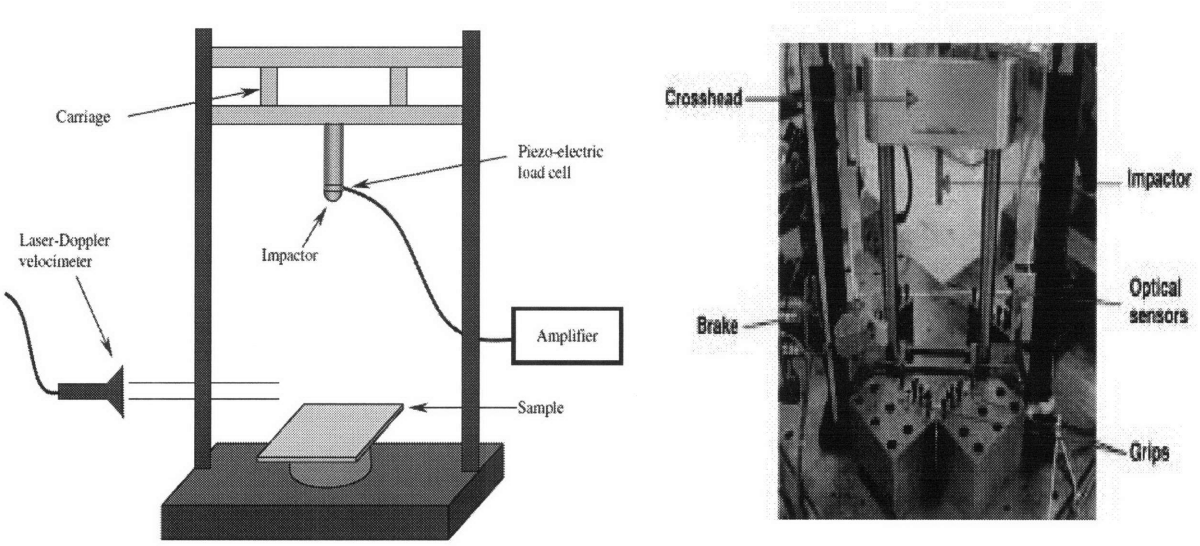

Figure A1: A schematic and a photograph of mechanism of a drop-weight impact test [217,219].

Charpy Pendulum Test

The Charpy test method was originally developed for testing metals. However, it has been used to conduct many impact studies on composite materials [110,142,220]. The reason for this choice is the fact that the Charpy pendulum is both simple to use and can be instrumented, and therefore, in principle, can yield information on the processes of energy absorption and dissipation in composites. The test specimen is generally a thick beam, sometimes incorporating a notch at its mid-point as shown in **Figure A2** [110]. The specimen is supported in a horizontal plane and impacted by the swinging pendulum directly opposite the notch. A dial on the test apparatus is used to record the energy dissipated during impact. By

instrumenting the impactor with a strain gauge, further information can be obtained , thereby enabling the determination of the variation of the impact force with time. By integrating the force/time signal the energy absorbed during impact can also be determined.

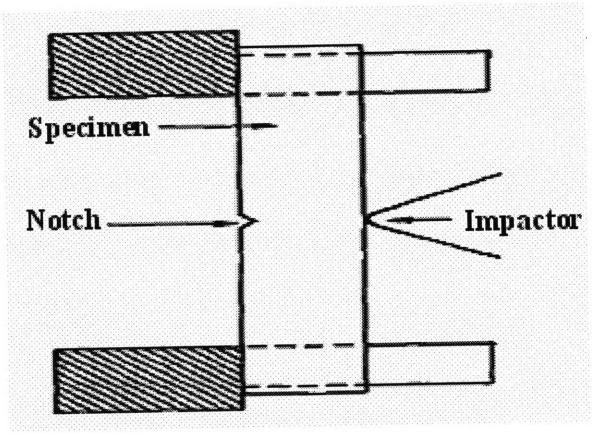

Figure A2: Test specimen for Charpy pendulum [110].

The test set-up suffers a number of disadvantages such as the fact that the load/time curves often contain high frequency harmonic oscillations resulting from the natural response of the impactor. Once the harmonic frequencies of the various components have been determined, these effects can generally be filtered out [219]. Another disadvantage is that the test specimen is a short, thick beam and is therefore not typical of engineering components. Further, the test is destructive, inducing failure modes that are not necessarily observed under low-velocity impact loading on operational structures.

It was shown that the Charpy energy of carbon fiber-reinforced plastic (CFRP) varied with specimen geometry, therefore, the applicability of the technique has been questioned [143]. The Charpy test is suitable only for ranking the impact performance of continuous fiber composites, and as a first step in determining the dynamic toughness of these materials.

Izod Test

The Izod impact test is shown schematically in **Figure A3**. The test set-up and procedure are similar to those outlined for the Charpy test. In the Izod test, the specimen is clamped in the vertical plane as a cantilever beam and impacted by a swinging pendulum at the unsupported end. This test has similar disadvantages to those reported for the Charpy pendulum test. It is best suited for ranking the impact resistance of composite materials.

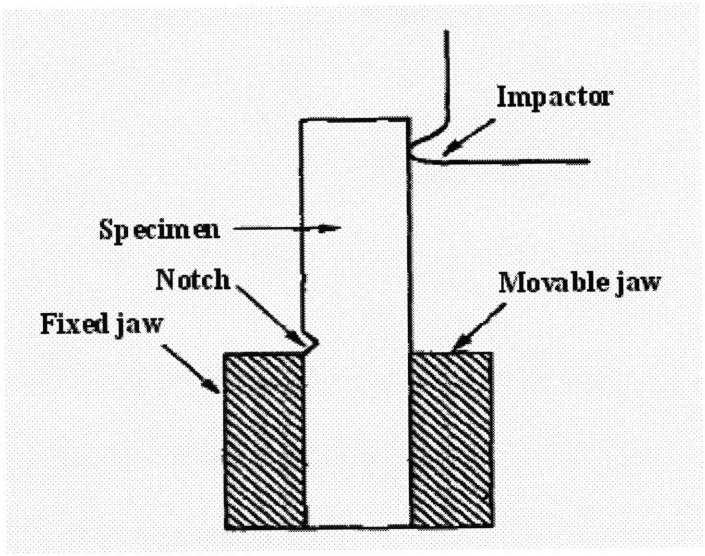

Figure A3: Izod test [146].

Hydraulic Test Machines

Hydraulic test machines have been used for assessing the deformation and failure characteristics of materials at high rates of strain [104,221]. Test specimens such as double cantilever beam (DCB) specimens or tensile dog-bone specimens can be tested over a wide range of strain rates. Bonded strain gauges or an optical transducer can be utilized to measure strain history of the specimen. If a strain gauge or any other displacement measuring device is bonded to the specimen, the strain rate sensitivity of the adhesive should be considered. One of the advantages of this technique is that the test specimens permit the evaluation of basic material

properties such as tensile strength, modulus, and interlaminar fracture toughness without the contact effects associated with falling weight impact. In order to ensure that the mass of the load cell and gripping system are as low as possible, extreme care has to be taken since inertial effects resulting from these components may conceal the true material response [104]. In addition, caution should also be exercised when applying fracture mechanics principles to geometries such as the DCB since the specimen may not be deforming in the same mode as a similar statically-loaded specimen [104].

Intermediate- and High-velocity Impact

Gas Gun Impact Test

Using a high pressure gas gun, impact testing at ballistic rates of strain can be achieved. Typically, a gas such as nitrogen is fed to a chamber located at one end of the barrel. Here the gas is restrained by a plastic diaphragm. When the gas has reached a predetermined value the diaphragm is burst by electrical heating or a mechanical puncturing device, accelerating a projectile down the barrel to strike a specimen or component supported vertically. The velocity of the impactor can be determined just prior to impact using optical sensors [222] or by using a simple break-wire technique[171]. Generally, the test frequently results in large-scale damage and/or target perforation. Instrumented gas guns have been developed, enabling force/displacement histories to be measured [223]. Gas guns are useful for assessing the high velocity impact response of composite material since they can be used to test large structures. A schematic of gas gun impact testing is shown in **Figure A4.**

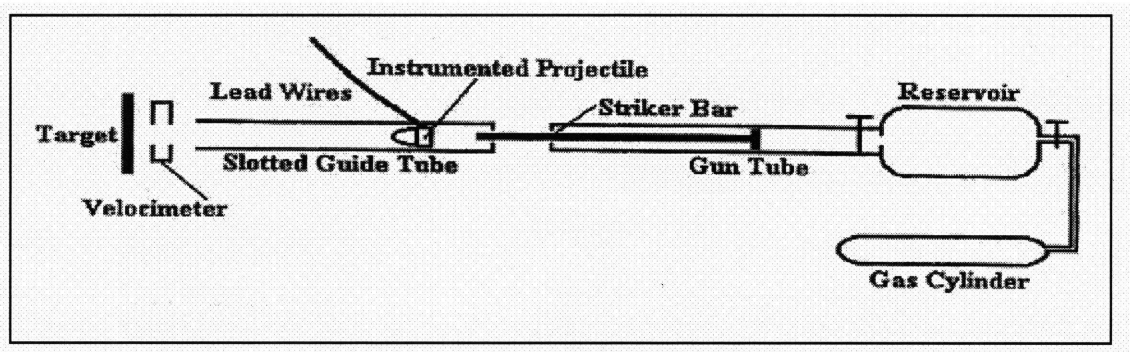

Figure A4: Schematic diagram of gas gun impact testing [223].

Hopkinson-bar Technique

The Hopkinson-bar technique permits the determination of the variation of basic material properties as a function of strain rate. Different types of Hopkinson-bar techniques are used: Punch-loaded Hopkinson-bar, the compression bar, the tensile bar, and the Hopkinson-bar shear test [224,225,226]. The set-up and experimental procedures associated with these tests have been discussed in detail in the literature [224]. The test set-up for undertaking dynamic tensile tests is illustrated in **Figure A5** [227]. Strain rates approaching 1000 s^{-1} can be achieved using gas-driven projectiles [224]. Strain gauges bonded to the input and inertia bars enable the incident and reflected stress waves to be analyzed and permit the determination of a dynamic stress/strain curve for the material.

To ensure that the interface between the specimen and loading bars is good, care has to be taken, otherwise a shear failure within the gripping section is likely to occur. Further, in order to minimize stress concentrations associated with the gripping area, relatively long specimens are required when testing composite materials [227]

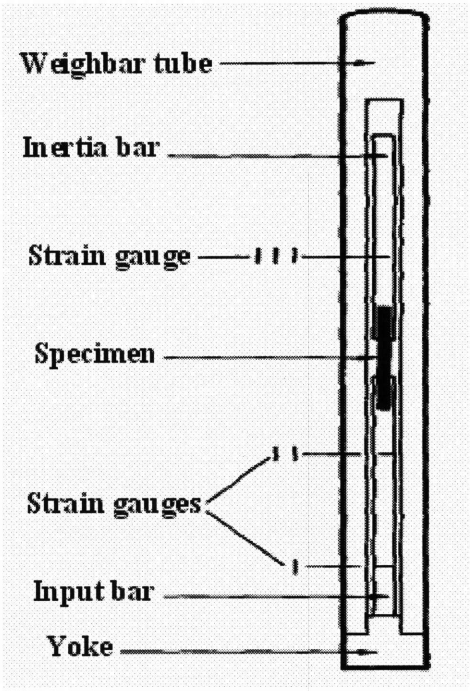

Figure A5: Hopkinson-bar technique [227].